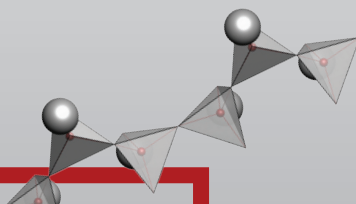


2014

international year of crystallography



Fifth National Crystallographic Symposium with International Participation



PROGRAM and ABSTRACTS



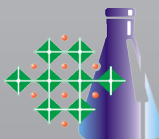
September 25–27, 2014, Sofia, Bulgaria
University of Chemical Technology and Metallurgy

With the support of



ROFA

Founded 1958



Симпозиумът се осъществява с финансовата подкрепа на Министерство на образованието, младежта и науката на РБългария

Fifth National Crystallographic Symposium with International Participation



PROGRAM and ABSTRACTS

organized under the auspices of the
Bulgarian Crystallographic Society (BCS) by:

University of Chemical Technology and Metallurgy
Institute of Mineralogy and Crystallography – BAS
Institute of General and Inorganic Chemistry – BAS
Geological Institute – BAS
Institute of Catalysis – BAS

September 25–27, 2014, Sofia, Bulgaria
University of Chemical Technology and Metallurgy

ORGANIZING COMMITTEE

Chair

Irena Mihailova, UCTM

Members

Boriana Mihailova, Universität Hamburg

Peter Tzvetkov, IGIC – BAS

Veronika Karadjova, UCTM

Milen Kadiyski, IMC – BAS

Daniela Karashanova, IOMT – BAS

Vladislav Kostov-Kytin, IMC – BAS

Galina Gencheva, Sofia University

Georgi Chernev, UCTM

Thomas Kerestedjian, GI – BAS

Daniela Kovacheva, IGIC – BAS Georgi

Avdeev, IPC – BAS

Zara Cherkezova-Zheleva, IC – BAS

Rositsa Nikolova, IMC – BAS

Ognyan Petrov, IMC – BAS

Yana Tzvetanova, IMC – BAS

Boris Shivachev, IMC – BAS

NCS2014 Program at a glance

THURSDAY	FRIDAY	SATURDAY
25 September	26 September	27 September
Registration 8:00-16:30	-	-
Opening ceremony 9:00-9:30	Plenary Lecture (in Bulgarian) Prof. Georgi Kirov	Session VII 9:00-10:20 Emre S. Tasci (I) Thomas Kerestedjian (PO) D. Nihtianova (PO)
Session I 9:30-10:30 J. Manuel Perez-Mato (I) Vesselin Tonchev (OP)	Session V 9 :50-10 :30 Jörg Rothe (I)	
Coffee break & NCS14 Photo	Coffee break	Coffee break
Session II 11:00-12:30 Ross Angel (I) Milen Gateshki (OP) Boris Shivachev (OP)	Session V (continued) 11:00-12 :20 Tonya Vitova (I) B. Mihailova (OP) Victor Ivanov (OP)	Session IX 10:50-12:10 Rossitza Pentcheva(I) Zara Cherkezova-Zheleva (OP) G. Avdeev (OP)
Lunch break	Lunch break	Closing remarks & Award for the best poster contribution by young scientists Rositsa Nikolova President of BCS 12:10 – 13:00
Session III 13:40-15:00 Ulrich Bismayer (I) Rossitsa. Titorenkova (OP) Tzanko. Doukov (OP)	Session VI 13:40-16:10 Biliana Gasharova (I) V. Karadjova (OP) Krassimir Garbev (I) Al. Karamanov (OP) Alaa Adam (OP) Aquachim (IT)	
Session IV 15:00-16:40 Maria Lalia-Kantouri (I) G. Gencheva (OP) L. Tzvetanova/T.Todorova (OP) Bas ter Mull, PANalytical (IT) Rofa/Rigaku (IT)		
Poster Session (snacks & drinks) Presenting <u>Odd</u> PS numbers 16:40-19:00	Poster Session (snacks & drinks) Presenting <u>Even</u> PS numbers 16:50-19:00	
Annual meeting of the Bulgarian Crystallographic Society 19:00-19:30		Legend: PL: Plenary Lecture, I: Invited Speaker, OP: Oral presentation, IT: Industrial talk PS: Poster session

SYMPOSIUM PROGRAM

Thursday 25 September

8:00 **Registration**

9:00–9:30 **Opening ceremony**

Chairing: Irena Mihaylova

Welcome address from **Mitko Georgiev**,
Rector of the University of Chemical Technology and Metallurgy

Introductory remarks by **Mois Aroyo**
Universidad del Pais Vasco, Bilbao, Spain

Welcome address by **Dr. Todor Chobanov**, deputy mayor of Sofia

Welcome musical performance

Session I **Chairing: Rositsa Nikolova**

9:30–10:10 **J. Manuel Perez-Mato* (invited)**, B. Kocsis, E. Tasci, M. Aroyo
** Dept. de Fisica de la Materia Condensada, Facultad de Ciencia y
Tecnologia, Universidad del Pais Vasco (UPV-EHU), Bilbao, Spain*
Single mode signature in distorted phases revealed by symmetry-mode analysis

10:10–10:30 **Vesselin Tonchev**
Institute of Physical Chemistry, Bulgarian Academy of Sciences
Transitions between regimes of new phase growth kinetics; illustration with
growth of equally-sized crystals

10:30–11:00 *Symposium Participants Photo*
Coffee break

Session II **Chairing: Ognyan Petrov**

11:00–11:40 **Ross J. Angel (invited)**
Department of Geosciences, University of Padova, Padova, Italy
In-situ high-pressure X-ray diffraction in materials and mineral science

11:40–12:00 **Milen Gateshki**, Th. Degen, Th. Dortmann
HighScore Plus: crystallography and more

12:00–12:20 H. Sbirikova and **Boris Shivachev**
Institute of Mineralogy and Crystallography, Bulgarian Academy of Sciences
Specifics of nucleic acid crystallization for diffraction experiments

12:20–13:40 **Lunch break**

Session III **Chairing: Thomas Kerestedjian**

13:40–14:20 **Ulrich Bismayer (invited)**
Fachbereich Geowissenschaften, Universität Hamburg, Germany
Interfaces in ferroic and non-ferroic systems

14:20–14:40 **Rossitsa Titorenkova***, B. Mihailova, G. Jegova, M. Rashkova
* *Institute of Mineralogy and Crystallography, Bulgarian Academy of Sciences*
Raman scattering and IR reflection micro-spectroscopic study of human teeth treated with ER:YAG dental laser

14:40–15:00 **Tzanko Doukov**
representing the SSRL structural biology team
Stanford Synchrotron Radiation Lightsource, SLAC, USA Remote Data Collection at the Stanford Synchrotron Radiation Lightsource

Session IV Chairing: Boris Shivachev

15:00–15:40 **Maria Lalia-Kantouri (invited)**, A. Zianna, M. S. Ristic, A. Hatzidimitriou
Laboratory of Inorganic Chemistry, Department of Chemistry, Aristotle University of Thessaloniki, Greece
Cadmium(II) complexes of salicylaldehydes, in the presence or absence of α -diimines

15:40–16:00 **Galina Gencheva**
Faculty of Chemistry and Pharmacy, Sofia University "St. Kliment Ohridski"
New insights for the design of ruthenium antitumor agents – amino-coordinated Ru(II) and Ru(IV) complexes of 3-amino-2-chloropyridine

16:00–16:20 **Totka Todorova, Yu. Kalvachev, V. Valtchev & Lilya Tsvetanova**, S. Ferdov, B. Shivachev, R. Nikolova
Institute of Mineralogy and Crystallography - BAS, Sofia, Bulgaria
Crystal structures of ion exchanged ETS-4 & Synthesis of mordenite type zeolite without organic template

16:20–16:30 **Bas ter Mull** (Industrial Talk)
PANalytical
Empyrean, the comprehensive platform for X-ray diffraction

16:30–16:40 Industrial Talk
Rofa-Rigaku

16:40–19:00 **Welcome party and Poster Session I (odd numbered posters) – Library of UCTM**

19:00–19:30 **Annual meeting of the Bulgarian Crystallographic Society**

Friday 26 September

9:00–9:50 **Chairing: Rositsa Nikolova**
Open public talk (in Bulgarian): **Prof. Georgi Kirov (invited)**
Faculty of Geology and Geography, Sofia University "St. Kl. Ohridski"
Бележки върху развитието на кристалографията в България

Session V Chairing: Daniela Kovacheva

9:50–10:30 **Joerg Rothe, (invited)**
Karlsruhe Institute of Technology, Institute for Nuclear Waste Disposal (KIT-INE), Karlsruhe, Germany
X-ray absorption fine structure spectroscopy (XAFS) with synchrotron radiation – an introduction

- 10:30–11:00 **Coffee break**
- 11:00–11:40 **Tonya Vitova (invited)**
Karlsruhe Institute of Technology (KIT), Karlsruhe, Germany
 High energy resolution X-ray absorption spectroscopy and inelastic X-ray scattering investigations of actinide and lanthanide materials
- 11:40–12:00 T. Vitova, S. Mangold, C. Paulmann, V. Marinova, M. Gospodinov,
Boriana Mihailova*
**FB Geowissenschaften, Universität Hamburg, Hamburg, Germany*
 Mesoscopic-scale atomic arrangements in Ru-doped perovskite-type relaxor ferroelectrics revealed by X-ray absorption spectroscopy
- 12:00–12:20 **Victor Ivanov**
Faculty of Physics, Sofia University "St. Kl. Ohridski"
 Crystallographic structure and vibrational modes of mercury telluride nanowires encapsulated in single walled carbon nanotubes
- 12:20–13:40 **Lunch break**
- Session VI Chairing: Galina Gencheva**
- 13:40–14:20 **Biliana Gasharova* (invited)**, Y.-L. Mathis, D. Moss, K. Garbev
** Institute for Photon Science and Synchrotron Radiation / ANKA synchrotron light source, Karlsruhe Institute of Technology, Karlsruhe, Germany*
 Synchrotron infrared microspectroscopy: basics and applications in mineralogy and materials science
- 14:20–14:40 **Veronika Karadjova***, M. Wildner, D. Manasieva, D. Stoilova
** Department of Inorganic Chemistry, University of Chemical Technology and Metallurgy, Sofia*
 Hydrogen bond strength in some beryllium compounds. Correlation between structural data and infrared spectra
- 14:40–15:20 **Krassimir Garbev* (invited)**, B. Gasharova, P. Stemmermann,
** Institute for Technical Chemistry, Karlsruhe Institute of Technology, Karlsruhe, Germany*
 New insights into the structure of cementitious materials
- 15:20–15:40 **Alexander Karamanov**
Institute of Physical Chemistry, Bulgarian Academy of Sciences
 Synthesis, structure and properties of innovative ceramics from industrial wastes
- 15:40–16:00 **Alaa Adam^{1,2}**, E. Lilov, P. Petkov
¹ *Physics Department, University of Chemical Technology and Metallurgy, Sofia;* ² *Physics Department, Faculty of Science, Sohag University, EGYPT*
 Structural and physicochemical properties of crystalline bismuth chalcogenides
- 16:00–16:10 **Industrial Talk**
Aquachim
 Particle size characterization instruments – innovative solutions from Beckman Coulter
- 16:10–18:30 **Poster Session II (even numbered posters) – Library of UCTM**

Saturday 27 September

Session VII *Chairing: Boriana Mihailova*

9:00–9:40 **Emre S. Tasci* (invited)**, S. Polad, T. Birol
* *Physics Department, Middle East Technical University, Ankara, Turkey*
Hunting for multiferroics via DFT modelling

9:40–10:00 **Thomas Kerestedjian**
Institute of Geology, Bulgarian Academy of Sciences
Match-2: Single and mixed phase identification from XRD data

10:00–10:20 **Diana Nihtianova***, L. Mihaylov, P. Tzvetkov, P. Markov, A. Yordanova, I. Koseva, V. Nikolov
* *Institute of Mineralogy and Crystallography, Bulgarian Academy of Sciences*
Characterization of nanosized $\text{Al}_{2-x}\text{Sc}_x(\text{WO}_4)_3$ solid solutions by transmission electron microscopy (SAED, HRTEM, XEDS)

10:20–10:50 **Coffee break**

Session VIII *Chairing: Daniela Karashanova*

10:50–11:30 **Rositsa Pentcheva (invited)**
Theoretical Physics, Faculty of Physics, University of Duisburg-Essen, Germany
Mechanisms of electronic reconstruction at oxide interfaces: Insights from DFT+U calculations

11:30–11:50 **Zara Cherkezova-Zheleva**
Institute of Catalysis, Bulgarian Academy of Sciences
Preparation of improved and nanodimensional catalytic materials by mechanochemical method

11:50–12:10 **Georgi Avdeev**
Institute of Physical Chemistry, Bulgarian Academy of Sciences
Institute of Physical Chemistry, Bulgarian Academy of Sciences
Високотехнологична лаборатория за специализирани рентгенови методи и томография за развитие на еко- и енергоспестяващи технологии и технологии, свързани със здравето

12:30–13:00 Award for the best poster contribution by young scientists
Closing remarks, Rositsa Nikolova, President of BCS

Poster Session

- P_1. M. Abdallah, N. Velikova, Y. Ivanova, Y. Dimitriev – Synthesis and characterization of poly sulfide-functionalized hybrid mesoporous silica
- P_2. B. Angelov, A. Angelova, S. K. Filippov, M. Drechsler, P. Štěpánek, S. Lesieur – Time resolved X-ray scattering of protein loaded lipid nanoparticle
- P_3. V. Angelov, E. Ivanov, R. Kotsilkova – The chemical composition and structure of three phase epoxy/organoclay/gold nanocomposites
- P_4. Z. A. Babakhanova, M. Kh. Aripova, J. Aripov – Studying the structure of quartz-graphite schists using SEM analysis
- P_5. B. Barbov, Yu. Kalvachev – Synthesis of Beta zeolites in the presence of seeds

- P_6. I. Bineva, T. Hristova-Vassileva, B. Pejova, D. Nesheva, Z. Levi, Z. Aneva – AFM and XRD Study on the recrystallization of nanocrystalline $\text{Zn}_x\text{Cd}_{1-x}\text{Se}$ thin films
- P_7. S. Chakarova, P. Gorolomova, B. Krebs, G. Momekov, G. Gencheva – Stabilization of higher oxidation states of platinum by coordination with flexible N,O,N-ligand dipyrindin-2-ylmethanone and rigid N,N-ligand pyridine-2-amine – synthesis, crystal structure and cytotoxicity
- P_8. I. Dakova, V. Dakov, I. Karadjova – Cu(II)-imprinted copolymer microparticles: synthesis, characterization and application for selective solid phase extraction of copper ions
- P_9. S. Dencheva, G. Kirov – Crystal morphology of simonkolleite ($\text{Zn}_9(\text{OH})_8\text{Cl}_2(\text{H}_2\text{O})$): A SEM study
- P_10. M. Dimitrov, R. Ivanova, V. Štengl, J. Henych, T. Tsoncheva – Optimization of $\text{CeO}_2\text{-ZrO}_2$ mixed oxide catalysts for ethyl acetate combustion
- P_11. S. Dimitrovska-Lazova, S. Aleksovska, P. Tzvetkov, V. Mirčeski, D. Kovacheva – Influence of Y-ion substitution on structural and electrochemical characteristics of $\text{YCo}_{0.5}\text{Fe}_{0.5}\text{O}_3$
- P_12. S. Dimova, K. Zaharieva, C. Jossifov, V. Sinigersky, Z. Cherkezova-Zheleva, B. Kunev, I. Mitov – Copolymerization of benzil with styrene in the presence of transition metal catalyst
- P_13. V. Divarova, K. Stojnova, P. Racheva, V. Lekova, A. Dimitrov – Extraction-spectrophotometric study of ion-association complex of cobalt(II)-4-(2-thiazolylazo)resorzinol with 2-(4-iodophenyl)-3-(4-nitrophenyl)-5-phenyl-2H-tetrazolium chloride
- P_14. L. Dimowa, I. Piroeva, S. Atanasova-Vladimirova, B. Shivachev, S. Petrov – Heulandite ion-exchange under identical conditions, comparison of results for various cations: Na^+ , K^+ , Mg^{2+} , and Ca^{2+}
- P_15. L. Djerahov, P. Vasileva, I. Karadjova, I. Dakova, R. M. Kurakalva – Silver nanoparticles embedded in biocompatible polymers: comparative study of extraction efficiency toward toxic metals
- P_16. N. I. Dodoff, N. G. Vassilev, R. P. Nikolova, O. E. Petrov, M. Lalia-Kantouri, V. Miletic, D. N. Kushev, M. D. Apostolova – Structural, spectroscopic and quantum-chemical studies of potentially cytostatic Pt(II) and Pt(IV) complexes of N-3-pyridinylmethanesulfonamide
- P_17. B. Donkova, V. Petkova – Comparison between thermal behaviour of $\gamma\text{-MnC}_2\text{O}_4\cdot 2\text{H}_2\text{O}$ in oxidative and inert media
- P_18. L. T. Dimowa, V. M. Dylulgerov, R. P. Nikolova, B. L. Shivachev – Carboxy phenylboronic acid potential template for isostructural MOFs of terephthalic acid
- P_19. V. M. Dylulgerov, L. T. Dimowa, K. Kossev, R. P. Nikolova, B. L. Shivachev – N,N'-(ethane-1,2-diyl) diformamide – Catalytic effect of 3-carboxyphenylboronic acid, cadmium acetate and theophylline
- P_20. S. M. Gechev, O. H. Vitov, J. T. Mouhovski – Growing simultaneously laser grade monocrystals of $(\text{Yb}^{3+}, \text{Na}^+): \text{CaF}_2$ & $(\text{Yb}^{3+}, \text{Na}^+): \text{Ca}_{1-x}\text{Sr}_x\text{F}_2$
- P_21. R. Gegova, A. Bachvarova-Nedelcheva, R. Iordanova, Y. Dimitriev – Synthesis and crystallization of gels in the $\text{TeO}_2\text{-TiO}_2\text{-ZnO}$ system
- P_22. Zh. Georgieva, A. Ugrinov, R. Petrova, B. Shivachev, S. Zareva, S. Varbanov, T. Tosheva, G. Gencheva – Synthesis, single-crystal structure and spectroscopic characterization of copper(II) complexes with bis((dimethylphosphinyl)methyl)amine
- P_23. D. Goranova, R. Rashkov, A. Kolevski, V. Tonchev – Ahead-Aside Aggregation (AAA) model: Towards modelling the electrodeposition of Ni–Cu alloys
- P_24. P. Gorolomova, B. Krebs, R. Petrova, B. Shivachev, S. Simova, G. Momekov, G. Gencheva – Structure, spectroscopic properties and *in vitro* antiproliferative effects of new Au^{III} complexes with dipyrindin-2-ylamine
- P_25. K. Hegetschweiler, V. Velcheva, A. Ugrinov, G. Momekov, G. Gencheva – Synthesis, structural characterization and *in-vitro* antiproliferative effects of octahedral platinum(IV) complexes with 1,3,5-triamino-1,3,5-trideoxy-cis-inositol
- P_26. Mohamed M. Ibrahim – Spectroscopic and kinetic studies of mixed ligand complexes of bipyridyl and glycine as intercalators and their behaviors as antioxidants
- P_27. Vi. Ivanova, A. Stoilova, Y. Trifonova, P. Petkov – Comparative analysis of some physico-chemical properties of the glassy systems $(\text{GeSe}_5)_{100-x}\text{In}_x$ and $(\text{GeTe}_2)_{100-x}\text{In}_x$
- P_28. N. Kaneva, A. Bojinova, K. Papazova – Aging effects on the structural and photocatalytic properties of ZnO sol-gel films for degradation of pharmaceutical drugs
- P_29. N. Kaneva, G. Lazarova, A. Bojinova, K. Papazova, D. Dimitrov – Effect of thickness on the photocatalytic properties of ZnO thin films
- P_30. V. Karadjova, M. Wildner, D. Manasieva, D. Stoilova – Hydrogen bond strength in some berillium compounds. Correlation between structural data and infrared spectra
- P_31. K. Koleva, N. Velinov, T. Tsoncheva, I. Mitov – Preparation, structure and catalytic properties of copper-zinc ferrites

- P_32. K. Kossev, N. Petrova, R. Nikolova, B. Shivachev – Crystal structure and properties of carbamide and thiocarbamide adducts of tetrabutyl ammonium hydrogen sulphate
- P_33. R. I. Kostov – Crystallography of the polyhedron, enantiomorphism and a five-fold symmetry code in Durer's "Melencolia I"
- P_34. B. Kostova, V. Petkova, M. Shopska, G. Kadinov, M. Baláz, P. Baláz – Influence of high energy milling activation on nano-to-micro-sized CaCO_3 crystals formation
- P_35. N. G. Kostova, M. Achimovičová, A. Eliyas, N. Velinov, V. Blaskov, I. Stambolova, P. Baláz – TiO_2 obtained from mechanically activated ilmenite ore and its photocatalytic properties
- P_36. Y. Kouzmanova, I. Dimitrova, G. Gentsheva, L. Aleksandrov, D. Kovacheva – Comparative study of the phase formation and interaction with water of calcium-silicate cements for dental applications
- P_37. L. Krasteva, N. Kaneva, A. Bojinova, K. Papazova, D. Dimitrov – Fe-doped ZnO thin films prepared by sol-gel methods, gas sensing and photocatalytic properties
- P_38. M. Kuneva, S. Tonchev – Proton exchanged layers in LiNbO_3 and LiTaO_3 : Characterization by ir spectra deconvolution
- P_39. Ts. Lazarova, D. Kovacheva, S. Aleksovska – Determination of the oxidation state of the B-cations in the structure of complex perovskite
- P_40. V. Lilova, E. Lilov, N. Nikiforov – IR study of lead-borate composites containing PbMoO_4 nanoparticles
- P_41. D. Marinkova, M. Michel, R. Raykova, L. Yotova, P. Griesmar – Proliferation of gram negative cells onto nanohybride sol-gel carriers
- P_42. P. Markov, S. Stanchovska, S. Harizanova, D. Nihtianova, E. Zhecheva, R. Stoyanova – TEM studies of local metal distribution in palladium doped $\text{LaCo}_{0.8}\text{Ni}_{0.1}\text{Fe}_{0.1}\text{O}_3$ perovskites
- P_43. A. Mazhdrakova, R. Harizanova, C. Bocker, G. Avdeev, I. Gugov, C. Rüssel – BaTiO_3 glass-ceramics: crystal growth and microstructure
- P_44. I. Mihailova, L. Radev, V. Aleksandrova, I. Colova, I. M. M. Salgado, M. H. V. Fernandes – Effect of phase composition on the in vitro bioactivity of glass-ceramics in the CaO-MgO-SiO_2 system
- P_45. K. Milenova, A. Eliyas, V. Blaskov, I. Avramova, I. Stambolova, S. Vassilev, P. Nikolov, N. Kasabova, S. Rakovsky – Comparative study of ZnO samples prepared by different methods
- P_46. K. Milenova, A. Eliyas, V. Blaskov, I. Avramova, I. Stambolova, S. Vassilev, P. Nikolov, Y. Karakirova, N. Kasabova, S. Rakovsky – Copper doped zinc oxide nanopowders used for degradation of residual AZO dyes in wastewaters
- P_47. Nasser Y. Mostafa, B. El-Deeb – Biosynthesized of smart gold nanoparticles: pH-induced reversible aggregation and Plasmon coupling
- P_48. G. Patronov, I. Kostova, D. Tonchev, Z. Stoeva – Influence of the content of samarium on the structure and the optical properties of zinc borophosphate materials
- P_49. R. Petkov, L. Atanasov, R. Gavrilova – Investigation of the possibility to increase the mechanical properties of ferritic nodular cast iron
- P_50. P. Petkova, P. Vasilev, M. Mustafa – Calculation of the refractive index of $\text{Bi}_{12}\text{SiO}_{20}:\text{Mn}$
- P_51. P. Petkova, P. Vasilev, M. Mustafa, R. Mimouni – Fermi energy and Urbach's rule of Ni doped Mn_3O_4 thin films
- P_52. V. Petrov, S. Terzieva, V. Tumbalev, V. Mikli, L. Andreeva, A. Stoyanova-Ivanova – Influence of treatment process on the surface and chemical composition of the thermally activated orthodontic archwires
- P_53. A. A. Petrova, S. M. Angelova, I. A. Nikolchina, V. B. Kurteva, B. L. Shivachev, R. N. Petrova – A novel 13-membered cyclic polyfunctional scaffold – synthesis and solution and solid state characterization
- P_54. V. Petrunov, L. Andreeva, S. Karatodorov, V. Mihailov, S. Terzieva, A. Stoyanova-Ivanova, V. Tumbalev, V. Mikli – Analysis of elemental composition of a variable force 3 orthodontic archwire
- P_55. I. Pronin, N. Yakushova, I. Averin, N. Kaneva, A. Bojinova, K. Papazova, D. Dimitrov – Obtaining oxide materials by alkoxide technology method
- P_56. E. Serafimova, V. Petkova, Y. Pelovsky, B. Kostova – Spectroscopic analysis of nitric-acid treated mixtures on the base of biomass and chicken litter
- P_57. A. Shalaby, D. Nihtianova, P. Markov, A. Staneva, L. Aleksandrov, R. Iordanova, Y. Dimitriev – Structural analysis of RGO and RGO/ SiO_2 nanocomposite by transmission electron microscopy
- P_58. M. Shopska, D. Paneva, G. Kadinov, Z. Cherkezova-Zheleva, I. Mitov – Composition and catalytic behaviour of biogenic iron containing material obtained by *Leptothrix* bacteria cultivation in adler's growth medium
- P_59. S. Siuleiman, D. Raichev, A. Bojinova, D. Dimitrov, K. Papazova – Degradation of the commercial colorant Orange II by nanocomposite photocatalysts based on $\text{TiO}_2\text{-ZnO}$ powders
- P_60. Ts. Stanimirova, Z. Delcheva – Structural prerequisites for cationic Cu-Zn isomorphism in Cu, Zn hydroxy-sulphate minerals

- P_61. A. Stoilova, Y. Trifonova, V. Ivanova – Compositional dependence of the optical properties of the $\text{GeTe}_3\text{-In}$ glasses
- P_62. A. Stoyanova-Ivanova, S. Terzieva, G. Ivanova, M. Mladenov, D. Kovacheva, R. Raicheff, S. Georgieva, B. Blagoev, A. Zaleski, V. Mikli – The use of high-temperature superconducting cuprate as a dopant to the negative electrode in Ni-Zn batteries
- P_63. A. Stoyanova, N. Ivanova, A. Bachvarova-Nedelcheva, R. Iordanova – Synthesis and photocatalytic activity of Fe and N-doped TiO_2
- P_64. V. Stoyanov, B. Kostova, E. Serafimova, V. Petkova – Effects of marble on phase formation in self-compacting type decorative cement composites
- P_65. E. Todorova, G. Chernev, S. Djambazov – Sol-gel silica hybrid materials applicable for external treatment of concrete defects
- P_66. M. Todorova, R. Bakalska, T. Kolev – Structural characterization of new merocyanine dye 4-[(E)-2-[4-(dimethylamino)naphtalen-1-yl]ethenyl]-1-pentylquinolinium bromide dihydrate
- P_67. S. Todorova, G. Gencheva, V. Kurteva, S. Simova, B. Shivachev, R. Petrova – A novel N,O-containing polydentate ligand and its palladium complex – a structural study
- P_68. T. Todorova, Yu. Kalvachev, V. Valtchev – Synthesis of mordenite type zeolite without organic template
- P_69. I. Tomov, S. Vassilev – Nullifying the extinction effect by reforming the extinction corrections
- P_70. D. Tsekova, Y. Zhelyazkova, R. Petrova, B. Shivachev, N. Vassilev, P. Gorolomova, S. Varbanov, T. Tosheva, G. Gencheva – A series of Zn^{2+} complexes of 1,2-bis(dimethylphosphinyl)methylenoxy) benzene ligand – synthesis, structural characterization and solution chemistry
- P_71. T. Tsoncheva, I. Genova, N. Scotti, M. Dimitrov, V. Dal Santo, D. Kovacheva, N. Ravasio – Silica supported copper and cobalt oxide catalysts for methanol decomposition: Effect of preparation procedure
- P_72. L. Tsvetanova, S. Ferdov, B. Shivachev, R. Nikolova – Crystal structures of ion exchanged ETS-4
- P_73. M. Tsvetkov, K. Zaharieva, Z. Cherkezova-Zheleva, M. Milanova, I. Mitov – Photocatalytic activity of nanostructure zinc ferrite-type catalysts in degradation of malachite green under UV-light
- P_74. Y. Tzvetanova, B. Shivachev, O. Petrov – Quantitative phase analysis of skarn rocks using Rietveld-based XRD method
- P_75. P. Tzvetkov, I. Koseva, L. Dimova, V. Nikolov, D. Kovacheva – Crystal structure of $\text{In}_2(\text{WO}_4)_3$ and high-temperature phase transitions in the series $\text{Al}_{2-x}\text{In}_x(\text{WO}_4)_3$
- P_76. S. Veleva, R. Angelova, L. Stoyanov, V. Grudeva, D. Kovacheva, M. Mladenov, N. Boshkov, D. Karashanova, R. Raicheff – Preparation and supercapacitive properties of biogenic and synthetic $\alpha\text{-Fe}_2\text{O}_3$ /active carbon nanocomposites
- P_77. N. Velikova, Y. Vueva, P. Vassileva, A. Datcheva, R. Georgieva, Y. Ivanova – Thiol-amine functionalized mesoporous silica based hybrid materials
- P_78. L. Vladislavova, R. Harizanova, C. Bocker, G. Avdeev, M. Abrashev, I. Gugov, C. Rüssel – BaTiO_3 crystallization from multicomponent oxide glasses – phase composition and microstructure investigation
- P_79. S. Yaneva, A. Hassaan, L. Yotova – Design of optical biosensors for detection of pharmaceutical products
- P_80. A. Yoleva, S. Djambazov, P. Djambazov – Study of medieval ceramics excavated at the Monastery of Karaachteke (Varna, Bulgaria)
- P_81. I. Yordanova, A. Ganguly, H. Kolev, S. Mondal, A. Naydenov, M. Shopka, Z. Cherkezova-Zheleva, N. Velinov, A.K. Ganguli, S. Todorova – Nano-oxides with controlled size modified with Pd for purification processes
- P_82. K. Zaharieva, K. Milenova, Z. Cherkezova-Zheleva, A. Eliyas, I. Mitov – Photocatalytic activities of nanodimensional cobalt-ferrite type of powders in the degradation of reactive BLACK 5 dye
- P_83. K. Zaharieva, Z. Cherkezova-Zheleva, B. Kunev, I. Mitov – Impact of chemical composition on preparation of nanodimensional spinel ferrites
- P_84. T. Apostolova – Intensity and SAR dependent changes in conformation of frog skeletal muscle total protein content after irradiation with 2.45 GHz electromagnetic field
- P_85. T. Malakova, K. Krezhov – Neutron powder diffraction investigation of a half hole-doped bismuth-based manganite
- P_86. V. G. Ivanov, J. Sloan, D. C. Smith, E. Faulques – Crystallographic structure and vibrational modes of mercury telluride nanowires encapsulated in single walled carbon nanotubes
- P_87. K. Kossev, R. Nikolova, B. Shivachev – Synthesis and crystal structure of magnesium chloride ureates

Speaker Information

IT and AV provision in “Asen Zlatarov” hall

Presenters are advised that the session room will be equipped with the following IT and AV equipment:

- Laptop PC connected to audio speakers
- Data projector and screen
- Microphones (two)

All presenters are responsible for ensuring that their presentation is compatible with the conference software (Powerpoint, AdobeAcrobar reader). The symposia helpdesk will be able to provide assistance if required.

However, all efforts should be made to convert files to comply with the following specifications in advance.

The following software will be provided:

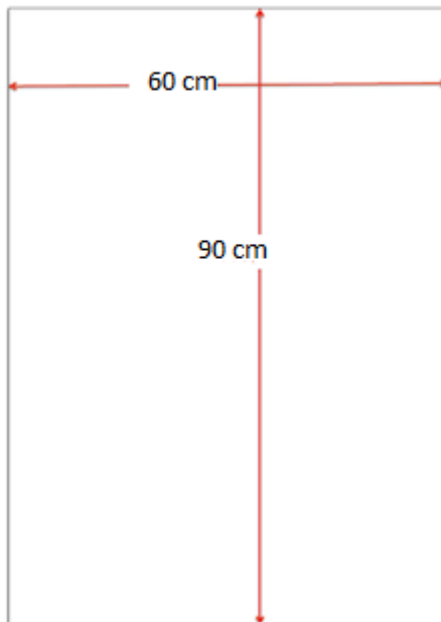
- **Windows 7 OS**
- **PowerPoint 2013 (Microsoft office 2013)**
- **Adobe Acrobat Reader**
- **Windows Media Player**
- **Internet browser (IE10, Firefox Mozilla).**

Installation of additional software may be requested by presenters in advance but only if it is freeware, demo version or is available for UCTM or partnering institutions use. IT/AV technicians will be available to assist session chairing and presenters on request.

Poster information

The poster exhibit hall (UCTM Library) will be open for setup on Thursday 25 at 10:30. Posters will remain on display at all times and must be removed by Saturday 27 at 11:30.

- Odd numbered posters will be presented on Thursday 25 and even numbered posters on Friday 26 (see poster sessions in program).
- Display boards will be numbered.
- Magnetic sticky holders will be provided (do not use any other material).
- Posters will be presented vertically (Portrait format with, preferred maximum size of 60 x 90 cm



CONTENTS

In-situ high-pressure X-ray diffraction in materials and mineral science	15
<i>R. J. Angel</i>	
Interfaces in ferroic and non-ferroic systems.....	16
<i>U. Bismayer</i>	
New insights into the structure of cementitious materials	17
<i>K. Garbev, B. Gasharova, P. Stemmermann</i>	
Synchrotron infrared microspectroscopy: Basics and applications in mineralogy and materials science	18
<i>B. Gasharova, Y.-L. Mathis, D. Moss, K. Garbev</i>	
Cadmium(ii) complexes of salicylaldehydes, in the presence or absence of α -diimines.....	19
<i>M. Lalia-Kantouri, A. Zianna, M. S. Ristovic, A. Hatzidimitriou</i>	
Mechanisms of electronic reconstruction at oxide interfaces: Insights from DFT+U calculations.....	21
<i>R. Pentcheva</i>	
Single-mode signature in distorted phases revealed by symmetry-mode analysis.....	22
<i>J. M. Perez-Mato, B. Kocsis, E. Tasci, M. Aroyo</i>	
X-ray absorption fine structure spectroscopy (XAFS) with synchrotron radiation – an introduction	23
<i>J. Rothe</i>	
Hunting for multiferroics via DFT modelling.....	24
<i>E. S. Tasci, S. Polad, T. Biroi</i>	
High energy resolution X-ray absorption spectroscopy and inelastic X-ray scattering investigations of actinide and lanthanide materials	25
<i>T. Vitova</i>	
Synthesis and characterization of poly sulfide-functionalized hybrid mesoporous silica.....	26
<i>M. Abdallah, N. Velikova, Y. Ivanova, Y. Dimitriev</i>	
Structural and physicochemical properties of crystalline bismuth chalcogenides	27
<i>A. M. Adam, E. Lilov, P. Petkov</i>	
Time resolved X-ray scattering of protein loaded lipid nanoparticles	27
<i>B. Angelov, A. Angelova, S. K. Filippov, M. Drechsler, P. Štěpánek, S. Lesieur</i>	
The chemical composition and structure of three phase epoxy/organoclay/gold nanocomposites.....	28
<i>V. Angelov, E. Ivanov, R. Kotsilkova</i>	
Biocompatible glass ceramic materials	29
<i>M. Kh. Aripova, R. V. Mkrtchyan, T. O. Nam</i>	
Studying the structure of quartz-graphite schists using SEM analysis.....	30
<i>Z. A. Babakhanova, M. Kh. Aripova, J. Aripov</i>	
Synthesis of Beta zeolites in the presence of seeds	31
<i>B. Barbov, Yu. Kalvachev</i>	
AFM and XRD study on the recrystallization of nanocrystalline $\text{Zn}_x\text{Cd}_{1-x}\text{Se}$ thin films	32
<i>I. Bineva, T. Hristova-Vassileva, B. Pejova, D. Nesheva, Z. Levi, Z. Aneva</i>	
Stabilization of higher oxidation states of platinum by coordination with flexible N,O,N-ligand dipyrindin-2-ylmethanone and rigid N,N-ligand pyridine-2-amine – synthesis, crystal structure and cytotoxicity	32
<i>S. Chakarova, P. Gorolomova, B. Krebs, G. Momekov, G. Gencheva</i>	
Cu(II)-imprinted copolymer microparticles: synthesis, characterization and application for selective solid phase extraction of copper ions	33
<i>I. Dakova, V. Dakov, I. Karadjova</i>	
Crystal morphology of simonkolleite ($\text{Zn}_5(\text{OH})_6\text{Cl}_2(\text{H}_2\text{O})$): A SEM study.....	34
<i>S. Dencheva, G. Kirov</i>	
Optimization of CeO_2 - ZrO_2 mixed oxide catalysts for ethyl acetate combustion	35
<i>M. Dimitrov, R. Ivanova, V. Štengl, J. Henych, T. Tsoncheva</i>	

Influence of Y-ion substitution on structural and electrochemical characteristics of $\text{YCo}_{0.5}\text{Fe}_{0.5}\text{O}_3$	36
<i>S. Dimitrovska-Lazova, S. Aleksavska, P. Tzvetkov, V. Mirčeski, D. Kovacheva</i>	
Copolymerization of benzil with styrene in the presence of transition metal catalyst.....	37
<i>S. Dimova, K. Zaharieva, C. Jossifov, V. Sinigersky, Z. Cherkezova-Zheleva, B. Kunev, I. Mitov</i>	
Heulandite ion-exchange under identical conditions, comparison of results for various cations: Na^+ , K^+ , Mg^{2+} , and Ca^{2+}	38
<i>L. Dimowa, I. Piroeva, S. Atanasova-Vladimirova, B. Shivachev, S. Petrov</i>	
Extraction-spectrophotometric study of ion-association complex of cobalt(II)–4–(2-thiazolylazo) resorzinol with 2–(4-iodophenyl)–3–(4-nitrophenyl)–5-phenyl-2H-tetrazolium chloride.....	39
<i>V. Divarova, K. Stojnova, P. Racheva, V. Lekova, A. Dimitrov</i>	
Silver nanoparticles embedded in biocompatible polymers: Comparative study of extraction efficiency toward toxic metals.....	40
<i>L. Djerahov, P. Vasileva, I. Karadjova, I. Dakova, R. M. Kurakalva</i>	
Structural, spectroscopic and quantum-chemical studies of potentially cytostatic Pt(II) and Pt(IV) complexes of <i>N</i> -3-pyridinylmethanesulfonamide	41
<i>N. I. Dodoff, N. G. Vassilev, R. P. Nikolova, O. E. Petrov, M. Lalia-Kantouri, V. Miletic, D. N. Kushev, M. D. Apostolova</i>	
Comparison between thermal behaviour of $\gamma\text{-MnC}_2\text{O}_4 \cdot 2\text{H}_2\text{O}$ in oxidative and inert media.....	42
<i>B. Donkova, V. Petkova</i>	
Remote data collection at the Stanford synchrotron radiation lightsource	43
<i>T. Doukov representing the SSRL structural biology team</i>	
<i>N,N'</i> -(ethane-1,2-diyl)diformamide – Catalytic effect of 3-carboxyphenylboronic acid, cadmium acetate and theophylline.....	44
<i>V. M. Dylgerov, L. T. Dimowa, K. Kossev, R. P. Nikolova, B. L. Shivachev</i>	
Carboxy phenylboronic acid potential template for isostructural MOFs of terephthalic acid	45
<i>L. T. Dimowa, V. M. Dylgerov, R. P. Nikolova, B. L. Shivachev</i>	
HighScore Plus: crystallography and more	46
<i>M. Gateshki, Th. Degen, Th. Dortmann</i>	
Intensity and SAR dependent changes in conformation of frog skeletal muscle total protein content after irradiation with 2.45 GHz electromagnetic field	46
<i>T. Apostolova</i>	
Growing simultaneously laser grade monocrystals of $(\text{Yb}^{3+}, \text{Na}^+): \text{CaF}_2$ & $(\text{Yb}^{3+}, \text{Na}^+): \text{Ca}_{1-x}\text{Sr}_x\text{F}_2$	47
<i>S. M. Gechev, O. H. Vitov, J. T. Mouhovski</i>	
Synthesis and crystallization of gels in the $\text{TeO}_2\text{--TiO}_2\text{--ZnO}$ system	48
<i>R. Gegova, A. Bachvarova-Nedelcheva, R. Iordanova, Y. Dimitriev</i>	
Synthesis, single-crystal structure and spectroscopic characterization of copper(II) complexes with bis((dimethylphosphinyl)methyl)amine.....	49
<i>Zh. Georgieva, A. Ugrinov, R. Petrova, B. Shivachev, S. Zareva, S. Varbanov, T. Tosheva, G. Gencheva</i>	
Ahead-Aside Aggregation (AAA) model: Towards modelling the electrodeposition of Ni–Cu alloys	50
<i>D. Goranova, R. Rashkov, A. Kolevski, V. Tonchev</i>	
Structure, spectroscopic properties and <i>in vitro</i> antiproliferative effects of new Au^{III} complexes with dipyridin-2-ylamine.....	51
<i>P. Gorolomova, B. Krebs, R. Petrova, B. Shivachev, S. Simova, G. Momekov, G. Gencheva</i>	
Synthesis, structural characterization and <i>in-vitro</i> antiproliferative effects of octahedral platinum(IV) complexes with 1,3,5-triamino-1,3,5-trideoxy-cis-inositol.....	52
<i>K. Hegetschweiler, V. Velcheva, A. Ugrinov, G. Momekov, G. Gencheva</i>	
Spectroscopic and kinetic studies of mixed ligand complexes of bipyridyl and glycine as intercalators and their behaviors as antioxidants	53
<i>Mohamed M. Ibrahim</i>	
Comparative analysis of some physico-chemical properties of the glassy systems $(\text{GeSe}_5)_{100-x}\text{In}_x$ and $(\text{GeTe}_5)_{100-x}\text{In}_x$	54
<i>Vi. Ivanova, A. Stoilova, Y. Trifonova, P. Petkov</i>	
Crystallographic structure and vibrational modes of mercury telluride nanowires encapsulated in single walled carbon nanotubes	55
<i>V. G. Ivanov, J. Sloan, D. C. Smith, E. Faulques</i>	

Aging effects on the structural and photocatalytic properties of ZnO sol-gel films for degradation of pharmaceutical drugs	56
<i>N. Kaneva, A. Bojinova, K. Papazova</i>	
Effect of thickness on the photocatalytic properties of ZnO thin films	57
<i>N. Kaneva, G. Lazarova, A. Bojinova, K. Papazova, D. Dimitrov</i>	
Hydrogen bond strength in some berillium compounds. correlation between structural data and infrared spectra.....	58
<i>V. Karadjova, M. Wildner, D. Manasieva, D. Stoilova</i>	
Synthesis, structure and properties of innovative ceramics from industrial wastes.....	59
<i>A. Karamanov</i>	
Preparation, structure and catalytic properties of copper-zinc ferrites	60
<i>K. Koleva, N. Velinov, T. Tsoncheva, I. Mitov</i>	
Crystal structure and properties of carbamide and thiocarbamide adducts of tetrabutyl ammonium hydrogen sulphate	61
<i>K. Kossev, N. Petrova, R. Nikolova, B. Shivachev</i>	
Crystallography of the polyhedron, enantiomorphism and a five-fold symmetry code in Durer's "Melencolia I"	62
<i>R. I. Kostov</i>	
Influence of high energy milling activation on nano-to-micro-sized CaCO_3 crystals formation.....	63
<i>B. Kostova, V. Petkova, M. Shopska, G. Kadinov, M. Baláz, P. Baláz</i>	
TiO_2 obtained from mechanically activated ilmenite ore and its photocatalytic properties	64
<i>N. G. Kostova, M. Achimovičová, A. Eliyas, N. Velinov, V. Blaskov, I. Stambolova, P. Baláz</i>	
Comparative study of the phase formation and interaction with water of calcium-silicate cements for dental applications	65
<i>Y. Kouzmanova, I. Dimitrova, G. Gentsheva, L. Aleksandrov, D. Kovacheva</i>	
Fe-doped ZnO thin films prepared by sol-gel methods, gas sensing and photocatalytic properties	66
<i>L. Krasteva, N. Kaneva, A. Bojinova, K. Papazova, D. Dimitrov</i>	
Proton exchanged layers in LiNbO_3 and LiTaO_3 : Characterization by ir spectra deconvolution.....	67
<i>M. Kuneva, S. Tonchev</i>	
Determination of the oxidation state of the B-cations in the structure of complex perovskite	68
<i>Ts. Lazarova, D. Kovacheva, S. Aleksovska</i>	
IR study of lead-borate composites containing PbMoO_4 nanoparticles.....	69
<i>V. Lilova, E. Lilov, N. Nikiforov</i>	
Proliferation of gram negative cells onto nanohybride sol-gel carriers	70
<i>D. Marinkova, M. Michel, R. Raykova, L. Yotova, P. Griesmar</i>	
TEM studies of local metal distribution in palladium doped $\text{LaCo}_{0.8}\text{Ni}_{0.1}\text{Fe}_{0.1}\text{O}_3$ perovskites	71
<i>P. Markov, S. Stanchovska, S. Harizanova, D. Nihtianova, E. Zhecheva, R. Stoyanova</i>	
BaTiO_3 glass-ceramics: crystal growth and microstructure	72
<i>A. Mazhdrakova, R. Harizanova, C. Bocker, G. Avdeev, I. Gugov, C. Rüssel</i>	
Effect of phase composition on the <i>in vitro</i> bioactivity of glass-ceramics in the CaO-MgO-SiO_2 system.....	73
<i>I. Mihailova, L. Radev, V. Aleksandrova, I. Colova, I. M. M. Salvado, M. H. V. Fernandes</i>	
Comparative study of ZnO samples prepared by different methods	74
<i>K. Milenova, A. Eliyas, V. Blaskov, I. Avramova, I. Stambolova, S. Vassilev, P. Nikolov, N. Kasabova, S. Rakovsky</i>	
Copper doped zinc oxide nanopowders used for degradation of residual AZO dyes in wastewaters.....	75
<i>K. Milenova, A. Eliyas, V. Blaskov, I. Avramova, I. Stambolova, S. Vassilev, P. Nikolov, Y. Karakirova, N. Kasabova, S. Rakovsky</i>	
New insights for the design of ruthenium antitumor agents – amino-coordinated Ru^{III} and Ru^{IV} complexes of 3-amino-2-chloropyridine.....	76
<i>G. Mirtcheva, R. Petrova, B. Shivachev, G. Momekov, G. Gencheva</i>	
Biosynthesized of smart gold nanoparticles: pH-induced reversible aggregation and Plasmon coupling.....	77
<i>Nasser Y. Mostafa, B. El-Deeb</i>	
Characterization of nanosized $\text{Al}_{2-x}\text{Sc}_x(\text{WO}_4)_3$ solid solutions by transmission electron microscopy (SAED, HRTEM, XEDS).....	78
<i>D. Nihtianova, L. Mihaylov, P. Tzvetkov, P. Markov, A. Yordanova, I. Koseva, V. Nikolov</i>	

Influence of the content of samarium on the structure and the optical properties of zinc borophosphate materials	79
<i>G. Patronov, I. Kostova, D. Tonchev, Z. Stoeva</i>	
Investigation of the possibility to increase the mechanical properties of ferritic nodular cast iron.....	80
<i>R. Petkov, L. Atanasov, R. Gavrilova</i>	
Calculation of the refractive index of $\text{Bi}_{12}\text{SiO}_{20}:\text{Mn}$	80
<i>P. Petkova, P. Vasilev, M. Mustafa</i>	
Fermi energy and Urbach's rule of Ni doped Mn_2O_4 thin films	81
<i>P. Petkova, P. Vasilev, M. Mustafa, R. Mimouni</i>	
Influence of treatment process on the surface and chemical composition of the thermally activated orthodontic archwires	82
<i>V. Petrov, S. Terzieva, V. Tumbalev, V. Mikli, L. Andreeva, A. Stoyanova-Ivanova</i>	
A novel 13-membered cyclic polyfunctional scaffold – synthesis and solution and solid state characterization	83
<i>A. A. Petrova, S. M. Angelova, I. A. Nikolchina, V. B. Kurteva, B. L. Shivachev, R. N. Petrova</i>	
Analysis of elemental composition of a variable force 3 orthodontic archwire	84
<i>V. Petrunov, L. Andreeva, S. Karatodorov, V. Mihailov, S. Terzieva, A. Stoyanova-Ivanova, V. Tumbalev, V. Mikli</i>	
Obtaining oxide materials by alkoxide technology method.....	85
<i>I. Pronin, N. Yakushova, I. Averin, N. Kaneva, A. Bojinova, K. Papazova, D. Dimitrov</i>	
Spectroscopic analysis of nitric-acid treated mixtures on the base of biomass and chicken litter.....	86
<i>E. Serafimova, V. Petkova, Y. Pelovsky, B. Kostova</i>	
Structural analysis of RGO and RGO/SiO_2 nanocomposite by transmission electron microscopy	87
<i>A. Shalaby, D. Nihianova, P. Markov, A. Staneva, L. Aleksandrov, R. Iordanova, Y. Dimitriev</i>	
Specifics of nucleic acid crystallization for diffraction experiments	88
<i>H. I. Sbirikova, B. L. Shivachev</i>	
Composition and catalytic behaviour of biogenic iron containing material obtained by <i>Leptothrix</i> bacteria cultivation in Adler's growth medium	89
<i>M. Shopska, D. Paneva, G. Kadinov, Z. Cherkezova-Zheleva, I. Mitov</i>	
Degradation of the commercial colorant Orange II by nanocomposite photocatalysts based on $\text{TiO}_2\text{-ZnO}$ powders.....	90
<i>S. Siuleiman, D. Raichev, A. Bojinova, D. Dimitrov, K. Papazova</i>	
Structural prerequisites for cationic Cu-Zn isomorphism in Cu, Zn hydroxy-sulphate minerals	91
<i>Ts. Stanimirova, Z. Delcheva</i>	
Compositional dependence of the optical properties of the $\text{GeTe}_3\text{-In}$ glasses	92
<i>A. Stoilova, Y. Trifonova, Vi. Ivanova</i>	
The use of high-temperature superconducting cuprate as a dopant to the negative electrode in Ni-Zn batteries	93
<i>A. Stoyanova-Ivanova, S. Terzieva, G. Ivanova, M. Mladenov, D. Kovacheva, R. Raicheff, S. Georgieva, B. Blagoev, A. Zaleski, V. Mikli</i>	
Synthesis and photocatalytic activity of Fe and N-doped TiO_2	94
<i>A. Stoyanova, N. Ivanova, A. Bachvarova-Nedelcheva, R. Iordanova</i>	
Effects of marble on phase formation in self-compacting type decorative cement composites	95
<i>V. Stoyanov, B. Kostova, E. Serafimova, V. Petkova</i>	
Raman scattering and IR reflection micro-spectroscopic study of human teeth treated with Er:YAG dental laser.....	96
<i>R. Titorenkova, B. Mihailova, G. Jegova, M. Rashkova</i>	
Sol-gel silica hybrid materials applicable for external treatment of concrete defects	97
<i>E. Todorova, G. Chernev, S. Djambazov</i>	
Structural characterization of new merocyanine dye 4-[(E)-2-[4-(dimethylamino)naphtalen-1-yl] ethenyl]-1-pentylquinolinium bromide dihydrate	98
<i>M. Todorova, R. Bakalska, T. Kolev</i>	
A novel N,O-containing polydentate ligand and its palladium complex – A structural study	99
<i>S. Todorova, G. Gencheva, V. Kurteva, S. Simova, B. Shivachev, R. Petrova</i>	

Synthesis of mordenite type zeolite without organic template.....	100
<i>T. Todorova, Yu. Kalvachev, V. Valtchev</i>	
Nullifying the extinction effect by reforming the extinction corrections.....	101
<i>I. Tomov, S. Vassilev</i>	
Transitions between regimes of new phase growth kinetics; illustration with growth of equally-sized crystals	102
<i>V. Tonchev</i>	
A series of Zn^{2+} complexes of 1,2-bis(dimethylphosphinylmethylenoxy)benzene ligand – synthesis, structural characterization and solution chemistry.....	103
<i>D. Tsekova, Y. Zhelyazkova, R. Petrova, B. Shivachev, N. Vassilev, P. Gorolomova, S. Varbanov, T. Tosheva, G. Gencheva</i>	
Silica supported copper and cobalt oxide catalysts for methanol decomposition: Effect of preparation procedure.....	104
<i>T. Tsoncheva, I. Genova, N. Scotti, M. Dimitrov, V. Dal Santo, D. Kovacheva, N. Ravasio</i>	
Crystal structures of ion exchanged ETS-4	105
<i>L. Tsvetanova, S. Ferdov, B. Shivachev, R. Nikolova</i>	
Photocatalytic activity of nanostructure zinc ferrite-type catalysts in degradation of malachite green under UV-light	106
<i>M. Tsvetkov, K. Zaharieva, Z. Cherkezova-Zheleva, M. Milanova, I. Mitov</i>	
Quantitative phase analysis of skarn rocks using Rietveld-based XRD method.....	107
<i>Y. Tzvetanova, B. Shivachev, O. Petrov</i>	
Crystal structure of $\text{In}_2(\text{WO}_4)_3$ and high-temperature phase transitions in the series $\text{Al}_{2-x}\text{In}_x(\text{WO}_4)_3$	108
<i>P. Tzvetkov, I. Koseva, L. Dimowa, V. Nikolov, D. Kovacheva</i>	
Preparation and supercapacitive properties of biogenic and syntetic $\alpha\text{-Fe}_2\text{O}_3$ /active carbon nanocomposites	109
<i>S. Veleva, R. Angelova, L. Stoyanov, V. Grudeva, D. Kovacheva, M. Mladenov, N. Boshkov, D. Karashanova, R. Raicheff</i>	
Thiol-amine functionalized mesoporous silica based hybrid materials.....	110
<i>N. Velikova, Y. Vueva, P. Vassileva, A. Detcheva, R. Georgieva, Y. Ivanova</i>	
Mesoscopic-scale atomic arrangements in Ru-doped perovskite-type relaxor ferroelectrics revealed by X-ray absorption spectroscopy	111
<i>T. Vitova, S. Mangold, C. Paulmann, V. Marinova, M. Gospodinov, B. Mihailova</i>	
BaTiO_3 crystallization from multicomponent oxide glasses – phase composition and microstructure investigation.....	112
<i>L. Vladislavova, R. Harizanova, C. Bocker, G. Avdeev, M. Abrashev, I. Gugov, C. Rüssel</i>	
Design of optical biosensors for detection of pharmaceutical products.....	113
<i>S. Yaneva, A. Hassaan, L. Yotova</i>	
Study of medieval ceramics excavated at the Monastery of Karaachteke (Varna, Bulgaria).....	114
<i>A. Yoleva, S. Djambazov, P. Djambazov</i>	
Nano-oxides with controlled size modified with Pd for purification processes.....	115
<i>I. Yordanova, A. Ganguly, H. Kolev, S. Mondal, A. Naydenov, M. Shopska, Z. Cherkezova-Zheleva, N. Velinov, A.K. Ganguli, S. Todorova</i>	
Photocatalytic activities of nanodimensional cobalt-ferrite type of powders in the degradation of reactive BLACK 5 dye	116
<i>K. Zaharieva, K. Milenova, Z. Cherkezova-Zheleva, A. Eliyas, I. Mitov</i>	
Impact of chemical composition on preparation of nanodimensional spinel ferrites.....	116
<i>K. Zaharieva, Z. Cherkezova-Zheleva, B. Kunev, I. Mitov</i>	
Preparation of improved and nanodimensional catalytic materials by mechanochemical method.....	117
<i>Z. Cherkezova-Zheleva</i>	
Neutron powder diffraction investigation of a half hole-doped bismuth-based manganite	117
<i>T. Malakova, K. Krezhov</i>	
Synthesis and crystal structure of magnesium chloride ureates	118
<i>K. Kossev, R. Nikolova, B. Shivachev</i>	

INVITED LECTURES

IN-SITU HIGH-PRESSURE X-RAY DIFFRACTION IN MATERIALS AND MINERAL SCIENCE

R. J. Angel*

Department of Geosciences, University of Padova, Via G. Gradenigo 6, 35131 Padova, Italy

Framework structures, built of relatively rigid atomic clusters, are of central importance to mineralogy, materials science, chemistry and physics. The perovskite structure, built of a framework of octahedra, is the most abundant mineral in the Earth and is also a key component of electronics because of the outstanding ferroelectric and relaxor electronic properties of certain compositions. Oxide perovskites are the mostly widely-used substrate material for electronics and perovskite thin films can exhibit exotic electronic and magnetic properties for memory devices. Metal-organic frameworks (MOFs) have recently been the focus of much chemical research for gas storage and the ability to control their catalytic properties by tailored synthesis to incorporate specific functional groups in to the frameworks. Zeolitic frameworks are the basis of the multi-billion euro industry in catalysis of petrochemicals.

High pressure studies of framework structures are valuable because they enable the various deformation mechanisms exhibited by the structures (tilting, polyhedral deformation, extra framework interaction, extra-framework exchange, and topology changes) to be separated and studied. Understanding these mechanisms separately contributes to the rational design of framework materials with specific properties. High-pressure single-crystal diffraction methods are now mature enough that they can be used routinely to determine the structural evolution of frameworks, especially by following the evolution of lattice parameters with pressure. I will review recent developments in methodologies in diffractometer control [1] and data analysis [2] that can be employed by any crystallography laboratory and show their application in recent studies of frameworks.

[1] R.J. Angel, L.W. Finger, J. Appl. Cryst., 44 (2011) 247.

[2] R.J. Angel et al., Z. Krist., 229 (2014) 405.

* E-mail: rossjohn.angel@unipd.it

Keywords: high-pressure, diffraction, frameworks, phase transitions.

INTERFACES IN FERROIC AND NON-FERROIC SYSTEMS

U. Bismayer*

*Fachbereich Geowissenschaften, Universität Hamburg,
Grindelallee 48, 20146 Hamburg, Germany*

Interfaces like twin boundaries or wall regions between amorphous and crystalline material are microstructures which occur in natural and synthetic solids on the nanoscale. Among such nanostructures are ferroic twin walls which develop as a consequence of phase transitions and crossed lamellar interfaces in bio-minerals. Individual interfaces can vary from thin walls extended over a few unit cells up to several thousand nm. Interfaces show distinct physical properties and influence the macroscopic materials properties essentially. Hence, functional properties may occur inside interfaces and not in the bulk of a device or functionality is determined by the composite. Examples of wall structures and their local features related with ferroic, non-ferroic and biomaterials will be given.

* E-mail: ubis@uni-hamburg.de

Keywords: twin walls, interfaces, ferroics, metamict minerals, biominerals.

NEW ISIGHTS INTO THE STRUCTURE OF CEMENTITIOUS MATERIALS

K. Garbev^{1,*}, B. Gasharova², P. Stemmermann¹

¹ *Institute for Technical Chemistry, Karlsruhe Institute of Technology,
P.O. Box 3640, 76021 Karlsruhe, Germany*

² *Institute for Photon Science and Synchrotron Radiation / ANKA synchrotron light source,
Karlsruhe Institute of Technology, P.O. Box 3640, 76021 Karlsruhe, Germany*

Cement is not only the technical material produced in the largest quantities by mankind, but also its demand is steadily increasing leading to a current growth rate of the cement production of 3% annually. The contribution of the manufacture of ordinary Portland cement (OPC) to the global CO₂ emissions increased correspondingly from 5% to 8% during the last decade. Because of the enormous impact on the society there is a great effort to reduce the atmospheric greenhouse gases in relation with the production of hydraulically reactive materials in the recent years. One example for a novel cementitious material with a reduced both CO₂-burden and energy demand by more than 50% is Celitement developed at Karlsruhe Institute of Technology (KIT). Celitement consists of previously unknown amorphous calcium-hydrosilicates. Just like OPC, they harden upon reaction with H₂O while forming amorphous calcium-silicate-hydrate (C-S-H) phases, which control to a large extend the physical properties of cement materials. The production of Celitement takes place in a two-stage process. First a precursor mainly consisting of C-S-H phases (crystalline and nanocrystalline) is synthesized during a hydrothermal process. In a further step the precursor is transformed into hydraulically reactive binding agents by means of tribochemical treatment.

Three main groups of compounds will be addressed in this talk: 1) Structural features of the X-ray amorphous calcium hydrosilicates (Celitement) based on spectroscopic methods will be discussed. 2) New insights into the structure of nanocrystalline C-S-H phases and their thermal behavior will be presented. 3) Examples of previously unknown phase transformations upon heating within the large group of crystalline C-S-H phases with various degrees of polymerization of the silicate tetrahedra will be shown.

* E-mail: krassimir.garbev@kit.edu

SYNCHROTRON INFRARED MICROSCOPY: BASICS AND APPLICATIONS IN MINERALOGY AND MATERIALS SCIENCE

B. Gasharova^{1,*}, Y.-L. Mathis¹, D. Moss¹, K. Garbev²

¹ *Institute for Photon Science and Synchrotron Radiation / ANKA synchrotron light source,
Karlsruhe Institute of Technology, P.O. Box 3640, 76021 Karlsruhe, Germany*

² *Institute for Technical Chemistry, Karlsruhe Institute of Technology, P.O. Box 3640,
76021 Karlsruhe, Germany*

Infrared microspectroscopy is a powerful technique for characterization of spatial variations in the crystallochemical composition of heterogeneous materials. This technique couples the high degree of chemical specificity of infrared spectroscopy with the microscale spatial resolution possible with modern infrared optics and sources. Microspectroscopy at high spatial resolution is traditionally one of the key areas of application for synchrotron infrared sources in the field of mineralogy and crystallography. It exploits the brilliance of synchrotron light sources (photon flux per unit source area into unit emission angle), which allows much higher measurement beam intensity through small sample areas compared to conventional infrared sources.

Two main points will be addressed in this presentation: (i) The infrared facilities for infrared micro and nanospectroscopy, and for research under extreme conditions at the ANKA synchrotron light source in Karlsruhe, Germany will be introduced and the advantages of synchrotron infrared light compared to conventional sources will be illustrated; (ii) Examples of mineralogical and crystallographic applications will be shown.

Acknowledgment: Research described in this paper was performed at ANKA, the synchrotron radiation facility at the Karlsruhe Institute of Technology (KIT). The authors gratefully acknowledge the excellent support by Michael Süpfle at the infrared beamlines.

* E-mail: gasharova@kit.edu

CADMIUM(II) COMPLEXES OF SALICYLALDEHYDES, IN THE PRESENCE OR ABSENCE OF α -diimines

M. Lalia-Kantouri*, A. Zianna, M. S. Ristovic, A. Hatzidimitriou

*Aristotle University of Thessaloniki, Department of Chemistry, Laboratory of Inorganic Chemistry,
Thessaloniki 54 124, Greece*

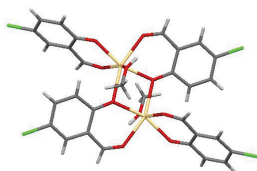
Introduction: The interaction of transition metal complexes with DNA has been in the center of scientific interest for many years, mainly due to their versatile applications in cancer research and nucleic acid chemistry. Cadmium is an extremely toxic element which is often present in the environment, also as a result of human activities. Therefore, an interesting area of research is to get compounds which are able to form stable complexes with cadmium, because they could be employed as detoxifying agents.

Aim: The aim of this work is to present a critical look at the coordination chemistry of some salicylaldehyde derivatives as ligands, in the presence or absence of α -diimines (bipy, phen, neoc, dpamH). Substituted salicylaldehydes are known to have versatility, regarding their binding modes and they may act as monodentate, bidentate or chelating ligands to the transition metals, and also possess antibacterial properties. Our group has been focused on the synthesis of metal complexes with salicylaldehydes and their interaction with DNA. Previous studies showed that Zinc (II) complexes with salicylaldehydes had interesting results concerning their interaction with DNA [1], while analogous Co(II) complexes in the presence of the base 2,2'-dipyridylamine showed anticancer activity [2]. For this respect, we prepared and characterized analogous compounds of Cd(II), while the investigation of their ability to bind to calf thymus DNA is in progress.

Synthesis: A methanolic solution of salicylaldehyde ligand (5-X-saloH), (deprotonated with CH_3ONa) was added to a methanolic solution of $\text{Cd}(\text{NO}_3)_2 \times 4\text{H}_2\text{O}$ in a 2:1 stoichiometric ratio at room temperature and afforded simple complexes formulated as $[\text{Cd}(5\text{-X-salo})_2(\text{CH}_3\text{OH})]_2$, where X = Cl or Br. If to the former solution 0.5 mmol of amine was added and the reaction mixture was heated at 50 °C and stirred for 1 h, yellow crystals suitable for X-ray structure determination were formed after few days. These compounds give different structures according to the α -diimines (bipy, phen, neoc, dpamH) used.

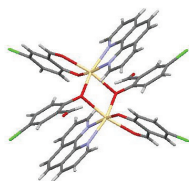
Characterization: The complexes were characterized physicochemically (elemental analysis, conductivity and magnetic susceptibility measurements) and spectroscopically (FT-IR, UV-Vis and $^1\text{H-NMR}$). The structure of the complexes was verified using single-crystal X-Ray diffraction analysis.

Crystal Structures: The simple compounds $[\text{Cd}(5\text{-Cl-salo})_2(\text{MeOH})]_2$ have dimeric structure with the salicylaldehyde ligand behaving in a normal bidentate manner through the phenolic and aldehyde oxygen atoms and also as a bridging ligand through the phenolic oxygen, connecting the two cadmium atoms in a distance of $\text{Cd} \cdots \text{Cd} = 3.482 \text{ \AA}$.

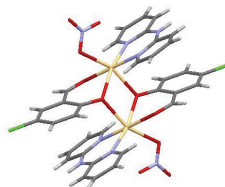


In the presence of the α -diimine, the mixed-ligand complexes retain their dimeric structure, with the exception of the complex $[\text{Cd}(5\text{-Br-salo})_2(\text{dpamH})]$, which is monomeric.

In the case of the amines = bipy or phen, the prepared complexes are formulated as dimeric: $[\text{Cd}(5\text{-X-salo})_2(\alpha\text{-diimine})]_2$, where the X = 5-Cl or 5-Br-salo ligands behave at the same time in both bidentate and monodentate coordination modes.



$[\text{Cd}(5\text{-Cl-salo})_2(\text{phen})]_2$



$[\text{Cd}(5\text{-Cl-salo})(\text{dpamH})(\text{ONO}_2)]_2$

In the case of the amines = neoc or dpamH, the prepared complexes are formulated as: $[\text{Cd}(5\text{-X-salo})(\alpha\text{-diimine})(\text{ONO}_2)]_2$, where the 5-Cl or 5-Br-salo ligands behave in their normal bidentate mode and also as bridging ligands, connecting the two cadmium atoms in a distance of $\text{Cd}\cdots\text{Cd} = 3.642 \text{ \AA}$. The nitrate anion is coordinated as monodentate ligand through one oxygen atom, while the α -diimine as neutral bidentate ligand in all cases.

- [1] A. Zianna, G. Psomas, A. Hatzidimitriou, E. Coutouli-Argyropoulou, M. Lalia-Kantouri, J. Inorg. Biochem., 127 (2013) 116.
- [2] M. Lalia-Kantouri, M. Gdaniec, T. Choli-Papadopoulou, A. Badounas, Ch. D. Papadopoulos, A. Czapiak, G. D. Geromichalos, D. Sahpazidou, F. Tsitouroudi, J. Inorg. Biochem., 117 (2012) 25.

* E-mail: lalia@chem.auth.gr

MECHANISMS OF ELECTRONIC RECONSTRUCTION AT OXIDE INTERFACES: INSIGHTS FROM DFT+U CALCUALTIONS

R. Pentcheva

Theoretical Physics, Faculty of Physics, University of Duisburg-Essen, Germany

Oxide interfaces exhibit a broad spectrum of functional properties that are not available in the respective bulk compounds, such as two-dimensional conductivity, superconductivity and magnetism. In this talk I will compare the mechanisms of electronic and orbital reconstruction in oxide quantum wells with (001) and (111) crystallographic orientation. The latter promise to host even more exotic electronic states compared to the much studied (001)-oriented systems due to their distinct topology. Material-specific density functional theory calculations with an on-site Coulomb repulsion term are used to explore the role of confinement, symmetry breaking, polarity mismatch and strain in the emergence of novel electronic phases. The results illuminate a rich set of competing ground states in polar $(\text{LaAlO}_3)_M/(\text{SrTiO}_3)_N(111)$ [1,2] and non-polar $(\text{LaNiO}_3)_N/(\text{LaAlO}_3)_M(111)$ [2] superlattices, ranging from spin-polarized, Dirac-point Fermi surfaces protected by lattice symmetry to charge-ordered Mott or Peierls insulating phases. Analogous to the (001) counterparts [3,4], orbital reconstructions and metal-to-insulator transitions depend critically on the thickness of the quantum well N and in-plane strain, thus opening avenues for engineering properties at the nanoscale.

Research in collaboration with D. Doennig, Dr. A. Blanca Romero and W.E. Pickett; supported by the DFG, SFB/TR80.

[1] D. Doennig, W. E. Pickett, and R. Pentcheva, Phys. Rev. Lett. 111, 126804 (2013).

[2] D. Doennig, W. E. Pickett, and R. Pentcheva, Phys. Rev. B 89, 121110 (R) (2014).

[3] D. Doennig and R. Pentcheva, in preparation.

[4] A. Blanca Romero and R. Pentcheva, Phys. Rev. B 84 195450 (2011).

SINGLE-MODE SIGNATURE IN DISTORTED PHASES REVEALED BY SYMMETRY-MODE ANALYSIS

J. M. Perez-Mato^{1,*}, B. Kocsis², E. Tasci³, M. Aroyo¹

¹ *Dept. de Física de la Materia Condensada, Facultad de Ciencia y Tecnología,
Universidad del País Vasco (UPV-EHU), Bilbao, Spain*

² *Ludwig-Maximilians Universität München, Crystallography section, Munich, Germany*

³ *Dept. of Physics, Middle East Technical University (METU) 06800, Ankara, Turkey*

Parameterization in terms of symmetry modes is an effective and efficient method for both the description and refinement of distorted structures [1]. Mode decomposition provides a hierarchical division of the degrees of freedom underlining the mechanism at the origin of a distorted phase and allows the detection of false refinement minima, typical of highly pseudo-symmetric structures. Symmetry-mode analysis is nowadays easily applicable using freely available programs as AMPLIMODES [2] or ISODISTORT [3]. Single crystal or powder diffraction direct refinements within a mode parameterization are also possible combining these programs with some refinement codes. In some cases, the number of refinable parameters can be reduced by setting to zero negligible marginal modes. The mode description is especially convenient when dealing with distorted structures of very low symmetry where the hierarchy between strong primary modes and weak secondary ones is specially pronounced. Primary distortions usually have their origin in a single set of unstable degenerate normal modes, which combined in different forms give place to phases of various symmetries. This fact introduces structural correlations between these phases that become patent in a mode description. These correlations can be used both to characterize the evolution of the relevant order parameters and as a crosscheck of the experimental structures. In the case of low symmetry phases, the single normal mode mechanism underlying primary distortions can even produce complex constraints in the structure, which are beyond conventional crystallography and are easily evidenced by a mode decomposition. We will illustrate these considerations by demonstrating the presence of this single-mode signature in the structures of the monoclinic phases of the ferroelectric $\text{PbZr}_{1-x}\text{Ti}_x\text{O}_3$ (PZT) and in the Verwey phase of magnetite.

[1] J. M. Perez-Mato, D. Orobengoa, and M. I. Aroyo, *Acta Cryst. A* 66, 558 (2010).

[2] D. Orobengoa et al., *J. Appl. Cryst.*, 42 (2009) 820.

[3] B. J. Campbell et al., *J. Appl. Cryst.*, 39 (2006) 607.

* E-mail: jm.perez-mato@ehu.es

Keywords: Symmetry-mode analysis, single-mode mechanism, PZT, magnetite.

X-RAY ABSORPTION FINE STRUCTURE SPECTROSCOPY (XAFS) WITH SYNCHROTRON RADIATION – AN INTRODUCTION

J. Rothe*

*Karlsruhe Institute of Technology, Institute for Nuclear Waste Disposal (KIT-INE),
P.O. Box 3640, 76021 Karlsruhe, Germany*

With the advent of dedicated synchrotron radiation sources in the eighties of the last century, X-ray Absorption Spectroscopy (XAS) has been developed into a powerful and versatile tool for the investigations of man-made materials and natural matter, nowadays contributing to almost any field of material and life sciences, e.g., [1]. By measuring XAS, the characteristic absorption of X-ray photons of energy E or wavelength λ ($E=h\cdot c/\lambda$, with c being the velocity of light) is determined with high precision in the vicinity of the specific binding energy of an inner shell electron of a selected sort of atoms in the sample. When the photon energy approaches or exceeds this binding energy, the electron is excited with a certain probability into a higher energy state. Thereby, the exciting photon is extinguished from the X-ray beam passing the sample. Thus, the absorption probability significantly increases when scanning the X-ray energy E across the electron binding energy, resulting in a specific “absorption edge”. Rather than being a simple step function, the absorption edge is modulated by pre-edge and post-edge resonance features - the so called “X-ray Absorption Fine Structure” (XAFS) – which reflect the binding properties of the excited atom in the sample (i.e., its coordination by neighboring atoms and the kind of chemical bonds connecting the absorbing and the neighboring atoms).

Detailed XAFS analysis provides functional understanding of a material on the basis of its atomic or molecular structure. With the exception of very low- Z atoms, XAFS can be derived from – and analyzed for – almost any kind of sample, regardless of aggregation state, degree of disorder or physical/chemical condition (e.g., pressure and temperature). Unlike the more common X-ray (powder or single crystal) diffraction method (XRD), XAFS does not require any long-range, crystalline ordering of atoms and molecules in the material under investigation. However, as a tunable and intense source of X-rays is required, XAS spectroscopy is almost exclusively performed at synchrotron radiation sources.

[1] J. Rothe, A. Léon, *X-ray absorption fine structure (XAFS) spectroscopy*, in A. Léon [Ed.], *Hydrogen Technology: Mobile and Portable Applications*, Berlin: Springer, 2008, 605–22.

* E-mail: rothe@kit.edu

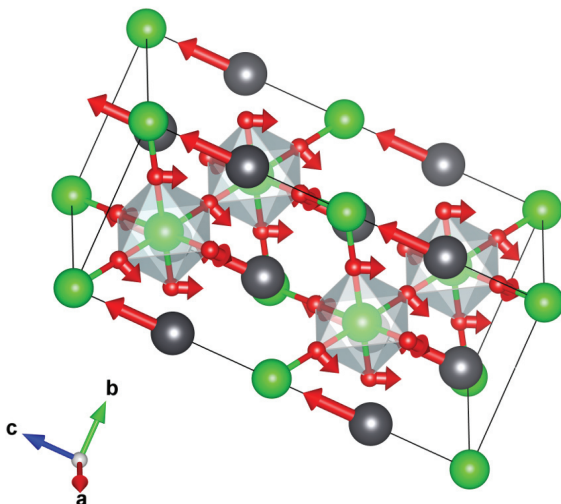
HUNTING FOR MULTIFERROICS VIA DFT MODELLING

E. S. Tasçi^{1,*}, S. Polad¹, T. Birol²

¹ Physics Department, Middle East Technical University, 06800 Ankara / Turkey

² Department of Physics and Astronomy, Rutgers University, 08854-8019 NJ / USA

Due to the advances in hi-tech components, the physical limits of size decrease propose challenges to find efficient materials that can couple multiple properties in this dimensionally restricted domain. One way to overcome this problem lies in multiferroics [1] and the perovskite family provides a wide range of applicability concerning the different fields [2].



The current state of computation enables us to efficiently evaluate the materials *in silico* yet one still has to cherry-pick the potential candidates from a vast pool of all possible combinations and materials informatics can act as a powerful guide in this search [3]. In our research, we are focusing on the octahedral tilting in perovskites [4] and thus building our roadmap.

[1] N.A. Spaldin & M. Fiebig, *Science*, 309 (2005) 391.

[2] J.B. Goodenough, *Rep. Prog. Phys.*, 67 (2004) 1915.

[3] I.E. Castelli & K.W. Jacobsen, *Modelling Simul. Mater. Sci. Eng.*, 22 (2014) 055007.

[4] N.A. Benedek & C.J. Fennie, *Phys. Rev. Lett.*, 106 (2011) 107204.

* E-mail: etasci@metu.edu.tr

Keywords: Perovskites; Multiferroics; Materials Informatics; *ab-initio* calculations.

HIGH ENERGY RESOLUTION X-RAY ABSORPTION SPECTROSCOPY AND INELASTIC X-RAY SCATTERING INVESTIGATIONS OF ACTINIDE AND LANTHANIDE MATERIALS

T. Vitova*

¹ Karlsruhe Institute of Technology (KIT), P.O. Box 3640, D-76021 Karlsruhe, Germany

High-energy resolution X-ray absorption spectroscopy (HR-XAS) [1] and inelastic X-ray scattering (IXS) [2] combined with quantum theoretical tools are gaining importance for understanding electronic and coordination structures as well as for speciation investigations of actinide (An) and lanthanide (Ln) materials. HR-XAS is successfully used to remove spectral broadening by registering the partial fluorescence yield emitted by the sample, thereby yielding highly resolved X-ray absorption near edge structure spectra (HR-XANES), which often display resonant features not observed in conventional XAS [1]. Resonant inelastic X-ray scattering (RIXS) is applied to obtain bulk electronic configuration information in solids, liquids and gases [1b]. Non-resonant inelastic X-ray scattering (NIXS) measures successfully, e.g., An O_{4,5} edge [2] and K edge XAS spectra of low Z elements in An/Ln materials. The high penetration depth of hard X-rays employed in NIXS (> 10 keV) enables flexible containment concepts, facilitating investigations of radioactive materials in the liquid phase or under extreme conditions.

We demonstrate the structural characterization capabilities of these novel techniques by discussing results from both model and complex An and Ln materials [1,2,3]. For example, we have investigated recently the U redox states of U interacted with magnetite nanoparticles and unambiguously demonstrated that U(V) can exist, along with U(IV) and U(VI), in samples kept under anoxic conditions. This result is of importance for understanding the interaction processes of uranium with corrosion products, which can potentially form in a long term nuclear waste repository.

The understanding of the long term behavior of vitrified nuclear waste stored in a long term nuclear waste repository requires a full and detailed characterization of the materials as they are synthesized and during exposure to the environment. Industrial glasses are complex, and we took a simplified separate effect approach to elucidate key properties of a simulated glass. In particular, results from U oxidation states characterization of U in simulated glass containing varying U loadings and a highly active glass sample from the “Verglasungseinrichtung Karlsruhe” (VEK) vitrification process of reprocessed high level nuclear waste will be presented and discussed.

- [1] a) T. Vitova et al., Phys. Rev. B 82 (2010) 235118; b) T. Vitova et al., Journal of Physics: Conference Series 430 (1) (2013), 012117.
[2] R. Caciuffo et al., Phys. Rev. B 81 (2010) 195104.
[3] a) R. Böhler et al., Journal of Nuclear Materials 448 (2013) 330; b) A. Walshe, Dalton Trans. 43 (2014) 4400; c) H. Damien et al., Chem. Eur. J., 20 (2014) 10431.

* E-mail: Tonya.Vitova@kit.edu

ORAL PRESENTATIONS AND POSTERS

SYNTHESIS AND CHARACTERIZATION OF POLY SULFIDE-FUNCTIONALIZED HYBRID MESOPOROUS SILICA

M. Abdallah*, N. Velikova, Y. Ivanova, Y. Dimitriev

*Department of Silicate Technology, University of Chemical Technology and Metallurgy,
Sofia, Bulgaria*

Poly sulfide-functionalized materials were synthesized by co-condensations of bis[3-(triethoxysilyl)propyl]tetrasulfide (BTPTS) and 1,2-bis(triethoxysilyl)ethane (BTESE) in the presence of the nonionic surfactant triblock copolymer poly(ethylene glycol)-block-poly(propylene glycol)-block-poly(ethylene glycol) ($\text{EO}_{20}\text{PO}_{70}\text{EO}_{20}$), Pluronic P123. The surfactant was used as a template for improving the porosity of the hybrid gels. In this work we synthesized samples with different amounts of (BTPTS) in acidic media. The final materials were soaked for 24 hours in ethanol and HCl for removing P123. In this work we investigate structure of the materials and the influence of the BTPTS amount incorporated in the silica framework after extraction of the surfactant. For this purpose we used thermo gravimetric analysis (DTA/TG), Fourier–transform infrared spectroscopy (FT-IR), nitrogen adsorption-desorption measurement, scanning electron microscopy (SEM), of ^{13}C NMR, ^{29}Si NMR analysis and element analysis. on the basis of the result of ^{13}C NMR, ^{29}Si NMR, and FT-IR we can concluded that the materials are hybrid Organic-inorganic materials BET and SEM results shows that BTESE amount has significant influence on the morphology and texture parameters of the final materials. With increasing BTPTS amount the hybrid network become more flexible, more density and more resistance of degradation in the result of it the decreasing of surface area and pore volume. Thermo gravimetric analysis (DTA/TG) results show that with increasing amount of BTPTS decreasing the thermal stability of the gel materials.

* E-mail: mohammed_abdla@yahoo.com

Keywords: Hybrid material, Mesoporous, Template, Thiol group.

STRUCTURAL AND PHYSICOCHEMICAL PROPERTIES OF CRYSTALLINE BISMUTH CHALCOGENIDES

A. M. Adam^{1,2}, E. Lilov¹, P. Petkov^{1,*}

¹ Physics Department, University of Chemical Technology and Metallurgy, Sofia, BULGARIA

² Physics Department, Faculty of Science, Sohag University, EGYPT

Crystalline bulk compositions of $\text{Bi}_2(\text{Se}_{1-x}\text{Te}_x)_3$ system, were prepared using the conventional melting method. Thin films of the proposed system were deposited based on the previously prepared bulk samples using the well known vacuum thermal evaporation technique.

The structural properties of the bulk samples and the as deposited thin films, have been studied with the aid of XRD, TEM, SEM and IR analysis. XRD patterns show that, the prepared samples are Crystalline materials with single phase of each composition. The grain size calculations performed using scherrer equation. Lattice parameters were also identified. Surface morphology and grain size of the bulk alloys as well as thin films were investigated using SEM and TEM characterization.

Physicochemical properties such as compactness, molar volume, mean coordination number and the free volume percentage were calculated for the concerned alloys based on the experimentally calculated densities. The effect of doping on the structural and physicochemical properties was investigated.

* E-mail: plamen.petkov@abv.bg

Keywords: Bismuth chalcogen; lattice parameters; physicochemical properties.

TIME RESOLVED X-RAY SCATTERING OF PROTEIN LOADED LIPID NANOPARTICLES

B. Angelov^{1,*}, A. Angelova², S. K. Filippov¹, M. Drechsler³, P. Štěpánek¹, S. Lesieur²

¹ Institute of Macromolecular Chemistry, Academy of Sciences of the Czech Republic, Heyrovsky Sq. 2, CZ-16206 Prague, Czech Republic

² CNRS UMR8612 Institut Galien Paris-Sud, Univ Paris Sud 11, F-92296 Châtenay-Malabry, France

³ Laboratory for Soft Matter Electron Microscopy, Bayreuth Institute of Macromolecular Research, University of Bayreuth, D-95440 Bayreuth, Germany

The kinetics of formation of lipid/protein complexes is investigated with the purpose of development of nanostructured lipid nanoparticles for drug delivery or nanocrystallisation. The complex formation was done via stopped flow mixing of PEGylated lipid intermediates and pure protein. The rapid nonequilibrium process was followed by millisecond time-resolved small-angle X-ray scattering (SAXS) at ID02 beamline, ESRF, Grenoble, France [1, 2]. The protein BDNF (brain derived neurotrophic factor) interacts with the flexible lipid membrane and induces an unusual overlay of two coexisting cubic lattices epitaxially connected to lamellar membrane stacks. The investigated system was imaged with cryo-transmission electron microscopy (cryoTEM) in its initial and final state. The results are important in the context of drug delivery of therapeutic proteins.

[1] B Angelov, A. Angelova, S. K., Filippov, T., Narayanan, M., Drechsler, P., Štěpánek, P., Couvreur, S., Lesieur, J. Phys. Chem. Lett., 4 (2013) 1959.

[2] B. Angelov, A. Angelova, S.K. Filippov, M. Drechsler, P. Štěpánek, S. Lesieur, ACS Nano, 8 (2014) 5216.

* E-mail: angelov@imc.cas.cz, www.imc.cas.cz

Keywords: Time resolved small angle X-ray scattering, protein, lipid, cubosome.

THE CHEMICAL COMPOSITION AND STRUCTURE OF THREE PHASE EPOXY\ORGANOCLAY\GOLD NANOCOMPOSITES

V. Angelov*, E. Ivanov, R. Kotsilkova

*Open Laboratory for Experimental Mechanics of Micro and Nanomaterials (OLEM),
Institute of Mechanics, Bulgarian Academy of Sciences*

The aim of this study is to investigate the chemical composition and structure of the Epoxy/ Organoclay/Gold nanocomposites. Gold nanoparticles are synthesized from precursor HAuCl_4 in aqueous solution and they are with different size and shape. The nanocomposites are prepared by “in-situ” polymerization method.

The composition of the final three phase nanocomposites is determined by XRF analysis. X-ray fluorescence (XRF) analysis is a fast and non-destructive method with very high accuracy and reproducibility.

XRD measurements are performed on the clay powder and the epoxy based nanocomposites. The X-Ray diffractograms are obtained using Bruker D8 Advance diffractometer. The crystalline phases are identified using the Joint Committee on Powder Diffraction Standards (JCPDS) files. The mean particle size (L) of gold nanoparticles is determined from the line broadening reflections, using the Scherer equation. The calculations are done using FIT computer program [1].

Transmission electron microscope JEOL JEM 2100 is used for characterization of the structure at micro- and nano-scale of the samples.

The sizes and the shapes of synthesized gold nanoparticles are estimated by XRD and TEM analysis.

This poster presents methods for preparation of gold nanoparticles on a substrate of layered silicates and the corresponding results from XRF, XRD, TEM analysis of the prepared nanocomposites [2].

Acknowledgements: The study was partially supported by the project COST Action MP1202.

[1] V. Petkov, N. Bakaltchev, J. Appl. Crystallography, 23 (1990) 138.

[2] V. Angelov, H. Velichkova, E. Ivanov, R. Kotsilkova, M-F. Ottaviani, M. Cangiotti, A. Fatori, M-H. Delville, Langmuir, in press.

* E-mail: v.angelov@imbm.bas.bg

Keywords: XRF, XRD, TEM, nanocomposites.

BIOCOMPATIBLE GLASS CERAMIC MATERIALS

M. Kh. Aripova*, R. V. Mkrtchyan, T. O. Nam

Tashkent Chemical Technological Institute, 32, Navoi str., Tashkent, Uzbekistan

It were synthesized opacified, opalescent and transparent glasses in the studied P_2O_5 – SiO_2 – Al_2O_3 – CaO – MgO – CaF_2 system; was determined an area of glass formation and liquation. The crystallization ability of synthesized glasses was investigated by mass crystallization method. It was established that the glasses in the temperature range 800–1000°C characterized by bulk crystallization, and the obtained crystallized material has high physical and technical characteristics and fine structure. Studies have shown that the developed glass-ceramic material exhibited biocompatibility, which is proven by morphological, biochemical and toxicological studies results.

Research on the biocompatibility of experimental glass-ceramic materials conducted for 1-3-12 months after implantation of bioceramics to animals – rabbits. The experimental results were evaluated based on clinical observation of the animals condition and the lower jaw preparations morphological studies at different times after surgery. In 1 month after replanting of implants in the main group of animals it has been an expansion of the defect at the edges of the bone defect as a result of bone edge' resorption. Between the implant and the bone defect edges was formed the rim of iso-connective tissue rich in capillary type' blood vessels. Subsequently resorb bone substance was replaced by cell-fibrous connective tissue. After 3 months along with strongly pronounced resorptive processes in the field of bone defect could be seen a neoplasm's consisting of coarse fiber structures constructed on the basis of the parent bone. 6 months after surgery in the control group, the newly formed bone structures had loose structure, after 12 months the implant was surrounded by a coarse fiber shell of thin connective tissue.

The investigation of tissue reactions in animals at the implant - natural tissue boundary showed that the developed bioceramics can serve as a replacement of bone tissue and it is not rejected by the body of the animal.

Biochemical and clinical studies have shown that implant in subcutaneous and intramuscular transplantation does not cause structural changes in the soft tissue belonging to the bone, has no toxic effects on the tissue surrounding the implant, causes no allergic, immunological reactions of the body and does not cause rejection reaction; it helps to restore the bone tissue.

* E-mail: aripova1957@yandex.ru

Keywords: biocompatibility, glass-ceramic material, the toxicological properties, bone tissue.

STUDYING THE STRUCTURE OF QUARTZ-GRAPHITE SCHISTS USING SEM ANALYSIS

Z. A. Babakhanova*, M. Kh. Aripova, J. Aripov

Tashkent Chemical Technological Institute, 32, Navoi str., Tashkent, Uzbekistan

A deposit of graphite named Taskazgan has been discovered in Uzbekistan. Moreover, there are 25 imprecise fields of graphite with variable perspectives. Almost all of the fields aren't studied thoroughly. The purpose of our work is to study the structure and composition of graphite ore suitable for further enrichment to produce a graphite concentrate.

According to the results of the semi-quantitative X-ray analysis, the graphitized schists of Taskazgan are consisting mainly of quartz crystals – 46, sericite – 28, albite – 18, small amounts of pyrite, goethite, dolomite – 5 and graphite – 2–3 (percentages by mass). SEM analysis (JXA 8800R “Superprobe”, JEOL, Japan) of the schist sample showed that the analyzed portion is mainly represented by massive aggregates of quartz and congestions of small-grained sericite (K_2O 11.25, MgO 2.20, Al_2O_3 31.82, SiO_2 48.08%), pyrite in the range of 10–15% (Fe 45.78, S 52.92 %) and arsenopyrite (Fe 35.07, As 43.35, S 21.72%). The minerals of dolomite (MgO 18.02, CaO 29.10, MnO 0.40, FeO 3.96%) and an ankerite (MgO 24.81, CaO 0.36, MnO 1.35, FeO 23.14%) have been observed in the cracks of the rock formations. Graphite in the rock formations is represented as fine-grained disseminations in the amount of 3–5%: there are also dotted allocations (less than 0.001 mm), lesser aggregates with the size of 0.025–0.1 mm and clusters of irregular shaped with vague outlines.

The rock formations of Rupert which contain graphite are represented by quartz-chlorite plagioclites of small and medium-grains with a different amount of graphite. The formation is silicified graphitized and penetrated with quartz and graphite veins. The graphite in the formation is distributed unevenly in the form of variable inclusions, disseminations and interlayers.

The mineral content of quartz-graphite schists of Rupert is – quartz, muscovite, albite, chlorite, small amounts of dolomite and graphite. The study of graphitized schists with the help of SEM analysis showed that the formation mainly consists of fused quartz aggregates sized from 25×25 to 50×38 μm and massive crystals of dolomite. The dolomite formations are intersected with whitish veins of ferruginous dolomite – ankerite. Potassium aluminosilicate is distributed in the pores between the quartz and dolomite crystals. Aluminosilicate contains up to 4.48% V_2O_5 ; 1.13% Cr_2O_3 ; 1.15% BaO . The genetic type of the ore in Rupert is metamorphic, graphite is represented in the form of flakes aggregates sized up to 1 mm and small flakes sized 0.001–0.1 mm, often interbedded by mica plates.

* E-mail: babax2013@yahoo.com, aripova1957@yandex.ru

Keywords: schists, graphite, flake, enrichment.

SYNTHESIS OF BETA ZEOLITES IN THE PRESENCE OF SEEDS

B. Barbov*, Yu. Kalvachev

*Institute of Mineralogy and Crystallography, Bulgarian Academy of Sciences,
Sofia, Bulgaria*

Zeolites are well known as active catalysts for oil refining, petrochemistry, organic synthesis and many different environmental processes. Among them zeolite Beta has special industrial importance. This interest originates from the broad Si/Al range in zeolite β ($5 - \infty$) and its particular structure, being an intergrowth of different polymorphs and therefore being disordered in one dimension. The combination of three-dimensional pore architecture composed of intersecting 12-ring channels with strong acid sites makes this zeolite useful catalyst in a number of processes – such as catalytic cracking, (hydro)isomerisation of alkanes, alkylation of aromatics, and esterification reactions, *etc.*

In order to obtain nanosized crystals of zeolite Beta hydrothermal seed-induced synthesis is performed. Nanosized zeolites are important in catalytic and adsorptive applications. Smaller crystals of zeolites will have larger surface areas and less diffusion limitations compared to zeolites with micrometer-sized crystals. Nanometer-sized zeolites also offer advantages in supramolecular catalysis, photochemistry, nanochemistry, electrochemistry, and optoelectronics. During the synthesis two types of seeds are used – crystal seeds and mother liquor. Seed-induced synthesis by using of mother liquor as seeds leads to smaller zeolite crystals.

Crystal growth kinetics of the material as a function of seed content, type of seeds and Si/Al ratio of the initial gel are studied. After the optimization of crystallization conditions a highly crystalline material with crystal size 100–200 nm is synthesized.

The obtained crystals were characterized by X-ray diffraction, scanning electron microscope, thermogravimetric analysis, and infrared spectroscopy.

Acknowledgements: The authors acknowledge the financial support from project BG051PO001-3.3-06-0027, financed by the operational programme “Human resources development”.

AFM AND XRD STUDY ON THE RECRYSTALLIZATION OF NANOCRYSTALLINE $\text{Zn}_x\text{Cd}_{1-x}\text{Se}$ THIN FILMS

I. Bineva^{1,*}, T. Hristova-Vassileva¹, B. Pejova², D. Nesheva¹, Z. Levi¹, Z. Aneva¹

¹ *Institute of Solid State Physics, Bulgarian Academy of Sciences,
72 Tzarigradsko Chaussee Blvd., 1784 Sofia, Bulgaria*

² *Institute of Chemistry, Faculty of Science, Ss. Cyril and Methodius University,
Skopje, Macedonia*

Single layers of $\text{Zn}_x\text{Cd}_{1-x}\text{Se}$ with various compositions ($x = 0.4, 0.6$, and 0.8) were prepared by thermal vacuum evaporation of consecutive small portions of ZnSe and CdSe layers with nominal thickness of 0.12, 0.25 or 0.37 nm. Atomic Force Microscopy (AFM) and X-ray diffraction (XRD) measurements were carried out to follow the films changes in a long time period – up to six years. The microstructure and morphology evolution seems to be strongly related to recrystallization process. Conversion of the images in Fourier space was performed using a two-dimensional fast Fourier transform algorithm (2DFFT) in order to observe patterns of periodicities.

The XRD investigations show typical solid solution patterns, proving that no decomposition occurs during the ageing process. The main XRD peak becomes narrower for $x=0.6$, while for $x=0.4$ and $x=0.8$ it changes weakly. For the latter compositions, in the small angles of XRD pattern ($2\theta < 15$) Bragg diffraction peaks appear, indicating ordering of nanocrystals in superstructures.

Progressive recrystallization with formation of layered structures on the surface is observed for the compositions with $x=0.8$ and 0.4 , being faster for the first ones. However, the recrystallization process of the films with $x=0.6$ is much slower – even after 6 years they are still nanocrystalline.

* E-mail: irka@issp.bas.bg

Keywords: ZnCdSe solid solution, AFM, XRD, Fast Fourier transform.

STABILIZATION OF HIGHER OXIDATION STATES OF PLATINUM BY COORDINATION WITH FLEXIBLE N,O,N-LIGAND DIPYRIDIN-2-YLMETHANONE AND RIGID N,N-LIGAND PYRIDINE-2-AMINE – SYNTHESIS, CRYSTAL STRUCTURE AND CYTOTOXICITY

S. Chakarova^{1,*}, P. Gorolomova¹, B. Krebs², G. Momekov, G. Gencheva¹

¹ *Sofia University "St. Kliment Ohridski", Faculty of Chemistry and Pharmacy, 1. J. Bourchier Blvd, 1164 Sofia, Bulgaria*

² *Anorganisch-Chemisches Institut der Universität Münster, Wilhelm-Klemm-Strasse 8, Germany*

The higher oxidation state platinum complexes offer increased opportunities for antitumor drug design due to their thermodynamic stability and inherent inertness. The octahedral constructs typical for mononuclear platinum(IV) complexes and for the metal centers in mixed-valence platinum(II,III) chain compounds provide additional axial coordination sites. These coordination

places can be exploited to create additional functionalities as well as for fine-tuning of lipophilicity, the redox potential, reactivity and kinetics of ligand substitution reactions. The presented studies are dedicated to design of new platinum compounds with octahedral environment and characterize their cytotoxic properties as a function of the structure. A stable mononuclear Pt^{4+} complex, 1 and two mixed valence platinum chain complexes, 2 and 3 were obtained during the interactions of 1:1 molar ratios of PtCl_6^{2-} and dipyrin-2-ylmethanone (dpk) in aqueous solutions and PtCl_4^{2-} and pyridine-2-amine (ap) in alkaline-aqueous solutions. The solid state structure of the compounds and their solutions chemistry were studied using single-crystal X-ray diffraction and spectroscopic methods. Single crystals of compound 1 ($\text{Pt}(\text{dpk-OH})\text{Cl}_3$) were grown by slow diffusion of ether into its DMF solution. Pt^{4+} cations exhibit distorted octahedral coordination of PtCl_3ON_2 units, as dpk is coordinated as a chelating tridentate ligand in its deprotonated *gem*-diol form. The chain structures of the compounds 2 and 3 were constructed through bridging coordination of the N,N-bidentate ap-ligand as the physicochemical properties of the compounds depend on a $\text{Pt}^{2+}/\text{Pt}^{3+}$ proportion. Extensive cytotoxic tests proved the perspectives of the compounds as proper structures for further anticancer drug design investigations.

* E-mail: ggencheva@chem.uni-sofia.bg

Keywords: platinum(IV) complexes, mixed valence platinum chain compounds, structural characterization, cytotoxic studies.

Cu(II)-IMPRINTED COPOLYMER MICROPARTICLES: SYNTHESIS, CHARACTERIZATION AND APPLICATION FOR SELECTIVE SOLID PHASE EXTRACTION OF COPPER IONS

I. Dakova^{1,*}, V. Dakov², I. Karadjova¹

¹ Faculty of Chemistry and Pharmacy, University of Sofia "St. Kliment Ohridski",
1 James Bourchier blvd., Sofia, Bulgaria

² University Laboratory of Ecology and Environmental Protection, University of Forestry,
10 Kliment Ohridsky blvd., Sofia, Bulgaria

Preparation and characterization of Cu(II)-imprinted copolymer microparticles are presented in this report. 4-(2-pyridylazo) resorcinol (PAR) is chosen as the specific chelating agent. In the first step, Cu(II) is complexed with PAR and Cu(II)-imprinted poly(hydroxyethyl methacrylate-co-trimethylolpropane trimethacrylate) microparticles (Cu-IIPs) are synthesized by a crosslinking dispersion copolymerization using ACN as solvent. After that, cavities in the copolymer network corresponding to the Cu(II) ions are created by elution with 2 M HNO_3 . The synthesized Cu-IIPs are characterized by elemental analysis, scanning electron microscopy and Fourier transform infrared spectroscopy. Extraction efficiencies of newly synthesized copolymers are investigated using batch experiments. The optimal pH value for the quantitative sorption is 7. The Cu(II)-IIPs show fast sorption/desorption kinetics, high selectivity and satisfied adsorption capacity for adsorption of Cu(II). Finally, the prepared Cu-IIPs are successfully applied to the selective recognition and determination of copper ions in surface waters.

* E-mail: i.dakova@chem.uni-sofia.bg

Keywords: Cu(II)-imprinted copolymer microparticles, copper ions, solid phase extraction.

CRYSTAL MORPHOLOGY OF SIMONKOLLEITE ($\text{Zn}_5(\text{OH})_8\text{Cl}_2(\text{H}_2\text{O})$): A SEM STUDY

S. Dencheva*, G. Kirov

*Department of Mineralogy, Sofia University "St. Kliment Ohridski" 1504 Sofia,
15 Tsar Osvoboditel Blvd., Bulgaria*

Simonkolleite is a rare mineral, first described as weathering product of zinc slags in natural conditions. It is an important component of the thin protective film of zinc hydroxysalts responsible for the excellent resistance of zinc and zinc-plated steel under natural conditions. Crystal morphology and arrangement of micro crystals in this film are important for its protective action.

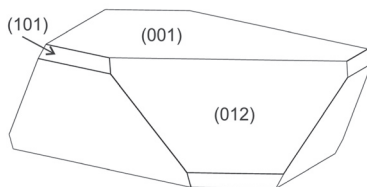
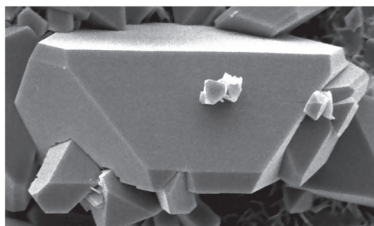
Simonkolleite samples were prepared from a solution of ZnCl_2 by alkalization with NaOH solution or by hydrolysis of urea and in the reaction with ZnO or zinc powder. The SEM investigations were carried out using a Jeol 5510 microscope.

In this work we use the possibilities of the computer program VESTA to generate crystal shapes in random orientation from structural data and comparison with SEM-images of synthetic and natural simonkolleite crystals.

Model images of the crystals were obtained using VESTA after the introduction of lattice parameters, space group and indexes of the attended morphological important forms in accordance with Bravais – Friedel – Donnay – Harker law and the method of PBC-vectors.

The largest interplanar distances in the X-ray diffractogram define as morphologically important forms the basic pinacoid {001} and the rhombohedrons {101} and {012}. The model images were matched with the real image by rotating around axis x, y and z with a step down to 0.1° .

The Figure shows a SEM picture of synthetic simonkolleite crystal (a) and its model image with aligned dimensions of the faces (b). The investigated simonkolleite crystals are composed of the combinations {001}, {101}, {012} or {001}, {012}.



* E-mail: zaneva@gea.uni-sofia.bg

Keywords: Simonkolleite, morphology, SEM study.

OPTIMIZATION OF CeO₂-ZrO₂ MIXED OXIDE CATALYSTS FOR ETHYL ACETATE COMBUSTION

M. Dimitrov¹, R. Ivanova^{1,2*}, V. Štengl³, J. Henych³, T. Tsoncheva¹

¹ *Institute of Organic Chemistry with Centre of Phytochemistry, BAS, Sofia, Bulgaria*

² *Sofia University, Faculty of Chemistry and Pharmacy, Sofia, Bulgaria*

³ *Institute of Inorganic Chemistry AS CR v.v.i, Husinec-Rez, Czech Republic*

Ceria (CeO₂) is a rare-earth metal oxide with important applications in areas of catalysis, electrochemistry, photochemistry, and materials science [1] due to its ability to undergo a facile conversion between “+4” and “+3” formal oxidation states [2]. To enhance the redox properties and thermal stability of pure ceria, zirconia (ZrO₂) is often mixed as an additive to form solid solutions of the Ce_{1-x}Zr_xO₂ type. It is very difficult for the Zr atoms to adopt the large metal-oxygen distances expected in the lattice of CeO₂. The consequence is the presence of perturbations in the Zr-O coordination sphere, which are responsible for the high oxygen mobility seen in ceria-zirconia mixed oxides thus enhancing the overall reoxidizing-reducibility capability of the mixed oxide system [3]. The enhanced reducibility is likely to lead to improved catalytic properties for some reactions such as volatile organic compounds combustion.

The aim of the investigation is to obtain Ce_{1-x}Zr_xO₂ mixed oxides with different composition varying the synthesis conditions. Ethyl acetate is used as representative VOC molecule for testing the catalytic behaviour of the obtained catalysts. An optimum mol ratio of CeO₂/ZrO₂=3/7 has been found to give the highest synergistic effect for ethyl acetate combustion.

[1] M. Boaro, M. Vicario, C. Leitenburg, G. Dolcetti, A. Trovarelli, *Catal. Today*, 77 (2003) 407.

[2] M.V. Ganduglia-Pirovano, A. Hofmann, J. Sauer, *Surf. Sci. Rep.*, 62 (2007) 219.

[3] P. Fang, J. Lu, X. Xiao, M. Luo, *J. Rare Earth*, 26 (2008) 250.

* E-mail: radostinaiv@abv.bg

Keywords: nanostructured ceria-zirconia catalysts, VOCs, ethyl acetate combustion.

INFLUENCE OF Y-ION SUBSTITUTION ON STRUCTURAL AND ELECTROCHEMICAL CHARACTERISTICS OF $\text{YCo}_{0.5}\text{Fe}_{0.5}\text{O}_3$

S. Dimitrovska-Lazova^{1,*}, S. Aleksovska^{1,2}, P. Tzvetkov³,
V. Mirčeski¹, D. Kovacheva³

¹ *Institute of Chemistry, Faculty of Natural Sciences and Mathematics, "Sts. Cyril & Methodius" University, Arhimedova 3, Skopje, R. Macedonia*

² *Research Center for Environment and Materials, Macedonian Academy of Sciences and Arts, Krste Misirkov 2, 1000 Skopje, R. Macedonia*

³ *Institute of General and Inorganic Chemistry, Bulgarian Academy of Science, "Acad. Georgi Bonchev" bl. 11, 1113 Sofia, Bulgaria*

The influence of partial substitution of Y^{3+} with Ca^{2+} in $\text{YCo}_{0.5}\text{Fe}_{0.5}\text{O}_3$ perovskite on the crystallochemical and electrocatalytic properties is presented. The perovskites $\text{YCo}_{0.5}\text{Fe}_{0.5}\text{O}_3$ and $\text{Y}_{0.8}\text{Ca}_{0.2}\text{Co}_{0.5}\text{Fe}_{0.5}\text{O}_{3-\delta}$ were synthesized by solution combustion method with citric acid as a fuel. The obtained powders were washed with diluted HCl and additionally heated 4 h at 800° and 6 h at 950°C .

The obtained perovskites were analyzed with powder XRD and cyclic voltammetry. The crystal structures of both compounds were determined by Rietveld refinement method. The XRD patterns showed that both perovskites are orthorhombic and crystallize in space group *Pnma*. In aim to obtain a clearer picture for the influence of substitution of Y^{3+} ion with Ca^{2+} ion on the structural characteristics, the lattice parameters and distances and angles were used to calculate several crystallographic parameters such as, cell distortion, orthorhombic distortion, bond and angle deformation, the tilting angles, bond valences, and global instability index. It was found that the distortion indices and tilting angles are lower for $\text{Y}_{0.8}\text{Ca}_{0.2}\text{Co}_{0.5}\text{Fe}_{0.5}\text{O}_{3-\delta}$ in comparison with $\text{YCo}_{0.5}\text{Fe}_{0.5}\text{O}_3$.

Taking into consideration the possible application of these compounds as catalysts in direct methanol fuel cells, their catalytic properties were studied by cyclic voltammetry using PIGE (paraffin impregnated graphite electrode) electrode. The recorded voltammograms showed substantial catalytic activity of Ca-containing perovskite, toward oxidation of methanol in basic solution.

* E-mail: sandra@pmf.ukim.mk

Keywords: perovskites, partial substitution, crystal structure, electrocatalytic properties.

COPOLYMERIZATION OF BENZIL WITH STYRENE IN THE PRESENCE OF TRANSITION METAL CATALYST

S. Dimova^{1,*}, K. Zaharieva², C. Jossifov¹, V. Sinigersky¹,
Z. Cherkezova-Zheleva², B. Kunev², I. Mitov²

¹ *Institute of Polymers, Bulgarian Academy of Sciences, Sofia, Acad. G.Bonchev str., bl. 103A*

² *Institute of Catalysis, Bulgarian Academy of Sciences, Sofia, Acad. G.Bonchev str., bl. 11*

Transition metal catalysts have been extensively used in carbon–carbon bond forming reactions. Carbon–carbon bond formation is a fundamental reaction in organic synthesis, one of its most important applications being the synthesis of polymers and copolymers [1].

The aim of this work was to study the polymer formation via coupling of diketone and styrene by transition metal catalysts. We starting from monomer benzil and comonomer styrene in appropriate molar ratio, catalyst WCl_6 and chlorobenzene as solvent. The molecular-weight range of the polymers obtained was from about 600–2000.

The products obtained were characterized by ^1H , ^{13}C NMR, FTIR spectroscopy and SEC (Size-exclusion chromatography). The morphology of the polymers was studied by scanning electron microscopy and X-ray diffraction analysis.

The results showed that depending on the reaction procedure (addition of the reagent or variation their molar ratio) were obtained polystyrene or a copolymer.

Acknowledgements: The authors from IC-BAS appreciate the financial help of the Bulgarian Science Fund of the Bulgarian Ministry of Education and Science by Project DFNI-E01/7/2012.

[1] F. di Lena et al., *Progress in Polymer Science*, 35 (2010) 959.

* E-mail: dimova@polymer.bas.bg

Keywords: Carbon–carbon bond formation, copolymerization, benzil, styrene.

HEULANDITE ION-EXCHANGE UNDER IDENTICAL CONDITIONS, COMPARISON OF RESULTS FOR VARIOUS CATIONS: Na⁺, K⁺, Mg²⁺, AND Ca²⁺

L. Dimova^{1,*}, I. Piroeva², S. Atanasova-Vladimirova², B. Shivachev¹, S. Petrov³

¹ *Institute of Mineralogy and Crystallography, Bulgarian Academy of Sciences,
"Acad. Georgi Bonchev" str. building 107, Sofia 1113, Bulgaria*

² *Academician Rostislav Kaishev Institute of Physical Chemistry, Bulgarian Academy of Sciences,
Acad. Georgi Bonchev str., building 11, Sofia 1113, Bulgaria*

³ *Department of Chemistry, University of Toronto, 80 St. George Street,
Toronto, ON, M5S 3H6 (Canada)*

Heulandite single crystals from Iskra deposit (Bulgaria) were the initial material for this study. Four samples were selected from initial heulandites and were ion exchanged with Na, K, Mg and Ca nitrates. The ion exchange procedure for all samples was carried out under identical conditions: 7 days at 100 °C and the 1M cation solution which was changed three times. The samples chemical composition was obtained by EDS analysis while single crystal X-ray structural refinement yielded the framework, cation and water positions. Weight losses associated with zeolitic water in the channels were obtained by DTA/TG analysis and used in the calculation of the common formulas of exchanged heulandites (72 framework oxygen atoms). Initial heulandite crystals (natural HEU from Iskra) contain predominantly Ca²⁺ as framework counter ion. Thus the EDS/TGA formula is (Na_{0.52}K_{0.5}Ca_{3.64}) Al_{8.32}Si_{27.68}O₇₂·nH₂O. The cations are distributed in positions M1 (channel A), M2 (channel B) and M3 (near the centre of channel C and the edge of A). The EDS and structural refinement show that for the employed procedure Mg²⁺ ion exchange is not observed. Different values for the uptakes of Na, K and Ca by the HEU structure are observed after the conducted ion exchange.

* E-mail: Louiza.Dimova@gmail.com

Keywords: Heulandite, ion exchange, single crystal.

EXTRACTION-SPECTROPHOTOMETRIC STUDY OF ION-ASSOCIATION COMPLEX OF COBALT(II)–4-(2-THIAZOLYLAZO) RESORZINOL WITH 2-(4-IODOPHENYL)-3-(4-NITROPHENYL)-5-PHENYL-2H-TETRAZOLIUM CHLORIDE

V. Divarova^{1,*}, K. Stojnova¹, P. Racheva², V. Lekova¹, A. Dimitrov¹

¹ *University of Plovdiv "Paisii Hilendarski", Department of General and Inorganic Chemistry, 24 Tzar Assen Street, 4000 Plovdiv*

² *Medical University Plovdiv, Department of Chemistry and Biochemistry, 15A Vasil Aprilov Boulevard, 4002 Plovdiv, Bulgaria*

Cobalt is a typical transition and complex formation metal, it refers to a group of essential biochemical elements. The complexes of cobalt with chelating ligands, containing N, O and S donor atoms play a key role in the field of the coordination chemistry. They are studied, because they have industrial, biological, pharmacological and medical applications. The ion-association complex between of anionic chelate of Co(II)–4-(2-thiazolylazo)resorcinol (TAR) with 2-(4-iodophenyl)-3-(4-nitrophenyl)-5-phenyl-2H-tetrazolium chloride (INT) in the liquid-liquid extraction system Co(II)–TAR–INT–H₂O–CHCl₃ were studied.

The optimum conditions for the formation of ternary ion-association complex Co–TAR–INT was determined. The molar ratio of the reagents was determined. The extraction equilibria were investigated and quantitatively were characterized by the equilibrium constants and recovery factor. The validity of Beer's law was checked and some analytical characteristics were calculated.

* E-mail: vitana_diva@abv.bg

Keywords: Co-chelates, ion-association complexes, extraction equilibria.

SILVER NANOPARTICLES EMBEDDED IN BIOCOMPATIBLE POLYMERS: COMPARATIVE STUDY OF EXTRACTION EFFICIENCY TOWARD TOXIC METALS

L. Djerahov^{1,2}, P. Vasileva^{1,*}, I. Karadjova², I. Dakova², R. M. Kurakalva³

¹ *Department of General and Inorganic Chemistry, Faculty of Chemistry and Pharmacy, University of Sofia "St. Kliment Ohridski", Bulgaria*

² *Department of Analytical Chemistry, Faculty of Chemistry and Pharmacy, University of Sofia "St. Kliment Ohridski", Bulgaria*

³ *Environmental Geochemistry Division, CSIR-National Geophysical Research Institute, Hyderabad, India*

Green chemical approach was developed for the preparation of hybrid organic/inorganic films of polyvinyl alcohol (PVA) or chitosan (CS) loaded down with pre-synthesized silver nanoparticles (AgNPs). The employed polymers are not toxic and biocompatible in nature. AgNPs have been generated by green chemical reduction utilizing starch or raffinose as capping agents. Solution of PVA or CS was mixed with AgNPs dispersion and cast hybrid films were obtained under drying at suitable temperature.

The structure and morphology of nanoparticles and films were studied by TEM and SEM. AgNPs were uniformly distributed in the membrane of PVA or CS without any aggregation. Even more the presence of AgNPs in the PVA/CS film remarkably increase their mechanical stability, the most probably AgNPs play a role of crosslinker. The assumption is that the extraction efficiency of PVA/CS will be combined with the chemical activity of AgNPs in the as prepared nanocomposite films and even more some synergetic sorption effect might be expected. In order to prove this hypothesis sorption behavior of most frequently determined chemical elements was studied with each of the materials: CS/PVA, AgNPs, CS-AgNPs and PVA-AgNPs. Sorption experiments were performed at pH 7-9, achieved with ammonia or NaOH (these pH values ensured deprotonation of CS/PVA functional groups).

After sorption time of 12 h, the effluat solution is easy decanted, the membrane is washed twice with doubly distilled water and dissolved in around 300 μ l HNO₃ followed by dilution to desired volume and ETAAS measurements. Results obtained undoubtedly confirmed high extraction efficiency of composite films CS-AgNPs and PVA-AgNPs ensuring quantitative sorption of all studied elements except Mn at optimal conditions. Preconcentration procedure developed based on sorption properties of CS-AgNPs and PVA-AgNPs was applied for the determination of priority pollutants Cd, Pb and Ni in surface waters and elements Al, Cd and Pb in chemodialysis solutions. Determination limits achieved satisfy permissible limits which makes developed analytical procedure suitable for routine laboratory practice.

* E-mail: pvasileva@chem.uni-sofia.bg

Keywords: Ag nanoparticles, hybrid films, extraction efficiency, toxic metal pollutants.

STRUCTURAL, SPECTROSCOPIC AND QUANTUM-CHEMICAL STUDIES OF POTENTIALLY CYTOSTATIC Pt(II) AND Pt(IV) COMPLEXES OF *N*-3-PYRIDINYLMETHANESULFONAMIDE

N. I. Dodoff^{1,*}, N. G. Vassilev², R. P. Nikolova³, O. E. Petrov³, M. Lalia-Kantouri⁴,

V. Miletić⁵, D. N. Kushev¹, M. D. Apostolova¹

¹ Acad. R. Tsanev Institute of Molecular Biology, Bulgarian Academy of Sciences (BAS), Acad. G. Bonchev Str., Bl. 21, 1113 Sofia, Bulgaria

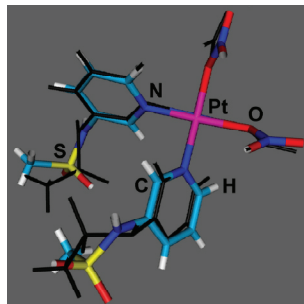
² Institute of Organic Chemistry with Center of Phytochemistry, BAS, Acad. G. Bonchev Str., Bl. 9, 1113 Sofia, Bulgaria

³ Acad. I. Kostov Institute of Mineralogy and Crystallography, BAS, Acad. G. Bonchev Str., Bl. 107, 1113 Sofia, Bulgaria

⁴ Department of Chemistry, Faculty of Science, Aristotle University of Thessaloniki, P.O. Box 135, 54124 Thessaloniki, Greece

⁵ Institute of Chemistry, Faculty of Science, University of Kragujevac, 34000 Kragujevac, Serbia

In continuation of our systematic studies on the coordination chemistry and cytotoxic effect of platinum-group metal complexes with *N*-3-pyridinylmethanesulfonamide (PMSA) [1-3], here we report the single crystal structure of *cis*-[Pt(PMSA)₂(NO₃)₂] (orthorhombic, *Pbca*, *a* = 19.8017(6), *b* = 9.8042(3), *c* = 24.0279(8), *Z* = 8) and compare it with that obtained by HF *ab initio* quantum-chemical calculations (the black structure in the Figure). The Pt(IV) complex *cis,cis,trans*-[Pt(PMSA)₂Cl₂(OH)₂]·2H₂O, previously synthesized and characterized by X-ray crystallography [3], has now been studied by powder XRD and HF *ab initio* quantum-chemical calculations. The free PMSA and its complexes have been characterized by IR and NMR (¹H, ¹³C, ¹⁵N, ¹⁹⁵Pt) spectroscopy. The IR spectra have been interpreted on the basis of HF *ab initio* vibrational analysis. The Pt(IV) complex exhibited moderate cytostatic activity against K562 human leukemic cells.



Acknowledgement: The work is part of the bilateral cooperation between BAS and AUTH.

[1] N. I. Dodoff *et al.*, Z. Naturforsch., 59 (2004) 1070.

[2] N. I. Dodoff *et al.*, J. Coord. Chem., 65 (2012) 688.

[3] N. I. Dodoff *et al.*, Chinese J. Struct. Chem., 31 (2012) 1476.

* E-mail: dodoff@obzor.bio21.bas.bg

Keywords: Platinum, sulfonamide, structure, cytostatic.

COMPARISON BETWEEN THERMAL BEHAVIOUR OF $\gamma\text{-MnC}_2\text{O}_4\cdot 2\text{H}_2\text{O}$ IN OXIDATIVE AND INERT MEDIA

B. Donkova¹, V. Petkova^{2,3}

¹ *Department of General and Inorganic Chemistry, Faculty of Chemistry and Pharmacy,
University of Sofia, 1 J. Bourchier Av., 1164 Sofia, Bulgaria*

² *Department Natural Sciences, New Bulgarian University, 21 Montevideo Str., 1618 Sofia, Bulgaria*

³ *Institute of Mineralogy and Crystallography, Bulgarian Academy of Sciences, Acad. G. Bonchev Str.,
bldg.107, 1113 Sofia, Bulgaria*

Sparingly soluble manganese oxalate is an appropriate precursor for preparation of various nano-sized manganese oxides which explains the growing interest to its utilization and investigation of its thermolysis.

Recently, three crystal forms of manganese oxalate are known – monoclinic $\alpha\text{-MnC}_2\text{O}_4\cdot 2\text{H}_2\text{O}$ (SG C2/c), orthorhombic $\gamma\text{-MnC}_2\text{O}_4\cdot 2\text{H}_2\text{O}$ (P2₁2₁2₁) and orthorhombic trihydrate $\text{MnC}_2\text{O}_4\cdot 3\text{H}_2\text{O}$ (Pcca). While the mechanism and products of thermal decomposition of monoclinic dihydrate have been extensively studied by various methods, the literature data for the trihydrate and orthorhombic dihydrate are quite scarce.

The aim of the present study is to investigate and compare the decomposition mechanism of the slightly known $\gamma\text{-MnC}_2\text{O}_4\cdot 2\text{H}_2\text{O}$ in oxidative and inert media under non-isothermal conditions with analysis of the evolved gases. Pure phase of pinkish orthorhombic dihydrate was obtained and characterized by X-ray diffraction and scanning electron microscopy. Le Bail whole pattern fitting analysis was performed in addition. The non-isothermal investigation was carried out in a static Air and Ar atmosphere (60 ml.min⁻¹) at a heating rate of 5°C.min⁻¹ in the range of 25–800°C, using a coupling system TG-MS - instrument SETSYS2400 combined with an mass-spectrometer. According to TG-DTA-DTG curves, dehydration proceeds in the interval 140–187°C in Ar and 140–182°C in air. The corresponding intervals of decomposition are 335–434°C in Ar and 230–361°C in air. In inert Ar atmosphere, CO and CO₂ are liberated simultaneously and MnO is obtained as a final product. In oxidative air atmosphere the evolved CO participate in additional oxy-reduction reactions and only CO₂ is detected. The decomposition is accompanied by oxidation of Mn(II) thus leading to formation of manganese oxides in higher and most probably mixed oxidation states. The investigations at other heating rates and calculation of the reaction enthalpy and activation energy of the processes under different atmospheres are in progress.

E-mail: nhbd@inorg.chem-uni.sofia.bg; vpetkova@nbu.bg; vilmapietkova@gmail.com

Keywords: manganese(II) oxalate; decomposition, DTA/TG, XRD, SEM.

REMOTE DATA COLLECTION AT THE STANFORD SYNCHROTRON RADIATION LIGHTSOURCE

T. Doukov^{1,*} representing the SSRL structural biology team

¹ *Stanford Synchrotron Radiation Lightsource, SLAC, MS 69, 2575 Sand Hill Road,
Menlo Park, CA 94025-7015, USA*

Technological advances in robotics and software coupled with the now global availability of internet access have revolutionized macromolecular crystallography methods enabling real-time experiments carried out by geographically separated collaborators. SSRL has pioneered remote access to the macromolecular beamlines since 2005. The majority of the users ship cryo-cooled samples. User support staff insert these samples into a sample mounting robot dewar. Remote users have complete control over their samples and may collect data from their laboratory or home. The Stanford Automated Mounter (SAM) robot, Blulce control software, and WebIce crystal analysis server handle sample visualization, mounting, dismounting, crystal centering, assessing crystal quality, calculating optimal data collection strategy, and writing notes for each sample into a spreadsheet. Multiple researchers from the same group may login at the same time and take turns, avoiding tiredness, stress, and unnecessary mistakes. Many groups screen large number of crystals and collect data only on the best ones. Automated crystal washing to remove ice bits from the surface of the frozen sample and remote crystal annealing often result in better diffraction data. Data processing is fast and done on a multi-computer linux cluster. Diffraction data backup could be requested using a web browser and the resulting DVDs are sent to the researcher by mail. Users are freed from almost every trivial burden, high travelling costs, stress at the beamline, and may concentrate on achieving the best scientific results.

Recent developments allow: (a) remote collection of UV-Visible spectra on the crystals before, during, and after the x-ray data collection; (b) remote teaching for the new users on simulated beamlines; (c) x-ray raster searches to locate small crystals; and (d) the use of new high density sample containers to very rapidly collect data multiples of crystals using one sample pin. Such approach was also used successfully for the protein sample delivery for the femto-second crystallography experiments at the X-ray free electron laser source (XPP station at the Linac Coherent Light Source (LCLS)).

[1] CA Smith at al., Remote access to crystallography beamlines at SSRL: novel tools for training, education and collaboration. *J. Appl. Crystallogr.* 43 (2010) 1261–1270.

* E-mail: tdoukov@slac.stanford.edu

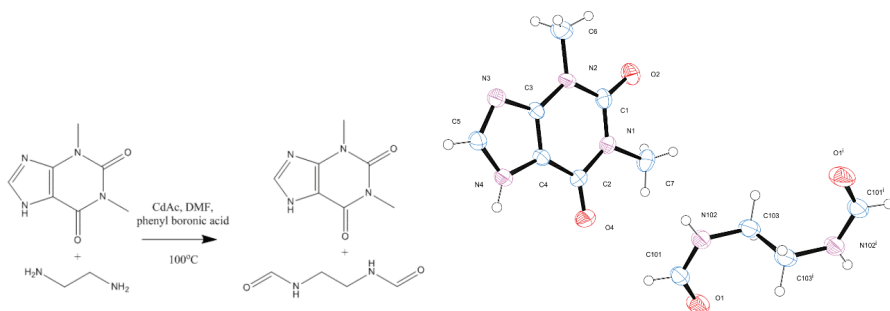
Keywords: protein crystallography, remote access, crystallographic education.

***N,N'*-(ETHANE-1,2-DIYL)DIFORMAMIDE – CATALYTIC EFFECT OF 3-CARBOXYHENYLBORONIC ACID, CADMIUM ACETATE AND THEOPHYLLINE**

V. M. Dylulgerov*, L. T. Dimowa, K. Kossev, R. P. Nikolova, B. L. Shivachev

*Institute of Mineralogy and Crystallography, Bulgarian Academy of Sciences,
1113 Sofia, Bulgaria*

Here we present the unexpected synthesis of *N,N'*-(ethane-1,2-diyl)diformamide. The reaction starting compounds were cadmium acetate, 3-carboxyhenylboronic acid, $C_7H_6BO_4$ and Aminophylline. The reaction was conducted in DMF at 100°C (Scheme 1). Cadmium acetate



Scheme 1. N-formylation of the ethylene diamine and ORTEP view of the co-crystal structure

acts as catalyst for the N-formylation of the diamine. The *N,N'*-(ethane-1,2-diyl)diformamide co-crystallized with theophylline in the triclinic space group P-1, with unit cell parameters $a=6.7437(8)$, $b=8.7847(14)$, $c=9.4656(15)$, $\alpha=91.825(13)^\circ$, $\beta=103.313(12)^\circ$, $\gamma=98.054(12)^\circ$, and $Z=1$. The co-crystal 3D structure is stabilized by intermolecular hydrogen bonds between *N,N'*-(ethane-1,2-diyl)diformamide and Theophylline. The excesses of Theophylline crystallized in a new polymorphic form.

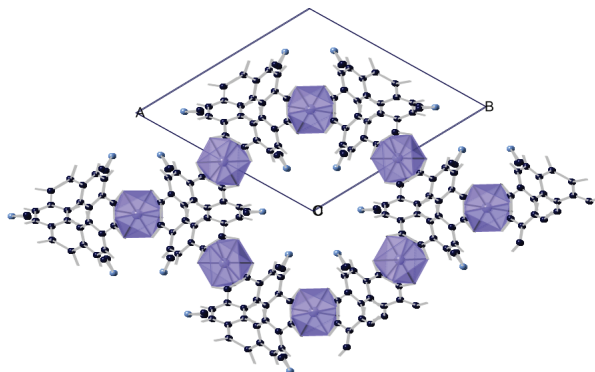
Acknowledgements: This work was supported by ESF (Grant BG051PO001-3.3.06-0027).

CARBOXY PHENYLBORONIC ACID POTENTIAL TEMPLATE FOR ISOSTRUCTURAL MOFs OF TEREPHTHALIC ACID

L. T. Dimova*, V. M. Dylgerov, R. P. Nikolova, B. L. Shivachev

*Institute of Mineralogy and Crystallography, Bulgarian Academy of Sciences,
1113 Sofia, Bulgaria*

A new Cd(II) based metal-organic framework (MOF), $\{[\text{Cd}(\text{CBA})](\text{CH}_3)_2\text{NH}_2\}_n$ (CBA = 3-carboxyphenylboronic acid) has been synthesized and structurally characterized. The MOF is isotypal to the previously reported $\{[\text{Cd}(\text{bdc})](\text{CH}_3)_2\text{NH}_2\}_n$ (bdc = terephthalic acid) exhibits



with slightly different cell parameters. The three-dimensional structural features are conserved (e.g. 1D micropore with ~10 Å diameter) that accommodate guest molecules though the amount of $\text{NH}_2(\text{CH}_3)_2$ is lowered. The picture below shows structural model as visible along c axis.

* E-mail: Louiza.Dimova@gmail.com

Keywords: MOF, single crystal, porous structures.

HIGHSCORE PLUS: CRYSTALLOGRAPHY AND MORE

M. Gateshki, Th. Degen, Th. Dortmann

Panalytical B.V. Lelyweg 1, 7602 EA Almelo, The Netherlands

HighScore Plus is a comprehensive software package for analysis of powder diffraction data with applications including phase identification and quantification, profile fitting, line profile analysis, structure determination, Rietveld analysis and many more.

A recent addition to the program is the possibility to perform statistical analysis of a large number of datasets by similarity analysis and partial least squares methods.

INTENSITY AND SAR DEPENDENT CHANGES IN CONFORMATION OF FROG SKELETAL MUSCLE TOTAL PROTEIN CONTENT AFTER IRRADIATION WITH 2.45 GHZ ELECTROMAGNETIC FIELD

T. Apostolova

*Department of excitable structures, Institute of Biophysics and Biomedical engineering,
Bulgarian Academy of Sciences, Sofia, Bulgaria*

The influence of 2.45 GHz electromagnetic field with high (20 mW/cm²) and low (10 mW/cm²) intensity on frog skeletal muscle protein conformation was studied. Two different fractions (with- and without mitochondria) were preliminary exposed with the electromagnetic field and others were sham exposed. The same ones were lyophilized after that and processed with Fourier transform infrared spectroscopy using Bruker IFS 113 v. Specific absorption rate (SAR) was calculated for both fractions and field intensities. The water mask was removed mathematically. The characteristic peaks and shoulders from Amid I and Amid II bands (descriptive for protein secondary structures) were decomposed and the area under them was calculated. The percentage decrease of α -helices after irradiation with the fields with both intensities and in both fractions after irradiation, was observed. The changes of β -sheets, parallel β -structures, turns, bends and random coils were intensity and SAR dependent. Because of the temperature controlled conditions at whole the time during irradiation, we argue that these conformational changes are specific, non-thermal.

Keywords: electromagnetic field, protein conformation, infrared spectroscopy, frog skeletal muscle.

GROWING SIMULTANEOUSLY LASER GRADE MONOCRYSTALS OF $(\text{Yb}^{3+}, \text{Na}^+): \text{CaF}_2$ & $(\text{Yb}^{3+}, \text{Na}^+): \text{Ca}_{1-x}\text{Sr}_x\text{F}_2$

S. M. Gechev*, O. H. Vitov, J. T. Mouhovski

*Institute of Mineralogy and Crystallography, Bulgarian Academy of Sciences,
Acad. Georgi Bonchev Str., bl. 107, 1113 Sofia, Bulgaria*

Artificially grown fluoride monocrystals should possess minimal structural defects and excellent uniform optical, mechanical and thermal characteristics [1]. The last requires OG conditions to be attained by adjusting the crystallization front (CF) in anyone crystal growth high-temperature gradient technique (TGT) so that the crystallization to proceed by normal growth mechanism and minimum melt supercooling. While the melt supercooling is closely related to the purity of the starting material, the growth mechanism depends itself on the latent heat of fusion and the thermal field configuration in the crucible/furnace unit assembly. All these, can be compensated by precise controlling and setting appropriately the furnace parameters of the growing apparatus. For that purpose, in the present report it is developed a semi-empirical model based on T-measurable variables influencing on the CF conditions in particular Bridgman-Stockbarger crystal growth system.

In the present survey it is used Bulgarian types of starting fluorspar which have several rare-earth and transition metal element traces [2]. Since that, a compositional phase diagram of $\text{Ca}_{1-x}\text{Sr}_x\text{F}_2$ solid solutions with varying x was specified via independently performed Differential Thermal Analysis (DTA) in accordance with the compounds' m.p. Furthermore, the DTA results were compared with other authors' results [3].

After orientation of the grown boules, they were cut appropriately and finely polished for finishing from them several samples as disks (windows), used for UV and IR spectroscopic measurements for finding the optical transmittance and laser generation characteristics. Thus one could determine the grade of the crystals according to their performance parameters.

[1] J.T. Mouhovski et al., Prog. Cryst. Growth Charact. Matter., 57 (2011) 1.

[2] S. Gechev et al., Geoscience, (2013) 21.

[3] D. Klimm et al., J. Cryst. Growth, 310 (2008) 152.

* E-mail: svilen.gechev@yahoo.com

Keywords: laser grade single crystals, optimum growth (OG), phase transformations.

SYNTHESIS AND CRYSTALLIZATION OF GELS IN THE TeO_2 – TiO_2 – ZnO SYSTEM

R. Gegova^{1,*}, A. Bachvarova-Nedelcheva¹, R. Iordanova¹, Y. Dimitriev²

¹ *Institute of General and Inorganic Chemistry, BAS, "Acad. G. Bonchev" str., bld. 11, 1113 Sofia, Bulgaria*

² *University of Chemical Technology and Metallurgy – Sofia, "Kl. Ohridski" blvd, 8, 1756 Sofia, Bulgaria*

The sol-gel processing offers an attractive route for the fabrication of TeO_2 -based materials but most of the authors applied it mainly for obtaining of thin films. Up to now, the investigations concerning bulk and powder materials are scarce. The purpose of this investigation is to study the synthesis and crystallization of gels in the TeO_2 - TiO_2 - ZnO system applying a sol-gel method. In order to overcome the problem with high hydrolysis rate of the Te (VI) alkoxide, the telluric (VI) acid (H_6TeO_6) along with zinc acetate and titanium butoxide were used as a new combination of precursors during the synthesis. The structure and optical properties of several representative compositions with different TeO_2 : TiO_2 : ZnO ratios were studied.

The crystallization tendency of the powders in the temperature range 300–700°C was investigated. By XRD analysis was established that the crystallization process started at heat treatment at 300°C and mixtures containing TiO_2 (anatase), ZnTiO_3 and ZnTeO_3 were obtained depending on composition and heating temperature. IR spectroscopy showed that the organic constituents existed below 300°C and characteristic bands for TiO_2 and ZnTiO_3 appeared in the range 300–500°C.

* E-mail: r.gegova@svr.igic.bas.bg

Keywords: sol-gel, telluric (VI) acid, crystallization.

SYNTHESIS, SINGLE-CRYSTAL STRUCTURE AND SPECTROSCOPIC CHARACTERIZATION OF COPPER(II) COMPLEXES WITH BIS((DIMETHYLPHOSPHINYLMETHYL)AMINE

Zh. Georgieva¹, A. Ugrinov², R. Petrova³, B. Shivachev³, S. Zareva¹,
S. Varbanov⁴, T. Tosheva⁴, G. Gencheva^{1,*}

¹ Faculty of Chemistry and Pharmacy, Sofia University "St. Kliment Ohridski",
1164 Sofia 1 J. Bourchier Blvd., Bulgaria

² Department of Chemistry and Biochemistry, North Dakota State University,
Fargo, ND 58102, United States

³ Institute of Mineralogy and Crystallography "Acad. Ivan Kostov", Bulgarian Academy of Sciences,
Acad. G. Bonchev str., bl. 107, 1113 Sofia, Bulgaria

⁴ Institute of Organic Chemistry with Center of Phytochemistry, Bulgarian Academy
of Sciences, 1113 Sofia

Recently coordination chemistry of tridentate O,N,O-ligand bis((dimethylphosphinyl)-methyl) amine, L, has been intensively investigated by reactions with transition metal ions such as Pt²⁺, Pd²⁺, Zn²⁺, Cu²⁺, Mn²⁺, etc. It was found that the reaction conditions and the nature of the metal ions used control the mode of the ligand coordination. The structural diversity of coordination polyhedra of copper(II) compounds is related to d⁹ electron configuration. Synthesis and structural characterization of octahedral copper(II) complex of the titled ligand are reported. The compound was obtained during the interaction with CuCl₂·H₂O at ligand excess (L:Cu=4)

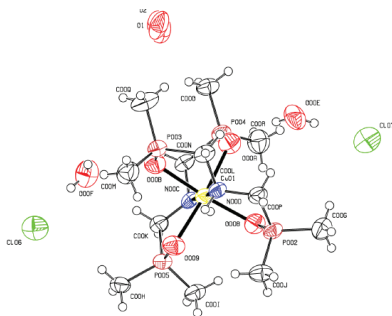


Fig. 1. Molecular structure of [Cu²⁺(L)₂]Cl₂·H₂O.

and recrystallized repeatedly in ethanol medium. The molecular structure of [Cu²⁺(L)₂]Cl₂·H₂O, Fig. 1, consists of discrete six-coordinate [Cu²⁺(L)₂]²⁺ cations, two chloride ions and two water molecules. The two ligands are coordinated in a tridentate mode. Cu²⁺ ions in the CuO₄N₂-chromophores exhibit tetragonally compressed octahedral coordination. The coordination octahedron is slightly affected by the Jahn Teller effect.

* E-mail: ggencheva@chem.uni-sofia.bg

Keywords: Copper(II) complexes, Tertiary phosphine oxides, Structural characterization.

AHEAD-ASIDE AGGREGATION (AAA) MODEL: TOWARDS MODELLING THE ELECTRODEPOSITION OF Ni–Cu ALLOYS

D. Goranova^{1,*}, R. Rashkov¹, A. Kolevski², V. Tonchev¹

¹ *Institute of Physical Chemistry, Bulgarian Academy of Sciences, 1113 Sofia, Bulgaria*

² *Aleksandrovskia University Hospital, 1431 Sofia, Bulgaria*

We extend our studies [1] of the electrodeposition of Cu-Ni alloys in the far-from-equilibrium range of parameters. Thus we are able, based on elemental analysis of the resulting morphologies, to conclude that Cu deposits preferentially in the convex regions while Ni prefers the concave ones. This *macroscopic* finding is translated into the *microscopic* deposition rules of a DLA-like model which we call Ahead-Aside Aggregation (AAA) model. AAA-model differs from our previous attempt [2] to model the growth of two distinct species in adopting asymmetric attachment rules – while “copper” particles attach only to these parts of the deposit that contain only copper, for the deposition of a “nickel” particle more than one occupied nearest neighbors of either kind are needed.

The rules for particle generation also differ. The “copper” particles are released far from the growing aggregate as in the original DLA model since Cu deposits in the range of diffusion limitations. We choose to generate a “nickel” particle from a site where a “copper” particle is just deposited but with a given probability. As an initial step of the model validation we compare the resulting morphologies and at the end of presentation discuss the further directions of model improvement through adopting suitable monitoring schemes aimed at achieving model validation on a quantitative level.

[1] D. Goranova, G. Avdeev, R. Rashkov, *Surface & Coatings Technology*, 240 (2014) 204.

[2] B. Rangelov, D. Goranova et al., *Compt. Rend. Acad. Bulg. Sci.*, 65 (2012) 913.

* E-mail: desislavagoranova@gmail.com

Keywords: Alloy electrodeposition, Far-from-equilibrium growth models, Convex-concave attachment, Morphology tuning

STRUCTURE, SPECTROSCOPIC PROPERTIES AND *IN VITRO* ANTIPROLIFERATIVE EFFECTS OF NEW Au^{III} COMPLEXES WITH DIPYRIDIN-2-YLAMINE

P. Gorolomova¹, B. Krebs², R. Petrova³, B. Shivachev³, S. Simova⁴,
G. Momekov⁵, G. Gencheva^{1,*}

¹ Faculty of Chemistry and Pharmacy, Sofia University "St. Kliment Ohridski", 1164 Sofia
1 J. Bourchier Blvd., Bulgaria

² Anorganisch-Chemisches Institut der Universität Münster, Wilhelm-Klemm-Strasse 8, Germany

³ Institute of Mineralogy and Crystallography "Acad. Ivan Kostov", Bulgarian Academy of Sciences,
Acad. G. Bonchev str., bl. 107, 1113 Sofia, Bulgaria.

⁴ Institute of Organic Chemistry with Centre of Phytochemistry, Bulgarian Academy of Sciences,
Acad. G. Bonchev str., bl. 9, 1113 Sofia, Bulgaria

⁵ Faculty of Pharmacy Medical University-Sofia 2 Dunav Str., 1000 Sofia, Bulgaria.

The development of novel metal-based compounds with a pharmacological profile different from that of the clinically-used platinum drugs is a way to address the disadvantages of cisplatin such as poor oral bioavailability, undesired toxic effects and drug resistance. Among them, the gold(III) complexes have great potential as anticancer agents, because there are many experimental evidences which proved that their growth inhibition effects pass through a variety of DNA-independent mechanisms. In this study we present the synthesis, structural characterization and cytotoxic studies of two Au^{III}-complexes of dipyrindin-2-ylamine (dpa). The complex cation [Au(dpa)Cl₂]⁺, *Au1*, was obtained in acidic medium and isolated as compounds: [Au(dpa)Cl₂]Cl, *Au1a*, (orthorhombic Pnma space group, *a* = 27.5104(17), *b* = 12.3308(16), *c* = 8.2024(12) Å), and [Au(dpa)Cl₂][AuCl₄], *Au1b*, (monoclinic P2₁ space group, *a* = 8.9273(6), *b* = 12.0903(10), *c* = 16.4352(14) Å, β = 105.684(3)°).

A neutral complex with a composition [Au(dpa₋₁)Cl₂], *Au2*, was produced in alkaline medium (pH=9.5). The structures of the complexes have been characterized by single-crystal X-ray diffraction, spectroscopic methods: IR and NMR and DFT calculations. The ligand is coordinated in a bidentate mode respectively: symmetrically through the pyridine N-atoms in *Au1* and asymmetrically via a pyridine N-atom and the N-atom from the deprotonated amine group in *Au2*. The new compounds exhibited prominent antiproliferative effects against a panel of human tumor cell lines in a micromolar range of concentrations as the difference in activity is a function from the mode of the ligand coordination.

Acknowledgements: The Fund "Scientific Research", Ministry of Education and Science, Project DDVU02-66 is acknowledged.

* E-mail: ggencheva@chem.uni-sofia.bg

Keywords: Gold(III) complexes, Structural characterization, DFT calculations.

SYNTHESIS, STRUCTURAL CHARACTERIZATION AND IN-VITRO ANTIPROLIFERATIVE EFFECTS OF OCTAHEDRAL PLATINUM(IV) COMPLEXES WITH 1,3,5-TRIAMINO-1,3,5-TRIDEOXY-CIS-INOSITOL

K. Hegetschweiler¹, V. Velcheva^{2,*}, A. Ugrinov³, G. Momekov⁴, G. Gencheva²

¹ *Anorganische Chemie, Universität des Saarlandes, Postfach 151150, D-66041, Saarbrücken, Germany*

² *University of Sofia "St. Kliment Ohridski", Faculty of Chemistry and Pharmacy, 1 James Bouchier blvd., 1164 Sofia, Bulgaria*

³ *Department of Chemistry and Biochemistry, North Dakota State University, Fargo, ND 58102, United States*

⁴ *Department of Pharmacology, Pharmacotherapy and Toxicology, Faculty of Pharmacy, Medical University-Sofia, 2 Dunav str., 1000 Sofia, Bulgaria*

A tridentate chelating ligand, 1,3,5-triamino-1,3,5-trideoxy-cis-inositol (taci), was used to synthesize stable octahedral mononuclear Pt⁴⁺ complexes. This ligand exhibits unique coordinating properties in consequence of the two kinds donor functional groups, spatially disposed as a set (N,N',N'' and O,O',O'') in equatorial or axial positions in the two distinct stable chair conformations. Thus, four modes of ligand coordination are accessible according to the steric requirements and electronic properties of the metal ions. The interaction of taci.3H₂O and PtI₆²⁻ in an aqueous solution resulted in the immediate precipitation of a mixture of complex species with variable composition and color depending on the acidity of the medium. Coordination compounds with defined composition were obtained by heating the solids with 0.5 M NaOH solution (a calculated amount). Single crystals of the red compound [Pt(taci)₃].1.3H₂O, 1A (monoclinic P2₁/c) were obtained through repeated recrystallization from water solution at pH=5. Crystals of anhydrous compound [Pt(taci)₃], 1B (triclinic P-1) were grown by slow diffusion of ether into DMF solution of 1A. Yellow crystals of [Pt(taci)₂](CO₃)₂.3H₂O, 2 (monoclinic C2/c) were obtained from an alkaline-water solution (at pH=9) and in the presence of CO₃²⁻. Pt⁴⁺ cations exhibit distorted octahedral coordination of PtN₃I₃ in 1 and PN₆ in the 1:2 bis-complex 2. The taci ligand adopts a chair conformation with axial amino groups coordinated to platinum. The compounds showed notable antiproliferative properties, which are superior for the complex 1 in *in vitro* tests with a panel of human malignant cell lines together with low nephrotoxicity.

* E-mail: vyara.velcheva@gmail.com

Keywords: 1,3,5-triamino-1,3,5-trideoxy-cis-inositol, Pt⁴⁺ complexes, single-crystal X-ray analysis, *in vitro* antiproliferative effect.

SPECTROSCOPIC AND KINETIC STUDIES OF MIXED LIGAND COMPLEXES OF BIPYRIDYL AND GLYCINE AS INTERCALATORS AND THEIR BEHAVIORS AS ANTIOXIDANTS

Mohamed M. Ibrahim*

*Department of Chemistry, Faculty of Science, Taif University,
Taif - Al-Haweiah - P.O.Box 888, Saudi Arabia*

A series of mixed ligand complexes, viz., $[\text{Cu}(\text{BPy})(\text{Gly})\text{X}]\text{Y}$ $\{\text{X} = \text{Cl}$ (**1**), $\text{Y} = 0$; $\text{X} = 0$, $\text{Y} = \text{ClO}_4^-$ (**2**); $\text{X} = \text{H}_2\text{O}$, $\text{Y} = \text{NO}_3^-$ (**3**); $\text{X} = \text{H}_2\text{O}$, $\text{Y} = \text{CH}_3\text{COO}^-$ (**4**); and $[\text{Cu}(\text{BPy})(\text{Gly})-(\text{H}_2\text{O})_2](\text{SO}_4)$ (**5**) have been synthesized. Their structures and properties were characterized by elemental analysis, thermal analysis, IR, UV–vis, and ESR spectroscopy, as well as electrochemical measurements including cyclic voltammetry, electrical molar conductivity, and magnetic moment measurements. Complexes **1** and **2** were structurally characterized by using X-ray crystallography. Complex **1** shows distorted square pyramidal CuN_3OCl coordination geometry in which the N,O-donor amino acid and the N,N-donor bipyridyl bind at the basal plane with chloride ion as the axial ligand. The crystal structure of complex **2** shows square planar CuN_3O coordination geometry, which exhibits chemically significant hydrogen bonding interactions besides showing coordination polymer formation. Spectral features led to the conclusion that complexes **1**, **3–5** display square-pyramidal geometries. While complex **2** displays square planar geometry, which suggests that the removal of the chloride ion has influence on the coordination geometry.

The superoxide dismutase and catalase-like activities of both complexes were tested and were found to be promising candidates as durable electron-transfer catalyst being close to the efficiency of the mimicking enzymes displaying either catalase or tyrosinase activity to serve for complete reactive oxygen species (ROS) detoxification, both with respect to superoxide radicals and related peroxides. On interaction with DNA, the quasi-reversible $\text{Cu}^{II}/\text{Cu}^I$ redox couple slightly improves its reversibility with considerable decrease in current intensity. The intercalation of these copper complexes into the DNA base pairs was also investigated by gel retardation assay method. All the experimental results indicate that the bipyridyl mixed copper(II) complexes intercalate more effectively into the DNA base pairs.

* E-mail: ibrahim652001@yahoo.com

Keywords: Enzyme mimics; characterization; Superoxide dismutase; Catalase.

COMPARATIVE ANALYSIS OF SOME PHYSICO-CHEMICAL PROPERTIES OF THE GLASSY SISTEMS (GeSe₅)_{100-x}In_x AND (GeTe₅)_{100-x}In_x

VI. Ivanova^{1,*}, A. Stoilova¹, Y. Trifonova¹, P. Petkov¹

¹ *University of Chemical Technology and Metallurgy , 8 Kl. Ohridski blvd,
Sofia 1756, Bulgaria*

Our study concerns the both glassy systems (GeSe₅)_{100-x}In_x and (GeTe₅)_{100-x}In_x, which contain different chalcogen elements. Se and Te-rich chalcogenide glasses are interesting because of its use in switching and memories device. But they exhibit high resistivity values implying certain limitations, as short lifetime and low sensitivity, in their applications. To get rid of limitations we add third element In info Ge-Se(Te) matrix. As a result of addition of In new properties are expected, which can be related with stucture transitions. The investigation of the physico-chemical properties gives more information about the real structure of glasses.

In this paper some physico-chemical properties have been obtained as density, compactness, molar volume, number of constrains per atom and overall mean bond energy and correlated with mean coordination number. The correlations between the composition and properties of the glasses are discussed with the view of structural transformation in the glassy matrix.

* E-mail: vladi_hr_iv@abv.bg

Keywords: chalcogenide glasses, physico-chemical properties, structure.

CRYSTALLOGRAPHIC STRUCTURE AND VIBRATIONAL MODES OF MERCURY TELLURIDE NANOWIRES ENCAPSULATED IN SINGLE WALLED CARBON NANOTUBES

V. G. Ivanov^{1,*}, J. Sloan², D. C. Smith³, E. Faulques⁴

¹ Sofia University, Faculty of Physics, 5 James Bourchier Blvd, BG 1164 Sofia, Bulgaria

² Department of Physics, University of Warwick, Coventry CV4 7AL, United Kingdom

³ School of Physics and Astronomy, University of Southampton,
Southampton SO17 1BJ, United Kingdom

⁴ Institut des Matériaux Jean Rouxel, University of Nantes, CNRS, UMR6502,
F-44322 Nantes, France

Confinement to lower spatial dimensions results in substantial modification of the structure and electronic properties of materials, as compared to those in their bulk forms. Filled single walled carbon nanotubes (SWCNT) provide the unique possibility for 1-dimensional (1D) controlled crystal growth and synthesis of structures having no analogues in the 3D world.

In this work we report on the density functional theory (DFT) calculation of the equilibrium structure and vibrational modes of HgTe nanowires encapsulated in SWCNT (HgTe@SWCNT). We confirmed the stability of the structure for the suggested rod symmetry group #29 ($p4_2/m$) by studying the phonon dispersion along the Γ –Z line of the 1D Brillouin zone (BZ). Our calculations confirm opening of an energy gap of ~ 1.35 eV in the 1D electronic band structure in contrast to the gapless band structure of the bulk HgTe material.

The calculated frequencies of the Γ -point Raman-active modes are in fair correspondence to those obtained experimentally on HgTe@SWCNT nanowires produced by melt infiltration into bundles of SWCNT. The strong resonant enhancement of Raman bands at excitation-photon energy of ~ 1.75 eV, as well as the appearance of multiple overtone bands, corroborate the opening of an energy gap in the 1D electronic spectrum.

* E-mail: vgi@phys.uni-sofia.bg

Keywords: nanowires, HgTe@SWCNT, DFT, Raman spectroscopy.

AGING EFFECTS ON THE STRUCTURAL AND PHOTOCATALYTIC PROPERTIES OF ZnO SOL-GEL FILMS FOR DEGRADATION OF PHARMACEUTICAL DRUGS

N. Kaneva*, A. Bojinova, K. Papazova

Laboratory of Nanoparticle Science and Technology, Department of General and Inorganic Chemistry, Faculty of Chemistry and Pharmacy, University of Sofia, 1164 Sofia, Bulgaria

In this work, ZnO thin films are prepared by sol–gel method and the effect of aging time of the ZnO sol on the structural and photocatalytic properties of the films is studied. ZnO sol is aged for different periods (0, 30 and 60 days). Nanocrystalline thin films with different thickness (one and five coats) are deposited on glass substrates via dip-coating technique. The structural properties of samples are analyzed by Scanning Electron Microscopy and X-ray diffractometer. The effect of the aging time of the starting sol is studied in respect to photocatalytic degradation of the pharmaceutical drugs (*Paracetamol (PCA)* and *Chloramphenicol (CA)*) by UV-vis spectroscopy. The experiments are conducted under UV and visible light irradiation.

The results show, that the increasing aging time of the starting solution with respect to ZnO generally promotes photocatalytic activity. The films with one coating have lower rate constants of degradation with comparison to the other samples. The thin films with five coats obtained from ZnO sol, aged 60 days exhibit highest photocatalytic degradation of the drugs (*PCA*: UV – 84.57% and Vis – 65.66%; *CA*: UV – 67.2% and Vis – 52.2%) in comparison to the freshly prepared ones (*PCA*: UV – 29.60% and Vis – 18.62%; *CA*: UV – 18.43% and Vis – 14.12%).

Acknowledgements: This research is financially supported by project FP7 project Beyond Everest and Russian Presidential Program of engineer advanced training.

* E-mail: nina_k@abv.bg

Keywords: Photocatalysis, ZnO sol-gel films, UV, visible, Paracetamol, Chloramphenicol.

EFFECT OF THICKNESS ON THE PHOTOCATALYTIC PROPERTIES OF ZnO THIN FILMS

N. Kaneva*, G. Lazarova, A. Bojinova, K. Papazova, D. Dimitrov

Laboratory of Nanoparticle Science and Technology, Department of General and Inorganic Chemistry, Faculty of Chemistry, University of Sofia, 1 James Bourchier Blvd., 1164 Sofia, Bulgaria

Nanostructured zinc oxide films are prepared by sol-gel method using dip-coating technique. The thin films are deposited on glass substrates with different thickness (1, 3, 5 and 7 coats). The samples are characterized by means of SEM, XRD and UV-visible analyses. The aim of our investigations is photocatalytic degradation of the organic dyes – *Malachite Green* (MG, triarylmethane dye) and *Methylene Blue* (MB, heterocyclic aromatic dye) under UV-light illumination.

The photocatalytic results show that the thickest films on glass exhibit the highest efficiency under UV-light. The thin films with one coating have lowest rate constants in comparison with the other samples. The ZnO films with 7 coats have better photocatalytic efficiency and faster degradation MG compared to MB. The reason for this is the formation of a stable intermediates in the reaction of OH radicals with triarylmethane dye (C=C bond) during the photocatalysis.

Acknowledgements: This research is financially supported by project FP7 project Beyond Everest and Russian Presidential Program of engineer advanced training.

* E-mail: nina_k@abv.bg (N. Kaneva)

Keywords: ZnO, thin films, thickness, photocatalysis, sol-gel, organic dyes.

HYDROGEN BOND STRENGTH IN SOME BERILLIUM COMPOUNDS. CORRELATION BETWEEN STRUCTURAL DATA AND INFRARED SPECTRA

V. Karadjova^{1,*}, M. Wildner², D. Manasieva³, D. Stoilova³

¹ Department of Inorganic Chemistry, University of Chemical Technology and Metallurgy,
8 Kl. Ohridski Str., 1756 Sofia, Bulgaria

² Universität Wien, Geozentrum, Institut für Mineralogie und Kristallographie, Althanstr. 14,
A-1090 Wien, Austria

³ Institute of General and Inorganic Chemistry, Bulgarian Academy of Sciences, bl. 11,
1113 Sofia, Bulgaria

The crystal structures of some beryllium compounds, $\text{BeSO}_4 \cdot 4\text{H}_2\text{O}$, and $\text{M}_2\text{Be}(\text{XO}_4)_2 \cdot 2\text{H}_2\text{O}$ ($\text{X} = \text{S}, \text{Se}$; $\text{M} = \text{K}, \text{Rb}$), as determined from single crystal X-ray diffraction data are discussed. The structure of $\text{BeSO}_4 \cdot 4\text{H}_2\text{O}$ is composed of isolated $\text{Be}(\text{H}_2\text{O})_4^-$ and SeO_4 tetrahedra, which are interconnected by strong hydrogen bonds. The double salts are characterized by three-membered chain fragments, composed of a central $\text{BeO}_2(\text{H}_2\text{O})_2$ tetrahedra sharing corners with two SO_4 tetrahedra. These bent $[\text{Be}(\text{SO}_4)_2(\text{H}_2\text{O})_2]^{2-}$ units are linked by potassium and rubidium ions and hydrogen bonds to double layers.

The strengths of the hydrogen bonds are analyzed in terms of the respective O_w/O bond distances, the $\text{Be}-\text{OH}_2$ interactions (*synergetic* effect), the proton acceptor capabilities of the oxygen atoms as deduced from Brown's bond valence theory, the *anti-cooperative* effect. The intramolecular $\text{O}-\text{H}$ bond lengths are derived from the νOD vs. rOH correlation curve.

The analysis of the infrared spectra reveals: (i) The water molecules in $\text{BeSO}_4 \cdot 4\text{H}_2\text{O}$ and in the double salts are strongly energetically distorted. (ii) The hydrogen bonds in $\text{K}_2\text{Be}(\text{SeO}_4)_2 \cdot 2\text{H}_2\text{O}$ are stronger than those in $\text{K}_2\text{Be}(\text{SO}_4)_2 \cdot 2\text{H}_2\text{O}$ due to the stronger proton acceptor capability of the SeO_4^{2-} ions. (iii) The proton donor strength of the water molecules in $\text{K}_2\text{Be}(\text{SO}_4)_2 \cdot 2\text{H}_2\text{O}$ and $\text{K}_2\text{Be}(\text{SeO}_4)_2 \cdot 2\text{H}_2\text{O}$ is greater than that of the water molecules in $\text{BeSO}_4 \cdot 4\text{H}_2\text{O}$ and $\text{BeSeO}_4 \cdot 4\text{H}_2\text{O}$ due to the different compositions of the respective beryllium tetrahedra. (iv) The formation of stronger hydrogen bonds in $\text{K}_2\text{Be}(\text{SO}_4)_2 \cdot 2\text{H}_2\text{O}$ than those in the respective rubidium compound is owing to the smaller ionic size of K^+ .

* E-mail: vkar@mail.bg

Keywords: beryllium compounds; crystal structures; infrared spectroscopy; hydrogen bond strength.

SYNTHESIS, STRUCTURE AND PROPERTIES OF INNOVATIVE CERAMICS FROM INDUSTRIAL WASTES

A. Karamanov

*Institute of Physical Chemistry, Bulgarian Academy of Sciences, Acad. G. Bonchev Str.,
Block 11, 1113 Sofia, Bulgaria*

New type of building ceramics, containing no traditional fluxes and huge amounts of industrial wastes, is discussed. The peculiarities of sintering behaviour and phase formation are elucidated by optical dilatometry and differential thermal analyses. The structures of and the phase compositions are studied by SEM-EDS and XRD. The main technological characteristics of the optimal compositions are also measured.

It is demonstrated that the chemical and phase compositions of these new building materials are similar to some glass-ceramics by industrial wastes, which however are produced by a more complicated and more expensive technology. In addition, the obtained samples are characterized with very low water soaking, moderate closed porosity and fine-polycrystalline structure, which lead to improvement of the mechanical properties.

The total crystallinity is estimated as 50–60 wt% and the main crystal phases are identified as anorthite solid solutions and pyroxene solid solutions, presented mainly by 3–6 μm hexagonal and 5–10 prismatic crystallites, respectively. This high amount of crystal phase and the observed unusual rough crystalline structure of formed closed pores are explained by an additional phase formation during the sintering and cooling steps.

* E-mail: karama@ipc.bas.bg

Keywords: ceramics, wastes, crystal phases, sintering.

PREPARATION, STRUCTURE AND CATALYTIC PROPERTIES OF COPPER-ZINC FERRITES

K. Koleva¹, N. Velinov^{1,*}, T. Tsoncheva², I. Mitov¹

¹ *Institute of Catalysis, BAS, Sofia, 1113, Bulgaria*

² *Institute of Organic Chemistry with Centre of Phytochemistry, BAS, Sofia, 1113, Bulgaria*

The ferrite materials are denoted with general formula AB_2O_4 . The distribution of metal ions in crystal lattice determines ferrites as normal, inverse and partial inverse one. In the $ZnFe_2O_4$ ferrite the tetrahedral (A) sites are occupied by only one type of cations. This is because of the preferences of Zn^{2+} to occupy the tetrahedral spinel sites forming normal spinel, while Cu^{2+} occupies mainly the octahedral [B] sites, and thus, the tetrahedral sites are occupied by half of Fe^{3+} and $CuFe_2O_4$ describes as inverse spinel. In the case of $Cu_{1-x}Zn_xFe_2O_4$, where $0 < x < 1$, the tetrahedral sites are occupied both by Zn^{2+} and Fe^{3+} cations and its spinel structure are denoted as partially inverse.

The aim of present work is to prepare samples with chemical compositions $Cu_{1-x}Zn_xFe_2O_4$ and to study the catalytic activity in reaction of methanol decomposition to CO and hydrogen. The cation distribution in ferrites and phase changes of catalysts under the reaction medium were also in the focus of the study.

The highest catalytic activity and significantly good selectivity of methanol decomposition to H_2 and CO was registered for the $Cu_{0.8}Zn_{0.2}Fe_2O_4$ ferrite. Mössbauer study of samples after the catalytic test reveals transformation of the initial ferrite phase with the formation of Zn-substituted magnetite ($Zn_xFe_{3-x}O_4$), Hägg carbide (Fe_2C_5), wuestite and α -Fe in different ratio.

Acknowledgements: The present work is financially supported by the Bulgarian National Science Fund under Project DFNI-E01/7/2012 and ДИД-02-38/2009.

* E-mail: nikivelinov@ic.bas.bg

Keywords: copper-zinc ferrite, Mössbauer spectroscopy, methanol decomposition.

CRYSTAL STRUCTURE AND PROPERTIES OF CARBAMIDE AND THIOCARBAMIDE ADDUCTS OF TETRABUTYL AMMONIUM HYDROGEN SULPHATE

K. Kossev*, N. Petrova, R. Nikolova, B. Shivachev

*Institute of Mineralogy and Crystallography "Acad. Iv. Kostov" Bulgarian Academy of Sciences,
Acad. G. Bonchev str., building 107, 1113 Sofia, Bulgaria*

Urea and its sulfur analog thiourea are products of large-scale chemical production. Thiourea and urea displays similar properties with the difference that thiourea is "softer" electron donor due to the higher energy of the bonding molecular orbitals of sulfur than those of oxygen. Both, urea and thiourea, form inclusion compounds with a number of inorganic and organic substances, i.e. urea clathrates of H_2O_2 , H_3PO_4 , CH_3OH . Methods based on clathrates formation were developed for industrial separation of linear from branched paraffinic hydrocarbons. Another example is the H_2O_2 clathrate (hydroperit) which is used in medicine as convenient and safe "solid form" of hydrogen peroxide for wound treatment. Complexes of urea and thiourea with transition and non-transition metals have been studied. Urea (thiourea) molecules replace completely or partially the crystallization water in the structure of the inorganic crystal hydrates. It is also known that urea and thiourea form salts with a number of inorganic and organic acids.

Urea adducts with tetraalkyl ammonium salts have been previously studied in order to solve their crystal structures and thermal properties [1]. The present communication concerns the preparation, structural and thermal characterization of two new urea and thiourea adducts. We investigated the co-crystallization of tetrabutyl ammonium hydrogen sulfate ($\text{Bu}_4\text{N}.\text{HSO}_4$) in the presence of urea and thiourea from aqueous or water-methanol solutions. The crystal structure of both adducts $\text{Bu}_4\text{N}.\text{HSO}_4.\text{U}$ (**1**) and $\text{Bu}_4\text{N}.\text{HSO}_4.\text{TU}$ (**2**) was solved. While **1** crystallizes in Monoclinic $P2_1/c$ space group the **2** crystallizes in tetragonal $I4_1/a$. The cations and anions in **1** produce a layer-like arrangement of alternating tetrabutyl ammonium and hydrogen-sulfate moieties. In the case of $\text{Bu}_4\text{N}.\text{HSO}_4.\text{U}$, the DTA analysis definitely shows an endothermic effect of melting at 97°C , while in the case of $\text{Bu}_4\text{N}.\text{HSO}_4.\text{TU}$, this effect is not observed due to the gradually softening up to 170°C . Probably the reason for this phenomenon is the lower polarity of the thiourea molecule comparing to that of urea. The melting behavior of both investigated adducts is rather similar of that of urea/thiourea adducts with tetraalkyl ammonium salts [1]. The main decomposition of (**1**) and (**2**) is observed on DTA and TG curves after 170°C .

[1] K. Kossev, H. Sbirikova, N. Petrova, B. Shivachev, R. Nikolova, Bulgarian Chemical Communications, 45, 4 (2013) 445.

* E-mail: k_kossev@yahoo.com

Keywords: Urea, thiourea, adducts, single crystal.

CRYSTALLOGRAPHY OF THE POLYHEDRON, ENANTIOMORPHISM AND A FIVE-FOLD SYMMETRY CODE IN DÜRER'S "MELENCOLIA I"

R. I. Kostov

University of Mining and Geology "St Ivan Rilski, Sofia 1700

Symmetry is a potential tool to find connections between science and art. The engraving "Melencolia I" (1514) by the famous German artist Albrecht Dürer (1471–1528) remains as one of the enigmatic art works. A large number of publications is devoted to the symbolism and interpretation of this engraving, representing a dominant crystal (polyhedron): cube, distorted (acute angle of crystal 80°) [1]; cube, oblique view (90°) [2]; truncated rhombohedron (72°), with the idea of golden section [3–4]; ($79^\circ 36'$) [5]; octahedron (60°) [6], fluorite octahedron (importance in metallurgy) [7]; (76°) linked to ancient pyramids [8]; ($81^\circ 47'$) ratio between two diagonals of the rhomb [9–10]; calcite ($79^\circ \pm 1^\circ$) truncated rhombohedron [11]; alunite (importance in paper industry) [12]; cube, enlarged vertically by a ratio [13]. The 72° hypothesis is most plausible to adopt, as related to five-fold symmetry (golden mean; the number 5 in the "magic square" is turned upside down; 5 keys): the center for a pentagon in a circle placed at the book of the angel can point to: key-foot-dog-(ladder+crystal)-head(angel) (c. also the hexagon, heptagon and nonagon "key"). As the engraving is made as a mirror image, the "real" enantiomorphic image must also be considered (a sketch by Dürer is known; Dresden, N22). Five-fold symmetry can be traced in some other of Dürer's engravings as "Knight, Death and the Devil" (1513) and "St. Jerome in His Study" (1514). The artist has applied five-fold symmetry in his geometric studies [14], constructing a pentagon or a dodecahedron in plan and elevation.

- [1] J. Harnest, Festschrift Luitpold Dussler (1972) 189.
- [2] F.A. Nagel, Der Kristall auf Dürers Melancholie (1922).
- [3] P. Grodzinski, Intern. Diamond Rev. 15 (1955) 66.
- [4] P. Schreiber, Historia Mathematica 26 (1999) 369.
- [5] D.H. Richter, Zt. Vermessungswesen 86 (1957) 284.
- [6] P.J. Federico, Mathematics Mag. 45 (1972) 30.
- [7] D.P. Grigoriev, I.I. Schafranovsky, Fortschr. Mineral. 50 (1973) 205.
- [8] F. Deckwitz, Dürer's Melencolia with Compasses and Ruler (1978).
- [9] E. Schröder, Dürer Kunst und Geometrie (1980).
- [10] A.L. Mackay, Nature 301 (1983) 652.
- [11] C.H. MacGillavry, Proc. Koninkl. Nederl. Akad. Wetensch. B 79 (1981) 287.
- [12] J.M. Frías, J. Nadal, Tierra y tecnología 30 (2006) 60.
- [13] I. Hideko, Aesthetics 13 (2009) 179. [14] G.P. Matvievskaia, Albrecht Dürer – Scientist (1987).

* E-mail: rikostov@yahoo.com

Keywords: five-fold symmetry, Dürer, "Melencolia I".

INFLUENCE OF HIGH ENERGY MILLING ACTIVATION ON NANO-TO-MICRO-SIZED CaCO_3 CRYSTALS FORMATION

B. Kostova^{1,*}, V. Petkova^{1,2}, M. Shopska³, G. Kadinov³, M. Baláž⁴, P. Baláž⁴

¹ *New Bulgarian University, Department of Natural Sciences, 1618 Sofia,
21 Montevideo Str., Bulgaria*

² *Institute of Mineralogy and Crystallography, Bulgarian Academy of Sciences, 1113 Sofia,
Acad. G. Bonchev Str., bldg.107, Bulgaria*

³ *Institute of Institute of Catalysis, Bulgarian Academy of Sciences, 1113 Sofia,
Acad. G. Bonchev Str., bldg.11, Bulgaria*

⁴ *Institute of Geotechnics, Slovak Academy of Sciences, Watsonova 45,
043 53 Košice, Slovak Republic*

It is well known that high energy milling (HEM) activation increase the crystals degree of reactivity enhancing their specific surface area (SSA) due to decreasing of particle size [1].

We inspected the behavior of eggshells CaCO_3 -crystals during HEM activation for 10, 130 and 360 min. The results show decrease of sample particles to nano-sized after 10 min activation and increase to micro-sized after 130 as well as 360 min activation. Further, the SSA of all investigated samples generally increase in comparison to non-activated sample.

The established results can be explained with: (i) recrystallization with increasing crystal size only and (ii) polymorph transformations, both investigated by Scanning Electron Microscopy [2], Powder X-Ray Diffraction [3] and Fourier Transform Infra-Red Spectroscopy [4].

[1] K. Tõnsuaadu, T. Kaljuvee, V. Petkova, R. Traksmäa, V. Bender, K. Kirsimäe, International Journal of Mineral Processing, 100 (2011) 104.

[2] W. Sekkal, A. Zaoui, Scientific Reports, 3 (2013) 1587.

[3] Powder Diffraction Files (2001) Joint Committee on Powder Diffraction Standards ICDD.

[4] M. Reichenbacher, J. Popp, Challenges in Molecular Structure developmen, Ch. 2, Springer 657.

* E-mail: bkostova@nbu.bg

Keywords: egg shells, CaCO_3 -polymorph, micro-sized crystals, high energy milling.

TiO₂ OBTAINED FROM MECHANICALLY ACTIVATED ILMENITE ORE AND ITS PHOTOCATALYTIC PROPERTIES

N. G. Kostova^{1,*}, M. Achimovičová^{2,3}, A. Eliyas¹, N. Velinov¹, V. Blaskov⁴,
I. Stambolova⁴, P. Baláž²

¹ *Institute of Catalysis, Bulgarian Academy of Sciences, 1113 Sofia, Bulgaria*

² *Institute of Geotechnics, Slovak Academy of Sciences, 043 53 Košice, Slovakia*

³ *Institute of Mineral and Waste Processing, Waste Disposal and Geomechanics,
Technical University-Clausthal, 38678 Clausthal, Germany*

⁴ *Institute of General and inorganic Chemistry, Bulgarian Academy of Sciences,
1113 Sofia, Bulgaria*

The ilmenite (FeTiO₃) is one of the basic raw materials for preparing titania. There are two industrial methods, that have been developed for the preparation of titania from ilmenite mineral: the pyrometallurgical and the hydrometallurgical one. The application of the industrial hydrometallurgical method leads mainly to rutile.

Mechanically activated FeTiO₃ concentrate, and TiO₂-the product after autoclave leaching of mechanically activated FeTiO₃ were characterized by XRD, specific surface area measurement (BET method), Infrared Fourier transform and Mössbauer spectroscopies. The photocatalytic properties of the so obtained titania samples were evaluated in the reaction of photo-discoloring of Methyl Orange aqueous solution. Mechanical activation accelerated the dissolution of FeTiO₃ in sulfuric acid due to decreasing crystallite size and revealing inner surface for contact with the acid. The ilmenite characteristic bands gradually disappeared after milling. A well-crystallized anatase TiO₂ was obtained with low content of impurities. The specific surface area was 28 m²g⁻¹. The photocatalytic activity of TiO₂ obtained from mechanically activated ilmenite ore was found to be merely lower than those of the commercially available TiO₂ photocatalyst.

Acknowledgement: The present investigations are financially supported by the Bulgarian National Science Fund at the Ministry of Education and Science-Project DNTS/SLOVAKIA 01/3, bilateral cooperation project between the Bulgarian Academy of Sciences and Slovak Academy of Sciences and project VEGA 2/0027/14.

[1] N.J. Welham, J.S. Williams, Metallurgical and Materials Transactions B, 30 (1999) 1075.

* E-mail: nkostova@ic.bas.bg

Keywords: crystallography, ilmenite, mechanical activation, photocatalytic property.

COMPARATIVE STUDY OF THE PHASE FORMATION AND INTERACTION WITH WATER OF CALCIUM-SILICATE CEMENTS FOR DENTAL APPLICATIONS

Y. Kouzmanova¹, I. Dimitrova¹, G. Gentsheva², L. Aleksandrov², D. Kovacheva^{2*}

¹ *Medical University-Sofia, Faculty of Dentistry, Dep. Conservative dentistry,
1 George Sofiiski Str., Sofia, Bulgaria*

² *Institute of General and Inorganic Chemistry, Bulgarian Academy of Sciences,
Acad. G. Bontchev Str. Bl. 11, 1113 Sofia, Bulgaria*

Mineral trioxide aggregate /MTA/ was first introduced to dentistry in 1993 by Torabinejad and co-workers [1]. Based on ordinary Portland cement it is composed of tricalcium silicate, dicalcium silicate, tricalcium aluminate, and tetracalcium aluminoferrite. Bismuth oxide is added as a radiopaquer for clinical applications. This cement was used for various dental clinical applications, including as endodontic material for repair. The search for better repair material during last 30 years has lead to introduction of various calcium silicate cements for dental applications. In clinical applications blood and oral fluid come in contact with calcium silicate cements during placement and setting. Despite similar content, due to the variations of manufacturing processes the purity of their constituents and hydration products as well as their behavior, can be different. The degree of solubility of calcium-silicate based cements is an object of debate among investigators. Most authors reported low solubility or no solubility, however increased solubility was reported in a long-term study. The aim of the present study is to compare the phase formation and evolution, as well as solubility of five different commercial calcium-silicate cements. Samples in a pellet form were prepared according to the manufacturer's instructions. After drying, the samples were immersed in distilled water for 28 days at room temperature. X-ray diffraction (XRD) analysis was applied to determine the phase composition of the initial powder mix, cement compositions, and cement compositions evolution after aging the material in distilled water. Thermal analyses (TG-DTA) were also performed to confirm the XRD results. The concentrations of Ca, Na, Mg, Al, K, Fe, Ti, Bi, Ta and Zr ions passed into the solution were determined by means of ICP-MS. The changes of elemental and phase composition were discussed.

[1] S. J. Lee, M. Monsef, M. Torabinejad, *Journal of Endodontics*, 19 (1993) 541.

* E-mail: didka@svr.igic.bas.bg

Keywords: calcium-silicate cements, dental applications.

Fe-DOPED ZnO THIN FILMS PREPARED BY SOL-GEL METHODS, GAS SENSING AND PHOTOCATALYTIC PROPERTIES

L. Krasteva, N. Kaneva*, A. Bojinova, K. Papazova, D. Dimitrov

¹ *Laboratory of Nanoparticle Science and Technology, Department of General and Inorganic Chemistry,
Faculty of Chemistry, University of Sofia, 1 James Bourchier Blvd., 1164 Sofia, Bulgaria*

The gas sensing and photocatalytic properties of Fe-doped ZnO are investigated in this work. The films are synthesized via sol-gel method and their structures are studied by EDS, SEM and water contact angle (WCA) analysis methods. All films are found to be hydrophobic in nature with a contact angle greater than 91.2–92.3°. The gas sensitive properties of the structures are analyzed in air and different ethanol vapour concentrations at fixed temperature. It is found that the contact potential difference increases nonlinearly with the increase ethanol concentration. The photocatalytic activity of the Fe-doped ZnO nanofilms is investigated for the Reactive Black 5 degradation in wastewaters under UV and visible light irradiation. Nanostructured films demonstrate higher photocatalytic efficiency and faster mineralization of dye, than the undoped ones.

Acknowledgments: This research is financially supported by project FP7 project Beyond Everest and Russian Presidential Program of engineer advanced training.

* E-mail: nina_k@abv.bg

Keywords: ZnO, Fe-doped films, gas sensing, photocatalysis, sol-gel, Reactive Black 5.

PROTON EXCHANGED LAYERS IN LiNbO_3 AND LiTaO_3 : CHARACTERIZATION BY IR SPECTRA DECONVOLUTION

M. Kuneva, S. Tonchev

*Institute of Solid State Physics – Bulgarian Academy of Sciences,
72 Tzarigradsko Chaussee Blvd., 1784 Sofia, Bulgaria*

IR reflection spectroscopy provides information about the structure and chemical bonds of the crystal surface region comparable in depth to the waveguide's one. It could be more useful for studying layered structures than IR absorption spectroscopy which is usually used in the case of proton-exchanged lithium niobate and lithium tantalate. Proton-exchanged waveguide layers containing various phases were studied by IR reflection spectroscopy.

The reflection spectra are strongly structured and differ substantially from the spectrum of the as-grown sample. The new bands appear at frequencies in the range of $700\text{--}1050\text{ cm}^{-1}$. The analysis is more complicated than the one based on the IR absorption spectra of proton-exchanged waveguides in both crystals and here, not only the presence or absence of the definite band but also the intensity ratio of the bands building the spectrum has to be taken into account. Gaussian deconvolution procedure was performed which allowed us to be more precise when determining the peak frequency and estimating the relative quota of each of the bands building the spectrum. The results discussed could contribute to the monitoring of the PE process when technology adjustment is needed for obtaining waveguides with definite phase content.

* E-mail: m_kuneva@yahoo.com

Keywords: Proton exchange, Optical waveguides, IR reflection spectroscopy.

DETERMINATION OF THE OXIDATION STATE OF THE B-CATIONS IN THE STRUCTURE OF COMPLEX PEROVSKITE

Ts. Lazarova^{1,*}, D. Kovacheva¹, S. Aleksovska^{2,3}

¹ *Institute of General and Inorganic Chemistry, Bulgarian Academy of Science,
"Acad. Georgi Bonchev" bl. 11, 1113 Sofia, Bulgaria*

² *Institute of Chemistry, Faculty of Natural Sciences and Mathematics, "Sts. Cyril & Methodius"
University, Arhimedova 3, Skopje, R. Macedonia*

³ *Research Center for Environment and Materials, Macedonian Academy of Sciences and Arts,
Krstе Misirkov 2, 1000 Skopje, R. Macedonia*

The perovskite structure is adopted by many oxides that have the chemical formula ABO_3 . The class of oxide perovskites is probably the best studied class of oxides due to its interesting physical and chemical properties. It is widely accepted that the type of B-cation influences the crystallography, phase transitions and other physical properties of the phase. Complex perovskite structures contain two different B-site cations. In the case of two transition metal cations in B-position a complex interaction between them results in a great number of intriguing electronic or magnetic properties. When both transition metals have possibility for different oxidation state it is rather difficult to determine the cation distribution in a proper way, but on the other hand this complexity is often essential for the functional properties of the materials.

A new series of complex perovskite compounds with general formula $PbLaFe_{2-x}Mn_xO_6$ ($0 < x < 2$, step 0.25) were prepared by solution combustion method. Thermal treatment for total 30 h at temperatures up to 850°C led to the synthesis of perovskite-type phases. Crystal structure refinement by Rietveld method was performed to determine the metal-oxygen distances and to extract the mean B-cation radius. Comparison of the theoretical and experimental compositional dependence of the mean B-cation radius is performed in a view to evaluate the oxidation state of iron and manganese in this series.

* E-mail: cveti_ura@abv.bg

Keywords: complex perovskites, crystal structure, oxidation state.

IR STUDY OF LEAD-BORATE COMPOSITES CONTAINING PbMoO_4 NANOPARTICLES

V. Lilova, E. Lilov, N. Nikiforov*

*University of Chemical Technology and Metallurgy, 8 Kl. Ohridski Blvd.,
1756 Sofia, Bulgaria*

Nanostructured composites based on an amorphous lead-borate matrix and crystalline PbMoO_4 nanoparticles are obtained by incorporation technique. The precursors used are chemically pure Pb_3O_4 and B_2O_3 reagents and powdered polycrystalline PbMoO_4 . The samples are prepared by conventional melting. The content of the PbMoO_4 varies in the range from 5 to 40 mol%.

The evolution in the network structure of the obtained materials is investigated by IR spectroscopy.

It is established that a part of the PbMoO_4 is dissolved and molybdenum ions act as network formers. The main structural units building the amorphous network are BO_3 and BO_4 in superstructures, PbO_n (where $n=3$ and/or 4) and MoO_4 . It is proved that the molybdenum favors the $\text{BO}_4 \rightarrow \text{BO}_3$ transformation.

* E-mail: vanya_di@yahoo.com

Keywords: nanocomposites, lead-borate glasses, network structure.

PROLIFERATION OF GRAM NEGATIVE CELLS ONTO NANOHYBRIDE SOL-GEL CARRIERS

D. Marinkova^{1,*}, M. Michel², R. Raykova¹, L. Yotova¹, P. Griesmar²

¹ *Department of Biotechnology, University of Chemical Technology and Metallurgy,
8 Kl. Ohridski blvd, 1756 Sofia, Bulgaria*

² *Université de Cergy-Pontoise, ENS, UMR CNRS 8029, SATIE,
F-95000 Cergy-Pontoise, France*

The mechanical properties of biofilms have a growing interest in science. Some scientists examine biofilms like rheological fluids. Surface energy controls many interesting properties that play a key role in the applications of surface design. The influence of matrixes is very important for the biofilm proliferation.

The aim of this study is to synthesize new hybrid sol-gel materials with nano-particles. The new synthesized matrixes show wide surface and it is investigated the biochemical properties of formed biofilms. Except the biological properties of obtained biofilms it is researched the rheological properties of fluids and the properties of synthesized matrixes.

Currently, research in the design of new materials is particularly interested in the connection between organic materials such as polymers and inorganic materials concerning application by the sol-gel (SG) method.

This work is related to the synthesis and characterization of new co-networks based on organic materials with incorporation of inorganic precursors

We report on the study and comparison of the formation of biofilms from model gram-negative bacteria onto different, newly synthesized hybrid carriers. By the TSM technology is monitored the complex materials and nano-structure in different scale.

* E-mail: dmarinkova@yahoo.com

Keywords: biofilm, matrices, nano-particles.

TEM STUDIES OF LOCAL METAL DISTRIBUTION IN PALLADIUM DOPED $\text{LaCo}_{0.8}\text{Ni}_{0.1}\text{Fe}_{0.1}\text{O}_3$ PEROVSKITES

P. Markov¹, S. Stanchovska¹, S. Harizanova¹, D. Nihtianova^{1,2},
E. Zhecheva¹, R. Stoyanova¹

¹ *Institute of General and Inorganic Chemistry, Bulgarian Academy of Sciences,
G. Bonchev str., bld. 11, 1113 Sofia, Bulgaria*

² *Institute of Mineralogy and Crystallography, Bulgarian Academy of Sciences,
Acad. G. Bonchev Str., bl. 107, 1113 Sofia, Bulgaria*

Nowadays, it is of importance to find alternative sources for “clean energy” storage and conversion. Lanthanum cobaltate, LaCoO_3 , with a perovskite type structure, is considered as a material with potential application in thermoelectricity due to its high Seebeck coefficient ($|S| > 500$ mV/K at room temperature). In addition, LaCoO_3 has been used as an effective catalyst in the reaction of complete oxidation of methane. To improve the thermoelectric and catalytic properties of LaCoO_3 , the structure approach is recently developed. This approach consists of the substitution of Co ions with transition metal ions (such as Ni and Fe) and with precious metal ions (such as Pd), as a result of which complex oxides $\text{LaCo}_{1-y}\text{M}_y\text{O}_3$ are formed. The knowledge on the type of local cationic distribution in $\text{LaCo}_{1-y}\text{M}_y\text{O}_3$ enables us to control their properties.

The aim of this contribution is to examine in details the local cationic distribution in palladium doped $\text{LaCo}_{0.8}\text{Ni}_{0.1}\text{Fe}_{0.1}\text{O}_3$ by means of TEM. Two compositions $\text{La}(\text{Co}_{0.8}\text{Ni}_{0.1}\text{Fe}_{0.1})_{0.95}\text{Pd}_{0.05}\text{O}_3$ and $\text{La}(\text{Co}_{0.80}\text{Ni}_{0.1}\text{Fe}_{0.1})_{0.85}\text{Pd}_{0.15}\text{O}_3$ are subject of this study. All perovskites are obtained by thermal decomposition of freeze-dried citrate precursors at 600 °C. It was found that, at this temperature, pure perovskite phase is formed. Detailed TEM investigations included study of morphology and local structure by SAED and HRTEM. It was determined that mean size of palladium particles is about 11 and 7 nm for low- and highly-doped perovskites with Pd. According to HRTEM images and SAED, palladium is distributed in the highly doped perovskite as La_2PdO_4 and PdO phases, while for low-doped perovskite Pd substitutes for transition metal ion in the perovskite structure.

BaTiO₃ GLASS-CERAMICS: CRYSTAL GROWTH AND MICROSTRUCTURE

A. Mazhdrakova^{1,*}, R. Harizanova¹, C. Bocker², G. Avdeev³,
I. Gugov¹, C. Rüssel²

¹ *Department of Physics, University of Chemical Technology and Metallurgy,
8 Kl. Ohridski Blvd., 1756 Sofia, Bulgaria*

² *Otto Schott Institute, University of Jena, Fraunhoferstr. 6, 07743 Jena, Germany*

³ *Institute of Physical Chemistry, Bulgarian Academy of Sciences, Block 11,
Acad. G. Bonchev Str., 1113 Sofia, Bulgaria*

The synthesis of alkali and alkaline-earth rich compositions in the system Na₂O/TiO₂/BaO/Al₂O₃/B₂O₃/SiO₂ is reported for different ratios [Na₂O]/[Al₂O₃] and for total glass-former concentration less than 30 mol%. The physicochemical properties of the obtained glasses are determined by using differential thermal analysis and conclusion is reached that increasing the alumina concentration leads to increase in both glass-transition and crystallization temperature.

Applying different time-temperature programs to the glasses with different Al₂O₃ concentrations, results mainly in crystallization of BaTiO₃ as established by x-ray diffraction. The scanning electron microscopy imaging shows formation and growth of globular crystals with sizes varying between about 300 nm and 20 micrometers depending on the time-temperature program applied and the ratio [Na₂O]/[Al₂O₃].

* E-mail: ruza_harizanova@yahoo.com

Keywords: barium titanate, crystallization, microstructure, crystal growth.

EFFECT OF PHASE COMPOSITION ON THE *IN VITRO* BIOACTIVITY OF GLASS-CERAMICS IN THE CaO–MgO–SiO₂ SYSTEM

I. Mihailova^{1,*}, L. Radev¹, V. Aleksandrova¹, I. Colova¹,
I. M. M. Salvado², M. H. V. Fernandes²

¹ *University of Chemical Technology and Metallurgy, 8 St. Kl. Ohridski Blvd.,
Sofia 1756, Bulgaria*

² *University of Aveiro and CICECO, Aveiro, Portugal*

The glass-ceramics in the system CaO–MgO–SiO₂ have recently received a great deal of attention because they exhibit good *in vitro* bioactivity and have potential use as bone implants. In order to investigate the effect of phase composition of calcium-magnesium-silicate ceramics with chemical composition 3CaO.MgO.2SiO₂ on *in vitro* bioactivity, two glass-ceramics were prepared by sol-gel method. The dried gels were thermally treated at 1100 and 1300°C. Structural behavior of the synthesized samples was examined by means of X-ray diffraction (XRD), Fourier Transform Infrared Spectroscopy (FTIR) and Scanning Electron Microscopy (SEM). Merwinite, as a main crystalline phase, and akermanite, as a minor phase, were identified in glass-ceramic sample sintered at 1300°C. Four crystalline phases (larnite, merwinite, akermanite and diopside) were detected after heat treatment at 1100°C.

In vitro bioactivity of the synthesized glass-ceramic samples was recorded in Simulated Body Fluid (SBF) for different times of soaking. The hydroxyapatite formation on the surface of the immersed samples was evaluated by using of XRD, FTIR, SEM and Energy Dispersive Spectroscopy (EDS) techniques. The concentration of the ions in SBF solutions after *in vitro* test was evaluated by Inductively Coupled Plasma Optical Emission Spectrometry (ICP-OES).

On the basis of the obtained results, good *in vitro* bioactivity was found for the both glass-ceramics. The peculiarities of the formation of apatite layer in dependence of the phase composition are analyzed and discussed.

* E-mail: irena@uctm.edu

Keywords: CaO–MgO–SiO₂, glass-ceramics, merwinite, larnite, *in vitro* bioactivity.

COMPARATIVE STUDY OF ZnO SAMPLES PREPARED BY DIFFERENT METHODS

K. Milenova^{1,*}, A. Elias¹, V. Blaskov², I. Avramova², I. Stambolova²,
S. Vassilev³, P. Nikolov⁴, N. Kasabova⁴, S. Rakovsky¹

¹ *Institute of Catalysis, Acad. G. Bonchev St, bl. 11, 1113 Sofia, Bulgaria*

² *Institute of General and Inorganic Chemistry, Acad. G. Bonchev St, bl. 11, 1113 Sofia, Bulgaria*

³ *Institute of Electrochemistry and Energy Systems, BAS, Acad. G. Bonchev bl. 10, 1113, Sofia, Bulgaria*

⁴ *University of Chemical Technology and Metallurgy, 8 Kliment Ohridski, 1756, Sofia, Bulgaria*

In the recent study ZnO powder, activated using original method was compared with ZnO prepared by usual precipitation method. The precursors of both samples were characterized by XRD and TG–DTA methods. After thermal decomposition of these precursors, ZnO nanoparticle powders were obtained and characterized by XRD, IR, XPS and BET methods.

A strong endothermic peak due to the zinc hydroxide precursor decomposition has been registered on the DTA curve for both precursors under 300°C temperature. The XRD analysis of ZnO photocatalysts shows wurtzite ZnO phase and IR proves formation of Zn–O bond. The specific surface area of the activated ZnO is 40 m²/g, compared to 23 m²/g for the usual ZnO sample. The photocatalytic properties of the samples were tested in the reaction of oxidative discoloration of Reactive Black 5 azo dye used as model waste water pollutant in a semi-batch reactor. Both photocatalysts show high effectiveness in the dye decomposition, with higher value (96%) achieved for the activated ZnO. The degree of degradation of Reactive Black 5 model contaminant is 33.8×10^{–3} min^{–1} for the activated ZnO and 23.6×10^{–3} min^{–1} for the usual one.

* E-mail: kmilenova@mail.ic.bas.bg

Keywords: ZnO; photocatalysis; ultraviolet light; azo dye.

COPPER DOPED ZINC OXIDE NANOPOWDERS USED FOR DEGRADATION OF RESIDUAL AZO DYES IN WASTEWATERS

K. Milenova^{1,*}, A. Eliyas¹, V. Blaskov², I. Avramova², I. Stambolova²,
S. Vassilev³, P. Nikolov⁴, Y. Karakirova¹, N. Kasabova⁴, S. Rakovsky¹

¹ *Institute of Catalysis, Acad. G. Bonchev St, bl. 11, 1113 Sofia, Bulgaria*

² *Institute of General and Inorganic Chemistry, Acad. G. Bonchev St,
bl. 11, 1113 Sofia, Bulgaria*

³ *Institute of Electrochemistry and Energy Systems, BAS,
Acad. G. Bonchev, bl. 10, 1113, Sofia, Bulgaria*

⁴ *University of Chemical Technology and Metallurgy,
8 Kliment Ohridski, 1756, Sofia, Bulgaria*

The influence of copper doping on the structural and on the photocatalytic properties of ZnO nanopowders was studied. Copper-doped ZnO samples with dopant content of 1.5 wt% were prepared by deposition method. Two types of ZnO were used – commercial one and ZnO activated by an original patented procedure. The crystalline structure, the oxidation state of the dopant and the specific surface area were investigated respectively by X-ray diffractometer (XRD), Electron paramagnetic resonance (EPR), X-ray photoelectron spectroscopy (XPS) and single point Brunauer-Emmett-Teller (BET) methods.

The EPR spectra registered isolated Cu²⁺ ions. The photocatalytic efficiency of the prepared nanosized samples were examined for photocatalytic degradation of Reactive Black 5 (RB5) dye under UV light. Examined powders have shown significant degree of degradation of the investigated textile dye pollutant, the maximum value of the constant rate ($35.9 \times 10^{-3} \text{ min}^{-1}$) was obtained for the activated Cu/ZnO. The photodegradation activity for Reactive Black 5 of activated Cu/ZnO is 99.5% and 98.0% for commercial copper doped ZnO. The present research study established that activated copper-doped ZnO can be used as an effective photocatalyst for the removal of azo dyes in wastewaters.

* E-mail: kmilenova@ic.bas.bg

Keywords: doping, ZnO, photocatalytic activity, azo dye pollutant.

NEW INSIGHTS FOR THE DESIGN OF RUTHENIUM ANTITUMOR AGENTS – AMINO-COORDINATED Ru^{III} AND Ru^{IV} COMPLEXES OF 3-AMINO-2-CHLOROPYRIDINE

G. Mirtcheva^{1,*}, R. Petrova², B. Shivachev², G. Momekov³, G. Gencheva¹

¹ Faculty of Chemistry and Pharmacy, Sofia University “St. Kliment Ohridski”, 1164 Sofia, 1 J. Bourchier Blvd., Bulgaria

² Institute of Mineralogy and Crystallography “Acad. Ivan Kostov”, Bulgarian Academy of Sciences, Acad. G. Bonchev str., bl. 107, 1113 Sofia, Bulgaria

³ Faculty of Pharmacy Medical University-Sofia 2 Dunav Str., 1000 Sofia, Bulgaria

In the field of antitumor drugs design, the ruthenium complexes possess significant advantages because of their specific kinetics of the ligand substitution reactions similar to that of the platinum(II) compounds. In addition, ruthenium is stable in different oxidation state (II, III and IV) even under physiological conditions and is capable to mimic iron in binding to biomolecules. Hence, mechanisms such as “activation by reduction” and “transferrin-targeted delivery” have been proposed for the ruthenium cytotoxic compounds, leading to improve the antitumor activity and diminish of their general toxicity. Recently a series of stable water-soluble octahedral Ru^{IV} and Ru^{III} complexes of 3-amino-2-chloropyridine (acp), have been synthesized in diluted hydrochloric acid. Their solid state structure, Fig. 1, and solution chemistry were characterized

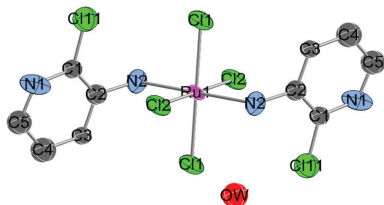


Fig. 1. Molecular structure of trans-[Ru^{IV}Cl₄(acp)₂].H₂O. (The compound crystallizes in triclinic P-1 space group; parameters: *a* = 6.3602(12) Å; *b* = 8.4175(15) Å; *c* = 9.8492(15) Å; α = 99.544(19)°; β = 106.897(14)°; γ = 100.80(2)°)

by elemental analysis, single crystal X-ray diffraction, magnetic measurements, EPR, IR, UV-Vis and ESI-MS analysis. The ligand used is coordinated in a monodentate mode via the lone pair of the sp³-hybridized N-atom of the external amine group. The complexes were found to undergo slow hydrolysis under pseudo-physiological conditions. The novel compounds showed moderate cytotoxicity against acute promyelocytic leukemia derived cell line HL-60 and specific activity against its cisplatin-resistant sub-line HL-60/CDDP. It was proved that the biological activity of the novel complexes strongly depends on the oxidation state of ruthenium, particular coordination sphere, number of dpa-ligands and their mode of coordination.

Acknowledgements: The Fund “Scientific Research”, Ministry of Education and Science, Project DDVU02-66 is acknowledged.

* E-mail: ggencheva@chem.uni-sofia.bg

Keywords: Ruthenium complexes, Structural elucidation, Ligand substitution reactions.

BIOSYNTHESIZED OF SMART GOLD NANOPARTICLES: pH-INDUCED REVERSIBLE AGGREGATION AND PLASMON COUPLING

Nasser Y. Mostafa^{*,1,2}, B. El-Deeb^{1,3}

¹ Faculty of Science, Taif University, P.O.Box: 888 Al-Haweiah, Taif, Saudi Arabia

² Chemistry Department, Faculty of Science, Suez Canal University, Ismailia 41522, Egypt

³ Botany Department, Faculty of Science, Sohag University, Sohag, Egypt

This paper reports the extracellular biosynthesis of gold nanoparticles (AuNPs) using the supernatant of *Proteus mirabilis* isolated from agricultural soil. UV spectra indicate that gold nanoparticles started to form within 3 hours reaction time. TEM micrographs indicated that the particles were well dispersed and near spherical in shape. The size range of the gold nanoparticles was around 20–50 nm. The secreted proteins reduce Au ions and stabilizes the produced AuNPs. ATR-FTIR confirmed the presence of a protein shell. The results of amide I band fitting revealed that secondary structure of proteins have been changed as a consequence of binding with AuNPs. AuNPs produced at pH higher than 5.0 were found to be

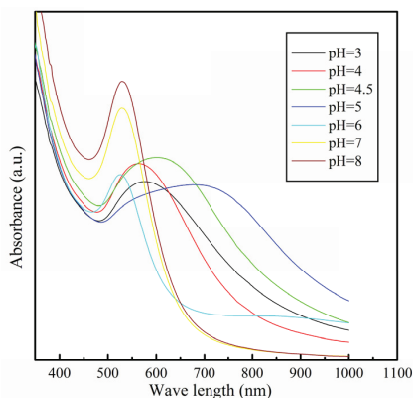


Fig. 1. UV-Vis absorption spectra of protein-AuNPs conjugate at different pH.

stable in solution for more than 6 months. However, the protein–AuNPs form aggregates at low pH (<5.0) as detected by the red shift of the plasmons resonance wavelength to far-red and near-infrared. This absorption shift of AuNPs upon aggregation is due to coupled plasmons between nanoparticles capped with protein [1]. The aggregation was related the pH-dependent conformational changes of protein molecules. This aggregation was proved to be reversible within 2 min.

[1] R. D. Kekatpure et al., Phys. Rev. Lett., 104 (2010) 243902.

* E-mail: nmost69@yahoo.com

Keywords: gold nanoparticles; protein; conjugate; plasmons.

CHARACTERIZATION OF NANOSIZED $\text{Al}_{2-x}\text{Sc}_x(\text{WO}_4)_3$ SOLID SOLUTIONS BY TRANSMISSION ELECTRON MICROSCOPY (SAED, HRTEM, XEDS)

D. Nihtianova^{1,2}, L. Mihaylov³, P. Tzvetkov², P. Markov², A. Yordanova²,
I. Koseva², V. Nikolov²

¹ *Institute of Mineralogy and Crystallography, Bulgarian Academy of Sciences,
Acad. G. Bonchev Str., bl. 107, 1113 Sofia, Bulgaria*

² *Institute of General and Inorganic Chemistry, Bulgarian Academy of Sciences,
Acad. G. Bonchev Str., bl. 11, 1113 Sofia, Bulgaria*

³ *Faculty of Chemistry and Pharmacy, University of Sofia "St. Kliment Ohridski",
James Bourchier Blvd, No. 1, 1164 Sofia, Bulgaria*

Some of the $\text{Me}_2(\text{WO}_4)_3$ compounds possess unusually low thermal expansion coefficients (including zero and even negative values) within a broad temperature range [1]. A very important advantage of this class of compounds is the aptitude of their structure to accumulate different trivalent ions. This provides possibilities to tailor the thermal expansion coefficient to desirable values by varying the composition of the solid solutions to obtain a structure suitable for specific applications. For example, a zero thermal expansion coefficient is reported for the $\text{Al}_{1.68}\text{Sc}_{0.02}\text{In}_{0.3}(\text{WO}_4)_3$ composition. Similar materials are particularly valuable for application in optics and optoelectronics. Another basic application of this class of compounds is as laser media for tunable lasers.

The object of our investigation were $\text{Al}_{2-x}\text{Sc}_x(\text{WO}_4)_3$ solid solutions with ($0 \leq x \leq 2$). The main aim of the present investigation was to find the controllable conditions for the syntheses of these materials and to obtain the main structural characteristics. The phase compositions and unit cell parameters were determined by XRD. These data were used for detailed interpretation of TEM (SAED, HRTEM) results. The crystal structure of these solid solutions is orthorhombic with space group Pnca . Several crystallographic sections are obtained by SAED method: [100], [010], [110], [111], [210], [212]. Some impurities of the triclinic phase $\text{Na}_5(\text{W}_{14}\text{O}_{44})$ PDF 89-6724 are detected in orientation [010] by SAED. HRTEM images in these crystallographic directions show the microstructure at unit cell level.

XEDS analysis is used to establish the chemical composition of these materials.

TEM (SAED, HRTEM, XEDS) results fully confirm the successful syntheses of the solid solutions with controllable chemical composition and particle size dimension from 10 to 70 nm in the whole range.

[1] A. Yordanova, I. Koseva, N. Velichkova, D. Kovacheva, D. Rabadjieva, V. Nikolov, *Materials Research Bulletin*, 47 (2012) 1544.

INFLUENCE OF THE CONTENT OF SAMARIUM ON THE STRUCTURE AND THE OPTICAL PROPERTIES OF ZINC BOROPHOSPHATE MATERIALS

G. Patronov^{1,*}, I. Kostova¹, D. Tonchev¹, Z. Stoeva²

¹ Dept. Chem. Technology, Plovdiv University "Paisii Hilendarski", 4000 Plovdiv, Bulgaria

² DZP Technologies Ltd., 22 Signet Court, Cambridge CB5 8LA, United Kingdom

Compositions based on ZnO, P₂O₅ and B₂O₃ have both scientific and technological importance because of their interesting characteristics. Doping with the rare earth elements not only leads to a change in the structure, but also to interesting the optical, magnetic and electrical properties.

This study presents samarium doped ZnO-rich borophosphate material of composition xSm₂O₃ – (72.31-x)ZnO – 9.69P₂O₅ – 18B₂O₃, where x = 0, 0.25, 0.5, 0.75, 1 mol%. Samarium doped ZnO-rich borophosphate compositions were investigated by differential thermal analysis, UV fluorescence, x-ray fluorescence, x-ray powder diffraction and scanning electron microscopy with energy-dispersive x-ray analysis (SEM-EDAX).

The results obtained show that samples we studied are predominantly amorphous, with the presence of crystalline structure in some of them. It is found that both UV fluorescence and x-ray fluorescence properties of the obtained materials depend on the excitation wavelength. Strongest UV fluorescence is found at 395nm. Interestingly, Sm³⁺ → Sm²⁺ conversion is observed at x-ray irradiation with green (535 nm) laser, whereas no conversion is found at excitation with purple (400nm) laser. The observed properties can be related to the structure and morphology of the obtained materials as evidenced by the SEM-EDAX investigation and powder x-ray diffraction data.

Acknowledgments: This research was funded by the "Scientific Research" fund at Plovdiv University, Grant № NI 13 HF 006.

* E-mail: patron@uni-plovdiv.bg

Keywords: samarium doped zinc borophosphates, thermal analysis, x-ray powder diffraction, fluorescence.

INVESTIGATION OF THE POSSIBILITY TO INCREASE THE MECHANICAL PROPERTIES OF FERRITIC NODULAR CAST IRON

R. Petkov*, L. Atanasov, R. Gavriloova

*University of Chemical Technology and Metallurgy, 1756 Sofia,
"Kl. Ochridski" blvd. 8*

In the last few decades production of ductile cast iron is constantly growing. The main reason for this development is the combination of high technological and operational characteristics, in particular – mechanical properties, which are characteristic of the carbon and low-alloy steels.

The aim of this study is by additional alloying to ensure ferrite structure of the metal base, solid-solution hardening of ferrite and hence higher mechanical performance. Generally, there are two elements which satisfy these conditions – silicon and aluminum. Aluminium inhibits spheroidizing effect of magnesium and has a lower stiffening effect. For this reason, studies have been conducted with the use of silicon.

For the purpose of the experimental work is designated as the base brand GGG500-7. In the own classic form this brand has perlite-ferrite structure. In the standard cooling conditions of the cast iron castings its chemical composition is 3.2–3.7% C; 2.0–2.5% Si; 0.3–0.7% Mn. To study the influence of the chemical composition of the structure and mechanical properties were carried out experiments with alloys with the same carbon equivalent, but the content of Mn is to 0.15% and the silicon content varied in the range of from 2.0 to 4.5%. The analysis of results allows conclusion, that in the presence of silicon within 3.5–3.7% and about 4.2 carbon equivalent can be obtained a ferritic ductile cast iron, which satisfies the brand GGG 500-7.

E-mail: castrum@uctm.edu

Keywords: ductile cast iron, ferrite structure, mechanical properties.

CALCULATION OF THE REFRACTIVE INDEX OF $\text{Bi}_{12}\text{SiO}_{20}:\text{Mn}$

P. Petkova^{1,*}, P. Vasilev¹, M. Mustafa¹

*¹ Shumen University "Konstantin Preslavsky", 115 Universitetska street,
9712 Shumen, Bulgaria*

The optical absorption spectra of Mn-doped $\text{Bi}_{12}\text{SiO}_{20}$ (with the sillenite structure) are investigated in the spectral range 400–1000 nm of Mn appearance. The absorption coefficient is presented in two cases: inside and outside the "core" region. The calculated second derivative of the optical absorption coefficient spectra contains information about d-electrons transitions in energy level diagram of Mn^{4+} ion in oxygen octahedron and Mn^{5+} in oxygen tetrahedron [1]. The Racah parameters B, C which correspond with individual d-electrons repulsions have been found and the crystal field parameter Dq is calculated also. Our analyzing of experimental data gives the value of refractive index [2] for BSO:Mn.

[1] Yu. F. Kargin, V. I. Burkov, A. A. Marin, A. V. Egorisheva, Crystals $\text{Bi}_{12}\text{MxO}_{20\pm\delta}$ with structure of sillenite. Synthesis, structure, properties. Moscow (2004).

[2] P. Petkova, Optical Materials, 36, 11 (2014), in press.

* E-mail: Petya232@abv.bg

Keywords: Mn-doped sillenite, optical absorption spectra, Racah parameters, crystal field parameter, refractive index.

FERMI ENERGY AND URBACH'S RULE OF Ni DOPED Mn_3O_4 THIN FILMS

P. Petkova^{1,*}, P. Vasilev¹, M. Mustafa¹, R. Mimouni²

¹ Shumen University "Konstantin Preslavsky", 115 Universitetska street,
9712 Shumen, Bulgaria

² ESSTT/63 Rue Sidi Jabeur 5100, Mahdia, Tunisia

The absorption coefficient of Ni doped manganese oxide thin films is measured in the spectral region 400–750 nm at room temperature. The parameters of electron-phonon interaction [1, 2], Urbach's energy [3] and the constants of Urbach's rule are calculated. The behavior of nickel ions in Urbach's rule region is also reported. The Fermi energy of Ni doped samples is determined also.

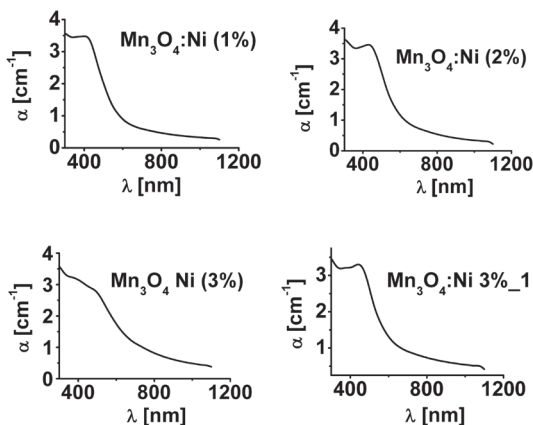


Fig. 1. Absorption coefficient of Ni doped Mn_3O_4 thin films in the spectral region 350–1100 nm

- [1] V. Kunets, N. Kulish, Vas. Kunets, M. Lisitsa, *Semiconductor Physics, Quantum Electronics & Optoelectronics*, 5, (2002) 9.
- [2] W. Woidovsky, T. Lukasiewicz, W. Nazariwicz, J. Zmija, *Phys. Status Solidi (b)*, 94 (1979) 649.
- [3] Sk. Faruque Ahmed, Myoung-Woon Moon, Kwang-Ryeol Lee, *Thin Solid Films*, 517 (2009) 4035.

* E-mail: Petya232@abv.bg

Keywords: nickel ions, absorption coefficient, Urbach's energy, Fermi energy.

INFLUENCE OF TREATMENT PROCESS ON THE SURFACE AND CHEMICAL COMPOSITION OF THE THERMALLY ACTIVATED ORTHODONTIC ARCHWIRES

V. Petrov¹, S. Terzieva^{2,*}, V. Tumbalev³, V. Mikli⁴,
L. Andreeva¹, A. Stoyanova-Ivanova²

¹ *Faculty of Dental Medicine, Medical University Sofia, 1 St. St. Georgi Sofiiski Blvd.,
1431 Sofia, Bulgaria*

² *Georgi Nadjakov Institute of Solid State Physics, Bulgarian Academy of Sciences,
72 Tzarigradsko Chaussee Blvd., 1784 Sofia, Bulgaria*

³ *Institute of General and Inorganic Chemistry, Bulgarian Academy of Sciences,
"Acad. Georgi Bonchev" str. bld.11, 1113 Sofia, Bulgaria*

⁴ *Centre for Materials Research, Tallinn University of Technology,
Ehitajate 5, Tallinn 19086, Estonia*

The thermally activated nickel-titanium archwires are widely employed in orthodontics because they present shape memory effect and super elasticity. The addition of copper to nickel-titanium alloy enhances the thermal properties of the wire while maintaining precise control of forces, comparing to "pure" nickel-titanium alloy. The purpose of this study is to investigate the chemical composition of the surface of thermally activated nickel-titanium and copper-nikel-titanium archwires with different cross sections (circle – 0.013 inch and rectangular – 0.016×0.022 inch). For the purpose of comparison, the origin wires (unused and sterilized ones) are also investigated as a control group. All studied orthodontic wires are produced byOrmco Ltd. and have transition temperature range at 35 °C. The analyses are carried out by three independent methods as X-ray diffraction analysis (XRD), Scanning Electronic Microscope (SEM) and by an Energy Dispersive X-Ray method (EDX).

The obtained results show that the processes of sterilizations of the investigated orthodontic archwires have no adverse effects on their properties. From the carried out tests it is established that there are no significant changes in the chemical composition of the surface of the thermally activated wires after treatment between 4 and 8 weeks. This period covers the average time of residence of the orthodontic wires at the mouth of the patient.

* E-mail: mira@issp.bas.bg

Keywords: thermally activated orthodontic wires, XRD, SEM-EDX, surface influence.

A NOVEL 13-MEMBERED CYCLIC POLYFUNCTIONAL SCAFFOLD – SYNTHESIS AND SOLUTION AND SOLID STATE CHARACTERIZATION

A. A. Petrova^{1,2}, S. M. Angelova^{1,2}, I. A. Nikolchina^{1,2}, V. B. Kurteva^{2,*},
B. L. Shivachev^{3,*}, R. N. Petrova³

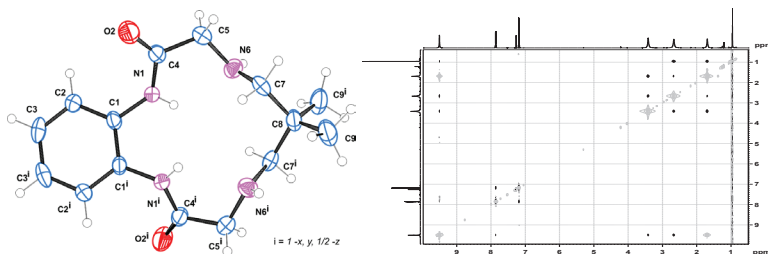
¹ University of Chemical Technology and Metallurgy, Department of General and Inorganic Chemistry, 8 Kliment Ohridski blvd. 1756 Sofia, Bulgaria

² Institute of Organic Chemistry with Centre of Phytochemistry, Bulgarian Academy of Sciences, Acad. G. Bonchev str., bl. 9, 1113 Sofia, Bulgaria

³ Institute of Mineralogy and Crystallography "Acad. Ivan Kostov", Bulgarian Academy of Sciences, Acad. G. Bonchev str., bl. 107, 1113 Sofia, Bulgaria

Macrocyclic polyfunctional molecules are of growing interest as they are widely applied as scaffolds in the combinatorial synthesis of receptor molecules; for instance, for constructing synthetic protein surface receptors.

The novel 13-membered cyclic compound 6,6-dimethyl-4,5,6,7,8,9-hexahydro-1H-benzo[e][1,4,7,10]tetraazacyclotridecine-2,10(3H,11H)-dione was obtained via two-step protocol from the cheap commercial source *o*-phenylenediamine. Its structure was determined by 1D and 2D NMR experiments and was confirmed by single crystal diffraction. The compound crystallizes



from *iso*-propanol in monoclinic *C* 2/*c* space group with cell parameters $a = 11.584(6)$, $b = 12.475(7)$, $c = 10.089(6)$ Å, $\beta = 93.20(3)^\circ$, $V = 1455.69$ Å³, $R_f = 8.73$ %.

Acknowledgments: The financial support by The Bulgarian Science Fund, projects UNA-17/2005, DRNF-02-13/2009, and DRNF-02/01, is gratefully acknowledged.

AP, SA and IN, students in UCTM, performed the synthetic work during their summer practices in IOCCP-BAS in August-September 2014.

* E-mail: vkurteva@orgchm.bas.bg (VK); blshivachev@gmail.com (BS)

Keywords: tetraazacyclotridecine-2,10-dione, NMR, X-ray.

ANALYSIS OF ELEMENTAL COMPOSITION OF A VARIABLE FORCE 3 ORTHODONTIC ARCHWIRE

V. Petrunov^{1,*}, L. Andreeva¹, S. Karatodorov², V. Mihailov², S. Terzieva²,
A. Stoyanova-Ivanova², V. Tumbalev³, V. Miki⁴

¹ *Faculty of Dental Medicine, Medical University Sofia, 1 St. St. Georgi Sofiiski Blvd.,
1431 Sofia, Bulgaria*

² *Georgi Nadjakov Institute of Solid State Physics, Bulgarian Academy of Sciences,
72 Tzarigradsko Chaussee Blvd., 1784 Sofia, Bulgaria*

³ *Institute of General and Inorganic Chemistry, Bulgarian Academy of Sciences,
"Acad. Georgi Bonchev" str. bld. 11, 1113 Sofia, Bulgaria*

⁴ *Centre for Materials Research, Tallinn University of Technology,
Ehitajate 5, Tallinn 19086, Estonia*

The Variable Force 3 Archwire is a heat activated, multi-force, nickel titanium archwire with three distinct force regions. This archwire places the correct force to the appropriate region (anterior, bicuspid and posterior) of the arch to quickly torque, level and align, without sacrificing patient comfort. In this work, analysis of a such archwire (cross section 0.16×0.22 inch.) with variable longitudinal elasticity is done. The elemental composition is obtained by different wire's regions with 5 mm separation by Laser-Induced Breakdown Spectroscopy (LIBS) and two other independent methods such as X-ray diffraction analysis (XRD) and Energy Dispersive X-ray method (EDX). The large area of application of LIBS is due to its ability to perform microprobe elemental analysis of wide variety of samples with no preliminary sample preparation. Pulsed Nd:YAG laser (λ 1,064 μm , pulse duration 8 ns) is focused on the sample surface, causing ablation and formation of laser-induced plasma plume. Collecting and processing the plasma emission gives us information of the sample elemental composition.

The obtained results of unused wire provide useful knowledge needs for further investigations on the wire changes during the treatment.

* E-mail: dr.petrnov@mail.bg

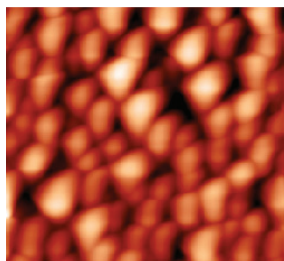
Keywords: Variable Force 3 Archwire, XRD, SEM-EDX, elemental composition.

OBTAINING OXIDE MATERIALS BY ALKOKSITEHNOLOGY METHOD

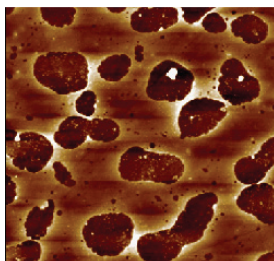
I. Pronin, N. Yakushova, I. Averin, N. Kaneva, A. Bojinova, K. Papazova, D. Dimitrov

*Laboratory of Nanoparticles Science and Technology, Department of General and Inorganic Chemistry,
Faculty of Chemistry and Pharmacy, University of Sofia*

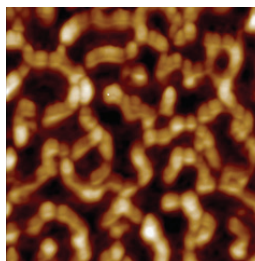
Obtaining inorganic oxide materials is an urgent task for micro- and nanoelectronics, optoelectronics, aerospace and other fields of science and technology. Predominative traditional technologies involving the use as precursors of inorganic metal salts, oxides and hydroxides are getting out of date. The alternative to traditional methods is the use of alkoxides as precursors of various chemical elements. This method is called alkoksotehnology. In other countries alkoksotehnology has been using for producing a number of materials for microelectronics, space technology. Today we can identify a number of alkoksotehnology advantages: high purity of the end products; chemical and structural homogeneity of multicomponent systems; easy creation of coatings; low temperature synthesis; environmental safety; the possibility of synthesis of new inorganic matters; simplicity of structure management. The figures 1–3 shows the structure of the coating composition of $\text{SnO}_2\text{--SiO}_2$, under different conditions of synthesis. It shows how to obtain nucleophilic spherical nuclei, the percolation cluster constricting and spinodal decomposition of the sol.



Nucleophilic cluster growth



Constricting percolation
cluster



Spinodal decomposition
sol

Despite the fact that the number of articles on this topic in the world is the thousands, in Russian ones they are rare and are often academic. In this regard, there is an underestimation alkoksotehnology as nano- synthesis method for the needs of industry. Thus, the development of scientific ideas of alkoksotehnology processes, as well as controlled thermonuclear fusion products obtained with its help is rather promising. In this presentation, physical and chemical alkoksotehnology basis is developed. The authors have studied the processes of sols forming suggested methods of managing their structure by varying the technological regimes. We propose fractal approach to the mechanisms of sols synthesis which help to increase the structure management and properties of the clusters in sols. Experimental studies involve a comprehensive study of sols properties and sols structure and coatings produced on their basis as well. The complex of the proposed methods and approaches will help to develop the scientific basic methods of alkoksotehnology applied to the creation of ceramic materials for aviation and aerospace industry.

SPECTROSCOPIC ANALYSIS OF NITRIC-ACID TREATED MIXTURES ON THE BASE OF BIOMASS AND CHICKEN LITTER

E. Serafimova^{1,*}, V. Petkova^{2,3}, Y. Pelovsky¹, B. Kostova²

¹ *University of Chemical Technology and Metallurgy – Sofia, 8 „St. Kliment Ohridski” Bul., Sofia 1756, Bulgaria*

² *Department Natural Sciences, New Bulgarian University, 21 “Montevideo” Str., 1618 Sofia, Bulgaria*

³ *Institute of Mineralogy and Crystallography, Bulgarian Academy of Sciences, “Acad. G. Bonchev” Str., Bldg. 107, 1113 Sofia, Bulgaria*

Poultry farming is a traditional branch of the Bulgarian national livestock in recent years for poultry meat and eggs. They are grown industrially between 15 and 22 million birds, of which 8–10 million hens, which produce daily between 4000–6000 t excrement. In one year aspect that defines an amount of about 500 000 t. As in other areas of the industry, and in this case, a major problem is the need to comply with regulatory requirements in the EU and in the country. In Bulgaria there are a few good practices implemented in poultry farms for the use of waste as secondary raw material or energy resource. This problem has not found the best solution globally too.

The proposed new solution is constructed on the basis of waste from poultry farms with additional waste products from other industries and biomass. The aim is to do integrated recovery of several wastes. These spectroscopic analysis have attempted application of the solid phase poultry waste and identifying the phases in it, in order to obtain organic products for agriculture.

It was found that the selected wastes and other raw materials have a structure and composition, which defines them as carriers of essential micro-nutrients without excessive content of heavy and toxic elements, which allows them to be classified as suitable components for obtaining soil improvers.

[1] Coates J. Interpretation of Infrared Spectra. A Practical Approach. Encyclopedia of Analytical Chemistry R. A. Meyers (Ed.) John Wiley & Sons Ltd, Chichester, 2000, 10815–10837.

[2] Dao T. H., H. Zhang, Annals of Environmental Science, 1 (2007) 69.

[3] Koukouzas N, Hamalainen J, Papanikolaou D, Tourunen A, Jantti T, Fuel, 86 (2007) 2186.

* E-mail: ekaterina_sr@abv.bg

Keywords: poultry excrements, biomass, soil improvers, IR, XRD, SEM.

STRUCTURAL ANALYSIS OF RGO AND RGO/SiO₂ NANOCOMPOSITE BY TRANSMISSION ELECTRON MICROSCOPY

A. Shalaby^{1,2,*}, D. Nihtianova^{3,4}, P. Markov⁴, A. Staneva², L. Aleksandrov⁴,
R. Iordanova⁴, Y. Dimitriev²

¹ *Science and Technology Center of Excellence (STCE), Cairo – Egypt*

² *University of Chemical Technology and Metallurgy, 8 Kl. Ohridski blvd., 1756 Sofia*

³ *Institute of Mineralogy and Crystallography, Bulgarian Academy of Sciences,
Acad. G. Bonchev Str., bl. 107, 1113 Sofia, Bulgaria*

⁴ *Institute of General and Inorganic Chemistry, Bulgarian Academy of Sciences,
G. Bonchev str., bld. 11, 1113 Sofia, Bulgaria*

Graphene has attracted scientific interest in recent years due to its unique properties. Graphene fabricated on silica depicts the interesting properties due to the local atomic configuration, and the binding sites of graphene with SiO₂. Reduced graphene oxide (RGO) was prepared by reducing of graphite oxide using sodium borohydride (NaBH₄). Sol-Gel method was used to obtain nanocomposite of RGO/ SiO₂ by mixing RGO with tetraethyl orthosilicate (TEOS). The transmission electron microscopy (TEM) investigations were performed on a TEM JEOL 2100 instrument at an accelerating voltage of 200 KV. The specimens were prepared by grinding and dispersing them in ethanol by ultrasonic treatment for 6 min. The suspensions were dripped on standard carbon/Cu grids. The measurements of lattice-fringe spacing recorded in HRTEM micrographs were made using digital image analysis of reciprocal space parameters. The analysis was carried out by the Digital Micrograph software. The obtained selected area electron diffraction (SAED) data show unambiguously that the sample RGO is different from Graphite 2H PDF 75-1621 and has typical interplanar distance d_{002} from 3.586 Å up to 4.016 Å. These crystallographic data are in good accordance to the published results of RGO materials, obtained by different methods [1]. The received SAED data for RGO/SiO₂ nanocomposite materials show largest values of interplanar distance d_{002} between 4.016 Å and 4.303 Å. Lattice fringes obtained by HRTEM method also give additional information about interplanar distance d_{002} : for RGO materials the value is 3.850 Å and for RGO/SiO₂ nanocomposite the value is 3.720 Å. The main phases are RGO and RGO/SiO₂ composite, but there are also some impurities of Graphite 2h PDF 75-1621.

[1] Huh, S. H. Physics and Applications of Graphene – Experiments (InTech, 2011), 73.

* E-Mail: ashalaby@outlook.com

Keywords: Reduced graphene oxide, TEOS, Nanocomposite, TEM analysis.

SPECIFICS OF NUCLEIC ACID CRYSTALLIZATION FOR DIFFRACTION EXPERIMENTS

H. I. Sbirikova, B. L. Shivachev*

*Institute of Mineralogy and Crystallography "Acad. Ivan Kostov"
Acad. Georgi Bonchev Str., bl. 107, 1113 Sofia, Bulgaria*

Most of our knowledge about nucleic acids (DNA, RNA and synthetic ones e.g. PNA, LNA) comes from fiber diffraction or single crystal structural studies. However high-resolution diffraction from a single-crystal experiment is indispensable in order to determine precisely the structural features and interactions in nucleic acids. In order to carry out such high-resolution experiments, the availability of sufficiently large single crystal $0.5 \times 0.5 \times 0.5 \text{ mm}^3$ and in addition exhibiting good diffraction is crucial. Interestingly the number of pure nucleic acid structures present in the PDB (and NDB) is quite low – 2715 when compared to the total number of structures +100 000. Moreover, sequence analysis shows that (i) most of the crystals structures (1800) contains less than 24 nucleotides (e.g. 12bp of dsDNA) and (ii) some of the sequences have been extensively "used" for co-crystallization experiments (e.g. the Dickerson-Drew dodecamer [1] sequence is present 137 times). In order facilitate the growth of nucleic acid crystals suitable for diffraction experiments we analyzed the crystallization conditions of the nucleic acids structures available in the PDB and NDB. As Spermine and magnesium are compounds that occur naturally in cells it is not surprising that one the findings is associated with their presence in almost all nucleic acid crystals. Another finding is that the amount of water in the crystallization condition should usually not drop below 60% and should not be higher than 80% v/v.

[1] Drew, H. R., Wing, R. M., Takano, T., Broka, C., Tanaka, S., Itakura, K., & Dickerson, R. E. Proceedings of the National Academy of Sciences, 78(4) (1981) 2179.

* E-mail: bls@@clmc.bas.bg

Keywords: single crystal, nucleic acid, crystal growth, DNA.

COMPOSITION AND CATALYTIC BEHAVIOUR OF BIOGENIC IRON CONTAINING MATERIAL OBTAINED BY *LEPTOTHRIX* BACTERIA CULTIVATION IN ADLER'S GROWTH MEDIUM

M. Shopska*, D. Paneva, G. Kadinov, Z. Cherkezova-Zheleva, I. Mitov

Institute of Catalysis, BAS, Acad. G. Bonchev, St., Bldg. 11, 1113 Sofia

The medium of Adler is selected for cultivation and isolation of iron bacteria because it favors intensive bacterial multiplication. The high population allows accumulation of large amounts of biogenic iron material and defines easier isolation. Biogenic iron-containing material is obtained after 6 month period of cultivation of *Leptothrix* genus bacteria. Infrared and Moessbauer spectroscopy are used for the sample characterization. Analyses showed that the studied material contained γ -FeOOH and α -FeOOH with particles sizes in the nanoscale. Carbonates, water and hydrocarbons are also registered. *In situ* DRIFTS technique is used to follow the material properties in the working conditions of CO oxidation reaction.

The biomass exhibits stable chemical composition under oxidative conditions up to 200°C. Small scale change in the surface hydroxyl cover is observed, only. The studied material has not considerable catalytic activity up to 200°C at the selected conditions (gas flow composition and rate). Measurable activity is registered at 250°C (the integrated intensity of the bands due to gaseous CO is decreased about 50%). Considerable change in the intensity of the band positioned at about 3240 cm⁻¹ was registered which is indicative for changes in the chemical composition. The Moessbauer spectral analysis showed that the initial sample contained 80% iron oxyhydroxides (lepidocrocite, goethite) and 20% iron oxide with spinel structure (maghemite). Only 5% lepidocrocite remains after the catalytic test. The predominant component is maghemite with particles of high dispersion. It can be concluded that the low catalytic activity at temperatures up to 200°C is result of the predominant work of iron oxyhydroxides but higher catalytic activity over 200°C is due to the formation of large amount of spinel iron oxide.

Acknowledgement: The authors are grateful to the Bulgarian National Science Fund at the Ministry of Education, Youth and Science for the financial support by project DID 02/38/2009.

* E-mail: shopska@ic.bas.bg

Keywords: nanosized biogenic iron-containing material, catalytic CO oxidation, *in situ* DRIFTS, Moessbauer spectroscopy.

DEGRADATION OF THE COMMERCIAL COLORANT ORANGE II BY NANOCOMPOSITE PHOTOCATALYSTS BASED ON TiO_2 -ZnO POWDERS

S. Siuleiman*, D. Raichev, A. Bojinova, D. Dimitrov, K. Papazova

*Laboratory of Nanoparticle Science and Technology, Department of General
and Inorganic Chemistry, Faculty of Chemistry and Pharmacy, University of Sofia,
1 James Bourchier Blvd., Sofia 1164, Bulgaria*

This study is focused on preparation, characterization and photocatalysis with ZnO/TiO_2 nanocomposites samples, prepared by solid-state thermal procedure from the commercial metal oxide powders. The content of ZnO in the powder samples is varied from 0, 10, 25, 40, 50 60, 75, 90 to 100%. The phase composition and morphology of the mixed composites and thin films is characterized by X-ray and SEM analysis. The surface area of mixed powders is determined by BET analysis. The photocatalytic efficiency is checked in photodegradation of the organic azo dye Orange II, used as cosmetic colorant CI 15510, in aqueous solutions under UV and visible light irradiation.

It is found that the mixed powder samples of 90% ZnO content manifest the highest photocatalytic efficiency.

Acknowledgements: This research is financially supported by FP7 project Beyond Everest.

* E-mail: shahin.elmali@gmail.com

Keywords: ZnO/TiO_2 composites, photocatalysis, photodegradation, Orange II, UV, visible light.

STRUCTURAL PREREQUISITES FOR CATIONIC Cu-Zn ISOMORPHISM IN Cu, Zn HYDROXY-SULPHATE MINERALS

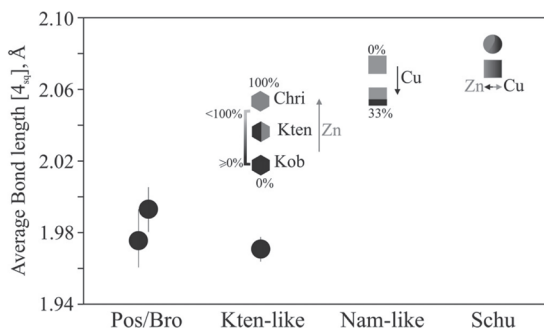
Ts. Stanimirova*, Z. Delcheva

University of Sofia "St. Kl. Ohridski", 15 Tzar Osvoboditel blvd., 1504 Sofia, Bulgaria

The crystal structural prerequisites for isomorphous substitution of $\text{Cu}^{2+} \leftrightarrow \text{Zn}^{2+}$ cations in the structures of copper hydroxy-sulphates ($[\text{Cu}^{2+}(\text{OH})_{2-x}\text{A}_{x/n}^{n-}][\pm\text{H}_2\text{O}]$ – brochantite, posnjakite, ktenasite, and shulenbergite) and zinc hydroxy-sulphates ($[\text{Zn}^{2+}(\text{OH})_{2-x}\text{A}_{x/n}^{n-}]\pm\text{H}_2\text{O}$ – namuwite, lahnsteinite and osakaite) were studied through series experiments – titration, ion-exchange, thermal treatment.

Depending on the different behavior of Cu^{2+} ($3d^9$) and Zn^{2+} ($3d^{10}$) in a strong ligand field, the two types of layered structures are formed [1, 2]. It was found that the different type of polyhedron of the two cations is main crystal structural factor that controls the rate of the isomorphism. The Cu–Zn cationic substitution was found to be possible only in structures with average bond length between the cations and the 4 closest coordinating anions (ABL[4_{sq}]) from 2.02 to 2.09 Å (Fig. 1). In the brochantite and posnjakite structures the Cu²⁺–Zn²⁺ isomorphism was not

Fig. 1. Cationic Cu-Zn isomorphous relationship depending on the ABL [4_{sq}] (○ – non-isomorphous; ◐, ◑ – isomorphous positions)



observed due to the small average bond length between the Cu^{2+} and 4 nearest OH groups (1.94–1.98 Å). The complete isomorphism in the ktenasite structure was found and proved only at one octahedral position, characterized by $\text{ABL}[4]=2.02$ Å. In the shulenbergite structure, the complete isomorphous substitution of Cu^{2+} by Zn^{2+} was obtained, while in opposite direction partially isomorphism was observed.

In the structures of Zn-hydroxide-type namuwite-like minerals the limited isomorphism was established. The amount of substitute cations was 1/3 of the cations in the octahedral position.

[1] A.C. Durand et al., J. Non-Crystal. Solids., 252 (2009) 125.

[2] Groat L. A., Am. Miner., 81 (1996) 238.

* E-mail: stanimirova@gea.uni-sofia.bg

Keywords: Cu-Zn hydroxy-salts, structures, isomorphism.

COMPOSITIONAL DEPENDENCE OF THE OPTICAL PROPERTIES OF THE $\text{GeTe}_3\text{-In}$ GLASSES

A. Stoilova¹, Y. Trifonova¹, V. Ivanova¹

¹ UCTM-Sofia, "Kl. Ohridski" blvd № 8, 1756 Sofia

In the current work we have investigated amorphous thin films from the system $\text{GeTe}_3\text{-In}$. This research continues our work on the study of tellurium-containing chalcogenide thin film materials. These materials exhibit unique physical properties that make them suitable for several potential applications such as infrared transmission and detection and memory switching. In this context, the analysis of the compositional dependence of their optical properties is an important aspect of their study [1].

We have produced them by using vacuum evaporation technique and investigated the structure and the electrical and optical properties of a multitude of amorphous thin films from the same ternary system by Ge/Te ratio 4 and 5. The results demonstrate changes in the optical properties such as decreases in the optical band gap and decreases in the value of the refractive index by increases in the In -content, that may be attributed to the formation of more numbers of defect centers and the increase in disorder with the increase in In content. The determination of the optical parameters of chalcogenide glasses from the system $\text{GeTe}_3\text{-In}$ contributes to the attempts to deepen the understanding of the basic mechanisms underlying the photoinduced phenomena of these materials [2–3].

The thin films from the system $\text{GeTe}_3\text{-In}$ were characterized by X-ray diffraction technique to test the amorphous nature of thin films. Transmission spectra of thin films were taken in the range of 400–2500 nm. The Swanepoel's method was used to calculate the optical parameters (refractive index and extinction coefficient) of the thin films.

- [1] Elliott S., Physics of amorphous materials, ed. Pitman Press Ltd., Bath, (2000).
- [2] Wong By H.-S. Philip, S. Raoux, S. B. Kim, J. Liang, J. P. Reifenberg, B. Rajendran, M. Asheghi, K. E. Goodson, Phase change memory, Proceedings of the IEEE, 98, 12, 2010.
- [3] A. Zaidan, V. Ivanova, P. Petkov, First principle electronic structure and atomic bonding calculations for chalcogenide GeTe_4 doped with indium, Advances in Natural Science: Theory & Applications, Volume 1 No. 1 2012, p. 37–46, Volume 1 No. 3 2012, p. 207–214.

* E-mail: ani_st@web.de

Keywords: Chalcogenide glasses, optical properties.

THE USE OF HIGH-TEMPERATURE SUPERCONDUCTING CUPRATE AS A DOPANT TO THE NEGATIVE ELECTRODE IN Ni-Zn BATTERIES

A. Stoyanova-Ivanova¹, S. Terzieva¹, G. Ivanova^{2,*}, M. Mladenov², D. Kovacheva³,
R. Raicheff², S. Georgieva⁴, B. Blagoev⁵, A. Zaleski⁶, V. Mikli⁷

¹ *Institute of Solid State Physics - BAS, Tsarigradsko Chaussee 72, 1784 Sofia, Bulgaria*

² *Institute of Electrochemistry and Energy Systems – BAS, G. Bonchev Street,
bl.10, 1113 Sofia, Bulgaria*

³ *Institute of General and Inorganic Chemistry – BAS, G. Bonchev Street,
bl.11, 1113 Sofia, Bulgaria*

⁴ *University of Chemical Technology and Metallurgy, 8 Kl. Ohridski, 1756 Sofia, Bulgaria*

⁵ *Institute of Electronics – BAS, 72 Tzarigradsko Chaussee Blvd., 1784 Sofia, Bulgaria*

⁶ *Institute of Low Temperature and Structure Research, Polish Academy of Sciences,
2 Okolna Str., 50-422 Wrocław, Poland*

⁷ *Centre for Materials Research, Tallinn University of Technology,
5 Ehitajate, 19086 Tallinn, Estonia*

Powder of $\text{YBa}_2\text{Cu}_3\text{O}_{7-\delta}$ (YBCO) ceramics is used as a conductive additive to the active mass of zinc electrodes in a laboratory nickel-zinc alkaline battery. The electrochemical studies are carried out by a specially designed electrochemical cell with demountable “coin” type zinc and nickel electrodes. The tests show that dopant of YBCO superconducting ceramic to the zinc electrode active mass improves cyclic operation ability as well as capacity stability and leads to higher specific capacity (with about 30%) of the cell compared to the cell with carbon as conductive additive to the active mass. The results obtained suggest a possible application of these structural type superconducting ceramics as additives to the electrode material of zinc electrodes for alkaline battery systems. The chemical stability of YBCO superconducting ceramics in alkaline medium is studied. The high chemical resistance of the ceramics in alkaline media is confirmed by structural observations and magnetic measurements.

* E-mail: aks_i_bg@abv.bg

Keywords: Superconducting ceramics; Alkaline treatment, Microstructure, Zn-electrode.

SYNTHESIS AND PHOTOCATALYTIC ACTIVITY OF Fe AND N-DOPED TiO₂

A. Stoyanova¹, N. Ivanova¹, A. Bachvarova-Nedelcheva², R. Iordanova²

¹ *Medical University, 5800 Pleven, Bulgaria*

² *Institute of General and Inorganic Chemistry, Bulgarian Academy of Sciences,
1113 Sofia, Bulgaria*

The present work reports on iron-, nitrogen-, and iron-nitrogen co-doped TiO₂ powders synthesis at low temperature using non-hydrolytic sol-gel method. It continues our investigations on the synthesis of nanosized TiO₂ powders with improved photocatalytic activity.

The structure of the obtained preparations was characterized by XRD, IR and UV-Vis spectroscopy. The average particle size was 15–25 nm.

The photocatalytic activity of doped TiO₂ powders was studied under both UV and visible light and was evaluated by the degradation of Malachite Green (MG) as model pollutant. It was found that the photocatalytic activity of N-modified TiO₂ was improved under UV irradiation, while Fe-N-co-doped sample showed the best photocatalytic sensitivity under visible light. Synthesized at low temperature Fe-doped TiO₂ did not show improved photo-activity under visible light.

The optimal dopant concentration was studied and an attempt was made to correlate it with photocatalytic activity.

* E-mail: a.stoyanova@mu-pleven.bg

Keywords: sol-gel synthesis, photocatalytic activity, TiO₂ doping.

EFFECTS OF MARBLE ON PHASE FORMATION IN SELF-COMPACTING TYPE DECORATIVE CEMENT COMPOSITES

V. Stoyanov¹, B. Kostova², E. Serafimova³, V. Petkova^{2,4}

¹ *University of Structural Engineering and Architecture (VSU) „Lyuben Karavelov“,
175 “Suhodolska” Str., 1373 Sofia, Bulgaria*

² *New Bulgarian University, Department of Natural Sciences, 21 “Montevideo” Str.,
1618 Sofia, Bulgaria*

³ *University of Chemical Technology and Metallurgy – Sofia, 8 “St. Kliment Ohridski” Bul.,
1756 Sofia, Bulgaria*

⁴ *Institute of Mineralogy and Crystallography, Bulgarian Academy of Sciences,
“Acad. G. Bonchev” Str., bldg.107, 1113 Sofia, Bulgaria*

The decorative cement mortars and concretes are an artificial imitation of the natural stones. The main advantage of these artificial stones is their better workability, but the durability and stability are the key objectives in the use of these cement composites. To achieve a good aesthetic surface of decorative composites, that allows their multilateral application (decorative stamp concrete, pots, balustrade, ornamental stones, restoration of architectural monuments, decoration of facades, fences, terraces, etc.), the use of white Portland cement and white or colour fine and coarse aggregates are necessary. These limitations both in phase and mineral composition of used cement, the disparate properties of the surface of the aggregates and the necessity of greater quantity of water suggest large differences in formed structure of these compositions, compared to conventional cement ones.

Due to their superior water-reduction capabilities the polycarboxylate-based admixtures strongly change the technology for producing Portland cement composites. The increase both of the dispersion of the cement particles and the amount of fines allow to create materials with high early-strengths caused by the dense structure, although the high workability of the fresh mixes.

Based on white Portland cement, three types of cementitious composites were studied. The density of their structure at 28 and 90 days of water curing were evaluated by measurement of some physical-mechanical properties such as density, compressive strength and porosity. X-ray diffraction analysis, IR and scanning electron microscopy were used to identify the crystal structures and their morphology.

The experimental data show that the cement composites with higher water content exhibit more variety of new-formed phases, like hydration products of C-S-H type. The structure of self-compacting type decorative mortars is so dense that there is no possibility of crystal hydrates development at late curing ages. The use of marble as filler leads to a partial inclusion of carbonate ions in the new-formed hydrated phases (carbo-aluminates).

* E-mail: vpetkova@nbu.bg, vilmapetkova@gmail.com

Keywords: White Portland cement, decorative mortar, cement hydration.

RAMAN SCATTERING AND IR REFLECTION MICRO-SPECTROSCOPIC STUDY OF HUMAN TEETH TREATED WITH Er:YAG DENTAL LASER

R. Titorenkova^{1,*}, B. Mihailova², G. Jegova³, M. Rashkova³

¹ *Institute of Mineralogy and Crystallography, Bulgarian Academy of Sciences,
Acad. G. Bonchev Str. 107, 1113 Sofia, Bulgaria*

² *Institute of Mineralogy and Petrology, University of Hamburg, Grindelallee 48,
D-20146 Hamburg, Germany*

³ *Faculty of Dental Medicine, Medical University Sofia, Georgi Sofiiski Str. 1,
1431 Sofia, Bulgaria*

Permanent and deciduous human teeth treated by a dental Er:YAG pulse laser ($\lambda = 2940$ nm) as well as by classical drilling tools were studied by UV Raman scattering (excitation wavelength of 325 nm) and Fourier transform infrared reflection microspectroscopy. Enamel was analyzed by both spectroscopic methods, whereas dentine was studied only by FTIR reflection due to the high level of photoluminescence continuum background even when a wavelength of 325 nm was used in inelastic light scattering experiments. The results [1] reveal that the apatite Ca-P-O framework remains intact, even the content of OH groups in the channels of the structure is preserved. The application of Er:YAG however causes mobilization and a consequent reduction of the carbonate groups incorporated into apatite. In addition, the laser treatment affects the conformation of the protein functional groups in a way, which seems to be similar to aging-related changes. The laser impact is most pronounced when a laser power of $8\text{ W} = 400\text{ mJ} \times 20\text{ Hz}$ was used. Both IR reflection and Raman scattering analyses show a negligible difference between deciduous and permanent teeth in their resistance upon Er:YAG laser irradiation.

[1] G. Jegova, R. Titorenkova, M. Rashkova, B. Mihailova. *Journal of Raman Spectroscopy*, 44(11) (2013) 1483.

* E-mail: rostitorenkova@dir.bg

Keywords: Er:YAG laser, teeth, UV Raman scattering, Fourier transform infrared (FTIR) reflection micro-spectroscopy.

SOL-GEL SILICA HYBRID MATERIALS APPLICABLE FOR EXTERNAL TREATMENT OF CONCRETE DEFECTS

E. Todorova*, G. Chernev, S. Djambazov

University of Chemical Technology and Metallurgy, 8 Kl. Ohrydski blvd, 1756 Sofia, Bulgaria

External treatment of concrete defects with materials which exhibit self - healing ability is a modern method for concrete protection. The self - healing process is connected with filling of the cracks and preventing their further distribution and materials, which can form calcium carbonate as filler are preferred, because of the durability of CaCO_3 . Combination of hybrid material containing calcium ions and bacterial cells is the optimal opportunity for that purpose. The hybrid material should exhibit stability, durability and flexibility to be able to penetrate in the crack. Furthermore, this material should be high reactive and biocompatible for providing interaction with bacterial cells, as well as formation of CaCO_3 . The synthesis technique, nature of initial components and structural characteristics are determined for development of material for external treatment of concrete defects.

Hybrid materials based on silica network and in situ incorporate two organic components (chitosan and polyethylene glycol) are synthesized via sol - gel method. The silica matrix obtained via hydrolysis and condensation reactions of tetraethyl orthosilicate provides the stability and durability of the hybrid. The organic components incorporated as monomers ensure the flexibility, biocompatibility and reactivity of the final material. The synthesis of the hybrid materials is carried out in neutral media, because of the compatibility with the bacterial cells and calcium ions are added for providing formation of CaCO_3 . The results from structural analysis (XRD, FTIR, SEM and AFM) showed, that obtained hybrid materials are characterized with amorphous, homogeneous structures. The FTIR spectra clearly demonstrated formation of the silica network, backbone organic units, as well as interactions between used organic components. Presence of free end groups of used components (Si-OH, C-OH, NH-) showed formation of high reactive hybrid materials. The AFM micrographs showed existence of particles (from 50 nm to 1 μm) on the surface, as their size vary with variation of organic component value. The obtained sol-gel silica hybrid materials can be combined with bacterial cells, because of the contact surface area and reactive centers, which ensure their possible interactions. The results from structural characterization showed, that obtained hybrids can be used as self - healing materials for external treatment of concrete defects.

* E-mail: elena.todorova.uctm@gmail.com

Keywords: Sol-gel, silica hybrids, nanomaterials, self - healing ability.

STRUCTURAL CHARACTERIZATION OF NEW MEROCYANINE DYE 4-[(E)-2-[4-(DIMETHYLAMINO)NAPHTALEN-1-YL]ETHENYL]-1-PENTYLQUINOLIUM BROMIDE DIHYDRATE

M. Todorova^{1,*}, R. Bakalska¹, T. Kolev²

¹ Plovdiv University "Paisii Hilendarski", Faculty of Chemistry, Department of Organic Chemistry, 24 Tsar Assen Str., 4000, Plovdiv, Bulgaria

² Bulgarian Academy of Sciences, Institute of Molecular Biology "Acad. Rumen Tsanev", 21 Acad. G. Bonchev Str., 1113, Sofia, Bulgaria

A merocyanine dye 4-[(E)-2-[4-(dimethylamino)naphthalen-1-yl]ethenyl]-1-pentylquinolinium bromide (**1**) has been synthesized by using a strategy D- π -A for the design of compounds with potential non-linear optical properties. The new compound has been characterized by X-ray diffraction. The crystal is monoclinic, space group $C2/c$, with **a** = 20.2988(18), **b** = 14.635(1), **c** = 19.8913(14), $V = 5155.5(8) \text{ \AA}^3$, **Z** = 8 (at 290 K). The unit cell consists of eight molecules of the dyes. The dye contains two water molecules in the solid state. The cation is nearly flat with a deviation of the planarity of -4.37° . All bond lengths of C-C are located between the normal C=C double bond (1.32 Å) and C-C single bond (1.53 Å), all C-C-C, C-N-C and C-C-N bond angles are close to 120° , which show that there is a highly π -electron delocalized system in the molecule. The structural parameter bond lengths alteration (BLA) – 0.134 Å has been calculated. The molecule is in trans-configuration as indicated by the torsion angle C(6)-C(20)-C(8)-C(10) 178.46° . The carbon-nitrogen bond lengths are as follows: N12-C28 1.430 Å, N12-C28 1.535 Å, N12-C16 1.407 Å. The N-dimethylamino group declines considerably from planarity with the torsion angle C(30)-N(12)-C(16)-C(15) – 71.06° , respectively.

* E-mail: mtodorova@uni-plovdiv.bg

Keywords: merocyanine dye, crystal structure, bond lengths alteration (BLA).

A NOVEL N,O-CONTAINING POLYDENTATE LIGAND AND ITS PALLADIUM COMPLEX – A STRUCTURAL STUDY

S. Todorova^{1,2}, G. Gencheva^{1,*}, V. Kurteva^{2*}, S. Simova², B. Shivachev³, R. Petrova³

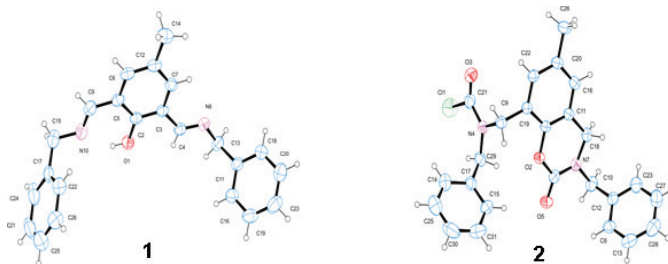
¹ Sofia University “St. Kliment Ohridski”, Faculty of chemistry and pharmacy, 1, blv. J. Bourchier, 1164 Sofia, Bulgaria

² Institute of Organic Chemistry with Centre of Phytochemistry, Bulgarian Academy of Sciences, Acad. G. Bonchev str., bl. 9, 1113 Sofia, Bulgaria

³ Institute of Mineralogy and Crystallography “Acad. Ivan Kostov”, Bulgarian Academy of Sciences, Acad. G. Bonchev str., bl. 107, 1113 Sofia, Bulgaria

In the search of metal-based drugs, able to improve the cisplatin spectrum of antitumor activity, the palladium compounds have been neglected, despite of their close electronic structure and coordination chemistry with these of platinum. One of the reasons is that they undergo aquation and ligand exchange reaction 10^4 to 10^5 times more rapidly than the corresponding complexes of platinum. An approach for modulation the kinetic behaviour and thus the corresponding cytotoxicity is to use proper ligand systems, which may increase the complex inertness. The palladium complex of a novel ligand **2** was obtained in acidic media and its structure in solution and solid state was characterized with NMR and IR.

The ligand **2** was obtained by a fast, efficient and simple protocol; conversion of *p*-cresol 2,6-bis-aldehyde into bis-imine compound **1** with benzyl amine followed by hydrogenation and reaction with phosgene. Its structure was determined by 1D and 2D NMR experiments and was confirmed by single crystal diffraction. The compound **2** crystallizes from methyl *t*-butyl ether in monoclinic *C*2/c space group with cell parameters $a = 27.8301(15)$, $b = 7.1729(4)$, $c = 22.2297(10)$ Å, $\beta = 91.577(4)^\circ$. The compound possesses a flat aromatic moiety.



Acknowledgments: The Scientific-Research Sector, SU “Sv. Kl. Ohridski”, Project 065/2014, is acknowledged.

* E-mail: ggencheva@chem.uni-sofia.bg (GG); vkurteva@orgchm.bas.bg (VK)

Keywords: carbamoyl chloride ligand, Pd-complex, NMR, X-ray.

SYNTHESIS OF MORDENITE TYPE ZEOLITE WITHOUT ORGANIC TEMPLATE

T. Todorova^{1,*}, Yu. Kalvachev¹, V. Valtchev²

¹ *Institute of Mineralogy and Crystallography, Bulgarian Academy of Sciences, Sofia, Bulgaria*

² *Laboratoire Catalyse & Spectrochimie, ENSICAEN, Université de Caen, Caen, France*

Mordenite is a zeolite with chemical formula: $| \text{Na}_8(\text{H}_2\text{O})_{24} | [\text{Al}_8\text{Si}_{40}\text{O}_{96}]$ having orthorhombic unit cell with space group Cmcn. Its structure is composed of five member rings forming characteristic building unit "Mor". Single crystals are elongated needle containing 8 and 12 member channels along [001].

Zeolite Mordenite has high thermal and acid stability because of its structure and high Si/Al ratio. Due to this stability mordenite has been used as a catalyst in many important reactions such as hydrocracking, hydroisomerization, alkylation, acid-catalyzed isomerization of alkanes and aromatics, reforming. Mordenite has also been used in the adsorptive separation of gas or liquid mixtures. Recently, mordenite has been applied in semiconductors, chemical sensors, and nonlinear optics.

This study reports the hydrothermal synthesis of mordenite crystals without organic template and characterization of the resulting crystals. Two synthesis techniques are applied. In the first one a standard initial gel $18\text{SiO}_2 : \text{Al}_2\text{O}_3 : 1,24 \text{ K}_2\text{O} : 1,21\text{Na}_2\text{O} : n\text{H}_2\text{O}$ ($n=600; 280; 22.5$) is subjected to hydrothermal crystallization at 160 and 180°C, for period ranging between 1 and 7 days. The second technique is in the presence of seeds. Seeds are added to the same starting gel. Mordenite crystals are used as seeds. The crystals growth kinetics of mordenite at different seed content (1, 2 and 5 wt.%) was studied. Resulting gel stays at room temperature for 24 hours, then placed for crystallization at 160 and 180°C for a different time (6–120 hours). The used reagents for the synthesis are: SiO_2 (100%, Degussa), Al (100% powder, Merck), KOH (85% pellets, Fluka), NaOH (98% pellets, Fluka) and distilled water. The obtained crystals were characterized by X-ray diffraction, scanning electron microscope, thermogravimetric analysis, and infrared spectroscopy. By using of seed-induced process we are able to synthesize mordenite crystals with relatively widely particle size distribution in nanometer scale. It is found that seed concentration and the synthesis temperature are important factors influencing the crystallization time and the characteristics of the products investigated.

Acknowledgements: The authors acknowledge the financial support from project BG051PO001-3.3-06-0027, financed by the operational programme "Human resources development".

NULLIFYING THE EXTINCTION EFFECT BY REFORMING THE EXTINCTION CORRECTIONS

I. Tomov^{1,*}, S. Vassilev²

¹ *Institute of Optical Materials and Technologies, BAS, 1113 Sofia, Bulgaria*

² *Institute of Electrochemistry and Energy Systems, BAS, 1113 Sofia, Bulgaria*

To nullify the secondary extinction (SE) effect by XRD characterizations of a crystal medium, one of the most significant discrepancy of the conventional approach [1,2] to treating the SE problem should be reconsidered. This discrepancy concerns severe approximations in the theoretical models of the inner morphology of the crystal, which do not accord with experimental evidence. To gain insight and resolve the problem, two expressions, $(I_{kin}/Q)=P I_0/(S/2\mu)$ and $\varepsilon=gQ[p_2/(p_1)^2]$, are herewith combined. Accounting for the pole density P , the first expression reveals explicitly the texture influence on powder diffraction [3]. The next expression is the SE correction itself [1,2] that is charged by above-mentioned discrepancy in terms of the SE coefficient g . Here, I_{kin} is the kinematical intensity, Q is the reflectivity per unit crystal volume, I_0 is the X-ray intensity of the incident beam, S is the beam cross section, μ is the ordinary linear absorption coefficient, P is the pole density, and p_n ($n=1, 2$) is the polarization of I_0 . The combined entities yield both a theoretically reformed SE correction, $\varepsilon=k I_{kin}[p_2/(p_1)^2]$, that has been empirically introduced earlier [4], and a relationship, $k=(g/P I_0)(2\mu/S)$, between diffraction and extinction. By its very nature, this relationship specifies the behaviour of the SE coefficients, k and g , and, hence, the respective SE corrections. This behaviour is adequately controlled by any variation of the level of interaction ($P I_0$) of the diffraction process (I_{kin}/Q) carried out in a crystal volume defined by the absorption factor ($S/2\mu$) that is a constant of the XRD pattern. To distinguish between the behaviour of k and g , we suppose a set of levels of interaction defined in particular. In this context, whereas I_0 varies from level to level, the pole density P is held to be a constant for the same set of levels of interaction. Only under such conditions, the term $(g/P I_0)$ is a constant since I_0 scales g by means of the constant P . Moreover, since the right hand side, $(g/P I_0)(2\mu/S)$, of the above-written relationship is a product of two constants, the coefficient k is also a constant. The constancy of k is used for analytical nullifying the SE effect. In this respect, the essence of k is thoroughly analysed. As a result, a pioneer technique for k calculation is developed using a series of intensities I_m measured at the above set of levels of interaction, the variation being controlled by I_0 alone in terms of a variation of the current density i of the generator tube under otherwise equal conditions. Except for the purposes of the XRD characterizations of the real structure of textures and powders, this approach allows for resolving problems of X-ray crystallography as well.

[1] Darwin, C. G., Phil. Mag., 43 (1922) 800.

[2] Zachariasen, W. H., Acta Cryst., 16 (1963) 1139.

[3] Bunge, H. J., Textures and Microstructures, 29 (1997) 1.

[4] Bragg, W. L., James, R. W., Bosanque, C. H., Phil. Mag., 42 (1921) 1.

* E-mail: iv.tomov39@gmail.com

Keywords: extinction, nullifying, effect, XRD measurements.

TRANSITIONS BETWEEN REGIMES OF NEW PHASE GROWTH KINETICS; ILLUSTRATION WITH GROWTH OF EQUALLY-SIZED CRYSTALS

V. Tonchev*

Institute of Physical Chemistry, Bulgarian Academy of Sciences, 1113 Sofia, Bulgaria

Using a general expression for the phase transformation kinetics, i.e. growth velocity as a function of the supersaturation, we study the possibility for transitions between different regimes of growth as described by the power g in the normal velocity equation. The model is restricted to the archetypical case when the deviation from equilibrium, i.e. the initial supersaturation S_0 , is defined in the beginning and not sustained further. Then, beyond the initial stage of new phase formation (nucleation), growth of the objects from the new phase starts. We focus our treatment on this second stage and assume that normal velocity r_g of the interface is proportional to the supersaturation S raised to a power g with proportionality coefficient β_g : $r_g = \beta_g S^g$. Invoking the postulate that when two kinetic regimes are simultaneously available in the system the one with higher velocity dominates the other, we show that transition between these regimes with decreasing supersaturation is possible only if the second regime has a lower value of g . Thus, in order to have transition into a regime with higher value of g it is expected to become available at some value of the decreasing supersaturation. This case has two variants: (i) when the new regime of growth replaces once and for all the former one and (ii) when the former regime is still available in the system, in this case a jump of the velocity is to be expected in order to enable the transition. In this second variant after further decrease of the supersaturation the growth rates of the two regimes will become equal again. Some of our predictions are compared with experimental data from literature. Finally, these regimes are illustrated for the case of growth of equally-sized crystals.

* E-mail: vesselin.tonchev@gmail.com

** The results to be presented in this talk are obtained in collaboration with *Georgi As. Georgiev* and *Hristo Nanev* (Sofia) and *Peter Vekilov* (Houston) but their presentation itself is a sole responsibility of the presenter.

Keywords: Batch crystallization, Equally-sized crystals, Crystal growth velocity, Morphology transitions.

A SERIES OF Zn^{2+} COMPLEXES OF 1,2-BIS(DIMETHYL-PHOSPHINYLMETHYLENOXY)BENZENE LIGAND – SYNTHESIS, STRUCTURAL CHARACTERIZATION AND SOLUTION CHEMISTRY

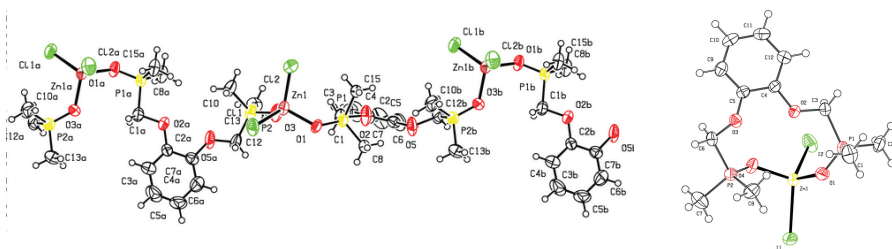
D. Tsekova^{1,*}, Y. Zhelyazkova¹, R. Petrova², B. Shivachev², N. Vassilev³,
P. Gorolomova¹, S. Varbanov³, T. Tosheva³, G. Gencheva¹

¹ Faculty of Chemistry and Pharmacy, Sofia University "St. Kliment Ohridski",
1164 Sofia 1 J. Bourchier Blvd., Bulgaria

² Institute of Mineralogy and Crystallography "Acad. Ivan Kostov", Bulgarian Academy of Sciences,
Acad. G. Bonchev str., bl. 107, 1113 Sofia, Bulgaria

³ Institute of Organic Chemistry with Center of Phytochemistry, Bulgarian Academy
of Sciences, 1113 Sofia

Nowadays chemistry of the coordination polymers is characterized with elaborating of large diversity of structural architectures as the challenge is to achieve particular chemical and physical functionalities. A successful approach for their construction is based on proper assembling of metal ions, multidentate organic ligands, inorganic counter ions and a precise choice of reaction conditions. Recently, several series of Mn^{2+} , Cu^{2+} and Zn^{2+} coordination polymers of O,O-bidentate and O,N,O-tridentate ligands containing two tertiary phosphine oxides as donor functional groups have been obtained. Herein we report the synthesis, structural characterization,



spectroscopic properties (IR, ^1H - and $^{31}\text{P}\{^1\text{H}\}$ NMR) of Zinc(II)-halide coordination compounds obtained with bidentate ligand 1,2-bis(dimethyl-phosphinylmethylenoxy)-benzene, L. Studying the influence of the counter ion on their self-assembly and crystallization in polymer structures we proved that the size of halide ions guides the supramolecular structure formation. Thus, the applying of the smaller in size Cl^- and Br^- ions favours the organic ligand bridging in a polymeric structure while the bigger I^- ions – directs to ligand chelation in a mononuclear structure.

* E-mail: DTsekova@chem.uni-sofia.bg

Keywords: Zn(II) complexes, Coordination polymers, single-crystal structure.

SILICA SUPPORTED COPPER AND COBALT OXIDE CATALYSTS FOR METHANOL DECOMPOSITION: EFFECT OF PREPARATION PROCEDURE

T. Tsoncheva¹, I. Genova^{1,*}, N. Scotti², M. Dimitrov¹, V. Dal Santo²,
D. Kovacheva³, N. Ravasio²

¹ *Institute of Organic Chemistry with Centre of Phytochemistry, BAS, Sofia, Bulgaria*

² *Institute of Molecular Sciences and Technologies of the National Research Council,
ISTM-CNR, Milano, Italy*

³ *Institute of General and Inorganic Chemistry, BAS, Sofia, Bulgaria*

Methanol (bio-methanol) is regarded as promising candidate for hydrogen production and storage, but the efficiency of its application depends on the possibility to obtain low-temperature and highly active and selective catalyst for its decomposition. Cobalt–copper oxides ($\text{Cu}_x\text{Co}_y\text{O}_z$) have attracted attention from many researchers worldwide for applications such as catalysis in Fischer–Tropsch process; synthesis of syngas-based alcohol, thermoelectricity material etc. The aim of present study is to follow the effect of preparation procedure on the preparation of supported on silica copper-cobalt bi-component materials. For the purpose, a modified “chemisorption-hydrolyses” method was first time applied to the deposition of copper-cobalt mixed oxide phase on silica. The samples were characterized with XRD, UV-Vis, XPS, TPR, FTIR of adsorbed pyridine, and compared with the similar materials obtained by simple incipient wetness impregnation technique. All materials were tested as catalysts in methanol decomposition. It was established, that the modification procedure strongly affects the interaction of copper and cobalt species. Well crystallized, easily reduced spinel phase with high catalytic activity in methanol decomposition is formed on silica by incipient wetness impregnation of silica support with nitrate precursors. The strong interaction of copper, and cobalt species with the silica support when “chemical-hydrolyses” procedure is applied renders difficult the formation of bulk spinel phase, but improved catalytic activity even though in lower extent as compared to the impregnated samples is also observed for bi-component materials. The formation of bi-component copper-cobalt oxide phase facilitates the preservation of metal particles in highly dispersed state under reduction atmosphere, which provides high catalytic activity.

Acknowledgments: Financial support project DFNI-E01/7/2012 and BAS-CNR bilateral project is acknowledged.

* E-mail: izabela_genova@abv.bg

Keywords: $\text{Cu}_x\text{Co}_y\text{O}_z$, chemisorption–hydrolyses method, methanol decomposition.

CRYSTAL STRUCTURES OF ION EXCHANGED ETS-4

L. Tsvetanova^{1,*}, S. Ferdov², B. Shivachev¹, R. Nikolova¹

¹ *Institute of Mineralogy and Crystallography, Bulgarian Academy of Sciences, Sofia, 1113, Bulgaria*

² *Department of Physics, University of Minho, 4800-058 Guimarães, Portugal*

Microporous titanosilicate Na-K-ETS-4 has been synthesized and exchanged to Mg, Cs, Ba, Al, Mn, Fe, Ni, Cu, Ag, Zn and Eu forms. The crystal structures were analyzed by single crystal X-ray diffraction and the chemical compositions were confirmed by energy dispersive X-ray spectroscopy. Chemical analyses showed that Na⁺ and K⁺ ions in ETS-4 could be fully exchanged by Zn²⁺, Ba²⁺, and Ag⁺ ions and only partially by Mg²⁺, Cs⁺, Mn²⁺ and Cu²⁺ ions. In the used conditions for ion exchange the Al³⁺, Fe²⁺, Ni²⁺ and Eu³⁺ ions do not replace Na⁺ and K⁺ from the as-synthesised sample.

Mg²⁺ ion occupy sodium position, Mn²⁺ and Zn²⁺ ions occupy sodium and potassium positions, while Ba²⁺, Cs⁺, Cu²⁺ and Ag⁺ ions are placed in both the positions of the charge compensating ions and positions of water molecules. The investigation shown that ion exchanged with different types of cations causes framework deformations and influences the volume of the unit cell. Increase in the volume of the unit cell is observed in the Cs-ETS-4, while for Ag and Mg forms volume remain almost the same. Significant decrease in volume was observed for Ba-ETS-4, Zn-ETS-4, followed by Mn-ETS-4 and Cu-ETS-4 (Fig. 1). The largest increase in the volume of the unit cell is observed in Cs-ETS-4, then Ag-ETS-4 and Mg-ETS-4 and reducing the volume is observed in the following order: Ba-ETS-4, Zn-ETS-4, Mn-ETS-4 and Cu-ETS-4.

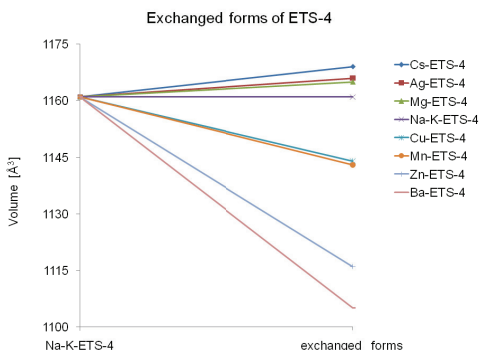


Fig. 1. Volume of the unit cell of Na-K-ETS-4 and the exchanged forms

The elastic behavior of the ETS-4 structure is most strongly expressed on decrease the parameter "a" in following order: Na-K-ETS-4 > Ag-ETS-4 > Mg-ETS-4 > Cs-ETS-4 > Cu-ETS-4 > Mn-ETS-4 > Ba-ETS-4 > Zn-ETS-4. The presented structural information can be of great value for elucidation of recently discovered antitumor, NO storage and gas separation applications of different ion exchanged forms of ETS-4.

PHOTOCATALYTIC ACTIVITY OF NANOSTRUCTURE ZINC FERRITE-TYPE CATALYSTS IN DEGRADATION OF MALACHITE GREEN UNDER UV-LIGHT

M. Tsvetkov^{1,*}, K. Zaharieva², Z. Cherkezova-Zheleva², M. Milanova¹, I. Mitov²

¹ University of Sofia, Faculty of Chemistry, 1, J. Bourchier Blvd., Sofia 1164, Bulgaria

² Institute of Catalysis, BAS, Acad. G. Bonchev Str., Bld. 11, Sofia 1113, Bulgaria

Series of nanosized zinc ferrite-type powders $\text{Zn}_x\text{Fe}_{3-x}\text{O}_4$ ($x = 0.25, 0.5, 1$) were synthesized using procedure described in [1]. The prepared samples by co-precipitation or co-precipitation and mechanochemical treatment were tested for photocatalytical degradation of malachite green (concentration 10^{-5} M) under UV-light. The catalysts showed good rate constant under these conditions. The obtained results established that co-precipitated zinc ferrite-type powders show the higher photocatalytic activity than the mechanochemically treated samples: ZnFe_2O_4 ($k=13.7 \times 10^{-3} \text{min}^{-1}$) > $\text{Zn}_{0.5}\text{Fe}_{2.5}\text{O}_4$ ($k=10.7 \times 10^{-3} \text{min}^{-1}$) > $\text{Zn}_{0.25}\text{Fe}_{2.75}\text{O}_4$ ($k=9.4 \times 10^{-3} \text{min}^{-1}$) > $\text{Zn}_{0.5}\text{Fe}_{2.5}\text{O}_4$ (MCT-2hours) ($k=8.1 \times 10^{-3} \text{min}^{-1}$) > ZnFe_2O_4 (MCT-1hour) ($k=6.3 \times 10^{-3} \text{min}^{-1}$). As can be seen the increasing of Zn^{2+} content in magnetite host structure of material prepared by co-precipitation leads to formation of photocatalyst with higher rate constant than the other co-precipitated ferrite-type samples. The photocatalytic measurements about mechanochemically treated zinc ferrite-type powders determined that photocatalytic activity increase with activation time and decreasing amount of Zn^{2+} ions incorporated in magnetite host lattice. The present study show that photocatalytic activity of zinc ferrite-type materials depends on the preparation method, degree of incorporation of Zn^{2+} ions in magnetite host structure and the milling time of mechanochemical treatment. The nanodimensional zinc ferrite-type samples possess good sorption ability of the dye after the dark period in the range 75–90% and such materials could be used as sorbents for organic dye pollutants.

[1] K. Zaharieva et al., Nanoscience and Nanotechnology (Eds. E. Balabanova, E. Mileva), 14 (2014) accepted.

* E-mail: mptsvetkov@gmail.com

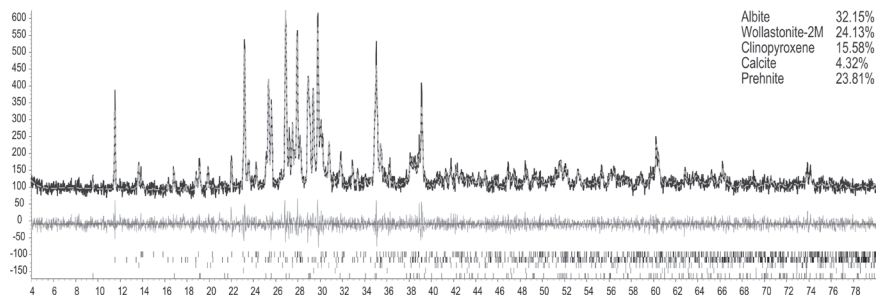
Keywords: zinc ferrite-type material, photocatalysis, Malachite Green.

QUANTITATIVE PHASE ANALYSIS OF SKARN ROCKS USING RIETVELD-BASED XRD METHOD

Y. Tzvetanova*, B. Shivachev, O. Petrov

*Institute of Mineralogy and Crystallography "Acad. Ivan Kostov", Bulgarian Academy of Sciences,
Acad. Georgi Bonchev Str., bl. 107, 1113 Sofia, Bulgaria*

The Rietveld method has become one of the most appropriate techniques for the quantification of mineral abundances in natural and industrial polycrystalline materials based on X-ray powder diffraction. In the Rietveld method, the difference between all data set points of the observed and the calculated profiles is minimized by a least squares refinement of selected parameters. The aim of this work is to present a technique for the rapid, inexpensive and accurate quantitative determination of mineral phases in large, heterogeneous samples of skarn rocks. The phase quantification procedure involved the identification of major and minor phases and a subsequent quantitative phase analysis of all data sets by the full profile Rietveld method implemented in the Topas v4.2. The skarn rocks selected for this study consist mainly of plagioclase, clinopyroxene, wollastonite-2M, garnets of the grossular-andradite series and epidote. The samples additionally contain varying amounts of prehnite, calcite, quartz, chlorite, thaumasite and accessory minerals – titanite, magnetite and apatite. Step-scan X-ray powder diffraction data were collected over a range of 4–80 2 θ with CuK α radiation on D2 Phaser – Bruker AXS Bragg-Brentano diffractometer operated at 30 kV and 10 mA with a step size of 0.02 2 θ and a counting time of 4 s/step. Starting values for the atomic positions and cell dimensions for each phase were obtained from published



crystal-structure refinements of minerals with compositions similar to those in the studied samples. Refinements for quantitative phase-analysis were done in the following general sequence: zero-shift parameter, scale factors for all phases, background polynomial parameters, unit cell dimensions of the phases, asymmetry parameters, and preferred orientation parameters for phases with marked grain-shape anisotropy. Phases in concentrations greater than about 20% were refined further for site occupancies and overall temperature factor alternatively, depending on the composition of the sample. The progress of the refinement is monitored by a number of agreement indices, among those commonly used are Rp, Rwp, Rexp, and the goodness of fit index GofF. Plots of the observed, calculated, and 'difference' powder diffraction pattern profiles for the Rietveld refinements of selected sample are given on Figure. The agreement indices are: Rexp – 13.76, Rwp – 15.00, Rp – 13.66, GofF – 1.09 DW – 1.97.

* E-mail: yana.tzvet@gmail.com

Keywords: Rietveld refinement, quantitative analysis, X-ray powder diffraction, skarn minerals.

CRYSTAL STRUCTURE OF $\text{In}_2(\text{WO}_4)_3$ AND HIGH-TEMPERATURE PHASE TRANSITIONS IN THE SERIES $\text{Al}_{2-x}\text{In}_x(\text{WO}_4)_3$

P. Tzvetkov^{1,*}, I. Koseva¹, L. Dimowa², V. Nikolov¹, D. Kovacheva¹

¹ *Institute of General and Inorganic Chemistry, Bulgarian Academy of Sciences,
Acad. G. Bonchev Street, bl. 10, 1113 Sofia, Bulgaria*

² *Institute of Mineralogy and Crystallography, Bulgarian Academy of Sciences,
Acad. G. Bonchev Street, bl. 107, 1113 Sofia, Bulgaria*

The compounds under investigation belong to the class with general formulae $\text{Me}_2(\text{WO}_4)_3$, where $\text{Me} = \text{Y}, \text{Sc}, \text{In}, \text{Al}$ or lanthanides with a small ionic radius – $\text{Ho}, \text{Er}, \text{Tm}, \text{Yb}, \text{Lu}$. They exhibit interesting properties such as Me^{3+} ionic conductivity, zero, low or negative thermal expansion coefficient and possibility Me^{3+} to be substituted by laser active ions. These make the compounds attractive for applications in special ceramics, sensors, optics and optoelectronics. In this study the crystal structure of $\text{In}_2(\text{WO}_4)_3$ was determined using single crystal x-ray diffraction at room temperature. The selected crystal was grown by the flux method. The crystal structure was solved in monoclinic space group $\text{P2}_1/\text{c}$ with lattice constants $a = 16.403(2)$, $b = 9.623(2)$, $c = 16.347(2)$ Å, $\beta = 109.12^\circ(3)$.

End members of the series $\text{Al}_{2-x}\text{In}_x(\text{WO}_4)_3$ are known to have structural phase transitions from low temperature monoclinic space group $\text{P2}_1/\text{c}$ to high temperature orthorhombic space group Pnca at very different temperatures (-15°C for $\text{Al}_2(\text{WO}_4)_3$ and 254°C for $\text{In}_2(\text{WO}_4)_3$ according to literature data). Morphotropic transition from orthorhombic to monoclinic structure was observed within the series $\text{Al}_{2-x}\text{In}_x(\text{WO}_4)_3$. We report on high-temperature powder x-ray diffraction measurements for members of the series $\text{In}_2(\text{WO}_4)_3$, $\text{In}_{1.5}\text{Al}_{0.5}(\text{WO}_4)_3$ and $\text{In}_{1.3}\text{Al}_{0.7}(\text{WO}_4)_3$. The temperature of phase transition decreases almost linearly with the increase of aluminum content. Variation of the crystal structure with the temperature change and chemical composition is discussed.

* E-mail: p-tzvetkov@gmx.net

Keywords: tungstates, crystal structure, phase transition.

PREPARATION AND SUPERCAPACITIVE PROPERTIES OF BIOGENIC AND SYNTETIC $\alpha\text{-Fe}_2\text{O}_3$ /ACTIVE CARBON NANOCOMPOSITES

S. Veleva^{1,*}, R. Angelova², L. Stoyanov¹, V. Grudeva², D. Kovacheva³,
M. Mladenov¹, N. Boshkov⁴, D. Karashanova⁵, R. Raicheff¹

¹ *Institute of Electrochemistry and Energy Systems – BAS, Acad. G. Bonchev Street,
bl.10, 1113 Sofia, Bulgaria*

² *Faculty of Biology, University of Sofia, 1164 Sofia, Bulgaria*

³ *Institute of General and Inorganic Chemistry – BAS, Acad. G. Bonchev Street,
bl.11,1113 Sofia, Bulgaria*

⁴ *Institute of Physical Chemistry – Acad. R. Kaishev BAS, Acad. G. Bonchev Street,
bl. 11,1113 Sofia, Bulgaria*

⁵ *Institute of Optical materials and Technologies “Acad. Jordan Malinovski”,
Acad. G. Bonchev Street, bl. 109, 1113 Sofia, Bulgaria*

The biogenic iron oxides/hydroxides nanosized materials were obtained by laboratory cultured *Leptothrix* bacteria. $\alpha\text{-Fe}_2\text{O}_3$ nanoparticles have been successfully obtained by annealing $\alpha\text{-FeOOH}$ precursor and by chemical synthesis method. The oxides are structurally and morphologically characterized by X-Ray diffraction (XRD), Transmission electron microscopy(TEM), Scanning electron microscopy (SEM) and low temperature nitrogen adsorption (BET). The nanocomposites $\alpha\text{-Fe}_2\text{O}_3$ / Active carbon were tested as electrode materials for asymmetric lithium-ion supercapacitors using galvanostatic charge/discharge cycling. The result indicates that the pseudocapacitor effect dominates the charge/discharge process. The $\alpha\text{-Fe}_2\text{O}_3$ synthesized at different temperature indicates that $\alpha\text{-Fe}_2\text{O}_3$ with a high crystallinity manifests relatively better cycling performance with a capacity of 120 F g⁻¹ at current density of 50 mA g⁻¹. While the current density increases to 500 mA g⁻¹, the corresponding discharge capacity can still remain as much as 20 F•g⁻¹. Meanwhile, XPS spectrum results of the active electrode material as-prepared and after a discharge process disclose that the electrochemical reaction mechanism happens in the half-cell lithium ion battery is the reduction of Fe_2O_3 to Fe.

Keywords: biogenic iron oxide, nanoparticles, hybrid lithium-ion supercapacitors.

THIOL-AMINE FUNCTIONALIZED MESOPOROUS SILICA BASED HYBRID MATERIALS

N. Velikova^{1,*}, Y. Vueva¹, P. Vassileva², A. Detcheva², R. Georgieva², Y. Ivanova¹

¹ *University of Chemical Technology and Metallurgy, 8 Kliment Ohridski Blvd., 1756 Sofia, Bulgaria*

² *Institute of General and Inorganic Chemistry, Bulgarian Academy of Sciences,
"Acad. G. Bonchev", bl. 11, 1113 Sofia, Bulgaria*

In recent years the mesoporous organic-inorganic hybrid materials have a wide range of application due to the presence of organic functional groups and pore size from 2 to 50 nm. The present work is focused on the synthesis, characterization and investigation of the adsorption properties toward the Hg(II) ions of hybrid materials in the system tetraethyl orthosilicate (TEOS)-bis-[3-(trimethoxysilyl)propyl] amine (BTPA)- bis[3-(triethoxysilyl)propyl]tetra sulfide (BTPTS). Silica based hybrid materials were prepared using sol-gel processing by co-condensation of the silica precursors in acidic media. The mesoporous were generated by surfactant templated method by using of Pluronic P123 as a porogen. The presence of the organic functional groups was confirmed by FTIR and NMR analysis. The textural characteristics were determined by BET analysis. SEM was used to observe the external morphology of the as synthesized hybrid gel materials.

In order to examine the potential of these mesoporous materials as adsorbents for heavy metals, Hg(II) adsorption were studied by means of the batch method. Mercury concentration was determined by flame AAS. Experiments were carried out in acidic media. Kinetic of adsorption was also investigated. We fixed the two hours as the optimum contact time to establish adsorption equilibrium. Pseudo-first order, pseudo-second order and intraparticle diffusion models were used to analyze kinetic data. Equilibrium experimental data were fitted to different mathematical equations. It was established that Langmuir isotherm most adequately describes the adsorption processes for all studied hybrids. Adsorption of Hg (II) ions from aqueous solutions showed high adsorption capacities suggesting that studied thiol-amine functionalized materials have good potential to be used as adsorbents for Hg (II) ions in acid solutions.

Acknowledgements: This material (presentation, paper, report) has been produced with the financial assistance of the European Social Fund, project number BG051PO001-3.3.06-0014. The author is responsible for the content of this material, and under no circumstances can be considered as an official position of the European Union and the Ministry of Education and Science of Bulgaria. The authors kindly acknowledge the financial support by the National Science Fund of Bulgaria (Contract No DCVP-02/2/2009 UNION).

* E-mail: nina.e.v@abv.bg

Keywords: Silica-based mesoporous organic–inorganic hybrid materials; Amine-functionalized organosilicas; Surfactant template method; Metal ion adsorption.

MESOSCOPIC-SCALE ATOMIC ARRANGEMENTS IN Ru-DOPED PEROVSKITE-TYPE RELAXOR FERROELECTRICS REVEALED BY X-RAY ABSORPTION SPECTROSCOPY

T. Vitova¹, S. Mangold², C. Paulmann³, V. Marinova⁴,
M. Gospodinov⁵, B. Mihailova^{3,*}

¹ Institut für Nukleare Entsorgung, Karlsruher Institut für Technologie, Hermann-von-Helmholtz-Platz 1, D-76344 Eggenstein-Leopoldshafen, Germany

² ANKA Synchrotronstrahlungsquelle, Karlsruher Institut für Technologie, Hermann-von-Helmholtz-Platz 1, D-76344 Eggenstein-Leopoldshafen, Germany

³ FB Geowissenschaften, Universität Hamburg, Grindelallee 48, 20146 Hamburg, Germany

⁴ Institute of Optical Materials and Technologies, Bulgarian Academy of Sciences, Acad. G. Bontchev Str. 109, 1113 Sofia, Bulgaria

⁵ Institute of Solid State Physics, Bulgarian Academy of Sciences, Blvd. Tzarigradsko Chaussee 72, 1784 Sofia, Bulgaria

The search for advanced materials with high response functions has spotted complex perovskite-type (ABO_3) relaxor ferroelectrics with Pb^{2+} on the A site. Ruthenium is a mixed-valence photochromic element and its incorporation into relaxor host matrices has the potential to induce new properties, which in turn is strong motivation for fundamental structural studies of Ru-doped relaxors. The aim of this study was to analyze the way of incorporation of Ru into $PbSc_{1/2}Ta_{1/2}O_3$, $PbSc_{1/2}Nb_{1/2}O_3$, and $0.9PbZn_{1/3}Nb_{2/3}O_3-0.1PbTiO_3$ by x-ray absorption spectroscopy and complementary optical and multi-wavelength Raman spectroscopy as well as synchrotron x-ray diffraction, to gain further insights on the mesoscopic-scale relaxor structure.

For all three compounds the incorporation of Ru hinders the development of ferroelectric long range order and leads to a red shift of the optical absorption edge, as the latter effect is much stronger for $PbB'_{1/2}B''_{1/2}O_3$ as for $PbB'_{1/3}B''_{2/3}O_3$ - $PbTiO_3$. Ruthenium enters $PbB'_{1/2}B''_{1/2}O_3$ as a point substitution defect on the B'' site, whereas in $PbB'_{1/3}B''_{2/3}O_3$ - $PbTiO_3$ Ru substitutes for both B and A-site cations, forming clusters of face-sharing elongated octahedra. Mesoscopic-scale chemical 1:1 B-site order is predominant in $PbB'_{1/2}B''_{1/2}O_3$, although the subtle/none degree of chemical long-range order. The $PbB'_{1/2}B''_{1/2}O_3$ relaxors also exhibit mesoscopic-scale dynamic BO_6 tilt order and the tilt angle correlates with the degree of Pb positional order.

[1] T. Vitova et al., Phys. Rev. B, 89 (2014) 144112.

* E-mail: boriana.mihailova@uni-hamburg.de

Keywords: x-ray absorption spectroscopy, relaxors, perovskite, ruthenium.

BaTiO₃ CRYSTALLIZATION FROM MULTICOMPONENT OXIDE GLASSES – PHASE COMPOSITION AND MICROSTRUCTURE INVESTIGATION

L. Vladislavova¹, R. Harizanova^{1,*}, C. Bocker², G. Avdeev³, M. Abrashev⁴,
I. Gugov¹, C. Rüssel²

¹ *Department of Physics, University of Chemical Technology and Metallurgy,
8 Kl. Ohridski Blvd., 1756 Sofia, Bulgaria*

² *Otto Schott Institute, University of Jena, Fraunhoferstr. 6, 07743 Jena, Germany*

³ *Institute of Physical Chemistry, Bulgarian Academy of Sciences, Block 11,
Acad. G. Bonchev Str., 1113 Sofia, Bulgaria*

⁴ *Faculty of Physics, Sofia University, 5 James Bourchier Str, 1164 Sofia, Bulgaria*

BaTiO₃ is dielectric material with numerous allotropic modifications which exhibit interesting electrical and mechanical properties. Usually, the cubic and tetragonal modifications of barium titanate are of practical interest due to their high dielectric constants which determine their potential application as parts of capacitors, different sensing or transducer devices.

The present work reports on the synthesis of oxide glasses with high concentrations of alkali, alkaline earth and 3d metals in which, after appropriate annealing, the crystallization of BaTiO₃ is achieved. The characteristic temperatures of the glasses are obtained by DTA and the subsequent annealing above the glass-transition temperature results in the precipitation of barium titanate with very high volume fraction. Initially, the phase composition identification is performed by x-ray diffraction and suggests formation of either cubic or tetragonal BaTiO₃. Further, to determine the exact allotropic modification of BaTiO₃ present, Raman spectroscopy is used and the presence solely of the cubic modification is established. The investigation of the microstructure is performed by scanning and transmission electron microscopy and suggests that first phase separation and further growth of barium titanate globular crystals in the unmixed regions occurs.

* E-mail: ruza_harizanova@yahoo.com

DESIGNE OF OPTICAL BIOSENSORS FOR DETECTION OF PHARMACEUTICAL PRODUCTS

S. Yaneva^{1,*}, A. Hassaan², L. Yotova²

¹ *University of Chemical Technology and Metallurgy, Department of Fundamentals of Chemical Technologies*

² *University of Chemical Technology and Metallurgy, Department of Biotechnology, blvd. Kl. Ohridski 8, Sofia, Bulgaria, 1756*

Sol–gel approach have rapidly become a fascinating new field of research in materials science. The use of some organic molecules in the gel formation process that may influence the dimensions of the forming pores represents another way to increase the immobilized enzyme activity.

The aim of our work is design of optical biosensors for detection of pharmaceutical products. We synthesized by sol-gel methods hybrid membranes contained silica precursors, cellulose derivatives and PAMAM dendrimers as perspective carriers for covalent immobilization. Horseradish peroxidase (HRP) was used as a model enzyme. Conditions were optimized, kinetic parameters, pH and temperature optimums were determined. Constructed biosensors were implemented to detect resorcinol, pirogallol, epinephrine and etc.

These biosensors can be potentially applied in medical, pharmaceutical, food and environmental monitoring fields.

* E-mail: sp_yaneva@uctm.edu

Keywords: optical biosensors, hybrid materials, toxic compounds detection.

STUDY OF MEDIEVAL CERAMICS EXCAVATED AT THE MONASTERY OF KARAACHTEKE (VARNA, BULGARIA)

A. Yoleva*, S. Djambazov, P. Djambazov

University of Chemical Technology and Metallurgy, Sofia, Bulgaria

The study of medieval ceramics is important in order to obtain information for development of ceramic production during this period. Various medieval unglazed and glazed ceramic artifacts discovered during archaeological excavations in the monastery of Karaachteke near Varna (Bulgaria) were first chemically and structurally characterized by ICP-OES, XRD, SEM-EDS and Archimedes method to understand the technology of medieval ceramics production. Water absorption of unglazed artifacts is ranging from 10 to 15 wt.%, which indicates that the ceramic is good sintered and possibly is fired at a high temperature, around 950–1050°C. The artifacts contain a certain amount of coloring oxides ($\text{Fe}_2\text{O}_3 + \text{TiO}_2$), which cause the slightly red color. The phase composition of the ceramic artifacts indicates the presence of crystalline phases of quartz and plagioclase, the amount of which varies in different samples. SEM proves the presence of coarse quartz grains having a size of 0.05 to 0.3 mm in the sintered ceramic body. This leads to the conclusion that it is used or highly sandy clay or ceramic body, consisting of red firing clay and quartz sand with dimensions of 0.05 to 0.3 mm.

The study of glazed artifacts proves that a transparent lead glaze with firing temperature about 950–1050°C was widely used in the Middle Ages. Part of glazed artifacts is typical sgraffito pottery. This fact shows that during this period ceramic masters knew and did ceramic bodies, engobes and glazes at recipe composition of different raw materials. Other part of glazed artifacts is almost identical with the famous Preslav ceramics of a white ceramic body and transparent green glaze with the Seger formula $\text{PbO} \cdot 0,16\text{Al}_2\text{O}_3 \cdot 2\text{SiO}_2$ and firing temperature above 1000°C.

* E-mail: djam@uctm.edu

Keywords: medieval ceramics, SEM, structure, glazes.

NANO-OXIDES WITH CONTROLLED SIZE MODIFIED WITH Pd FOR PURIFICATION PROCESSES

I. Yordanova^{1,*}, A. Ganguly⁴, H. Kolev¹, S. Mondal², A. Naydenov³, M. Shopska¹,
Z. Cherkezova-Zheleva¹, N. Velinov¹, A.K. Ganguli^{2,4,5}, S. Todorova¹

¹ *Institute of Catalysis, Bulgarian Academy of Sciences, Acad. G. Bonchev St., Block 11,
1113 Sofia, Bulgaria*

² *Department of Chemistry, Indian Institute of Technology, Hauz Khas, New Delhi 110016, India*

³ *Institute of General and Inorganic Chemistry, Bulgarian Acad. of Sciences, Acad. G. Bonchev St.,
Block 11, 1113 Sofia, Bulgaria*

⁴ *Nanoscale Research Facility, Indian Institute of Technology, Hauz Khas, New Delhi 110016, India*

⁵ *Institute of Nano Science & Technology, Habitat Centre, Phase – X, Mohali, Punjab, 160062, India*

The second chemical compound responsible for the global warming, after carbon dioxide, is methane. During the last decades catalytic combustion of methane has been extensively investigated for emission control and power generation. The most active catalyst is the Pd/Al₂O₃ catalyst. The order of activity Co₃O₄ > CuO > NiO > Mn₂O₃ > Cr₂O₃ was established for different oxides in the complete oxidation of methane. Suitable combination of Pd and various metal nano-oxides with controlled shape, size and morphology are expected to give stable and highly active catalysts in the complete CH₄ oxidation. Monodisperse and nano sized oxides were prepared by hydrothermal (Mn₃O₄ and Co₃O₄) and co-precipitation (Fe₃O₄) methods. Palladium was deposited by impregnation with aqueous solutions of Pd(NO₃)₂·2H₂O. The samples were calcined for 2h at 450°C. Physico-chemical characterization of the samples have been done by powder X-ray diffraction, Moessbauer spectroscopy, DRIFT, X-ray photoelectron measurements and BET method. Phase composition, structure, crystallite size, specific surface area and other important characteristics were established. Their impact on catalytic behavior of samples was registered in methane and CO oxidation reactions.

Acknowledgements: The authors are gratefully acknowledge the National Science Fund of Bulgaria (Grants No01/8-India and No TO1/6) for the financial support.

* E-mail: yordanova@ic.bas.bg

Keywords: monodisperse nanosized oxides Co₃O₄, Mn₃O₄ and Fe₃O₄, Pd modified, purification processes.

PHOTOCATALYTIC ACTIVITIES OF NANODIMENSIONAL COBALT-FERRITE TYPE OF POWDERS IN THE DEGRADATION OF REACTIVE BLACK 5 DYE

K. Zaharieva, K. Milenova, Z. Cherkezova-Zheleva, A. Eliyas, I. Mitov

*Institute of Catalysis, Bulgarian Academy of Sciences, Acad. G. Bonchev St.,
Block 11, 1113 Sofia, Bulgaria*

The photocatalytic activities of cobalt-ferrite type of powders, prepared by co-precipitation or co-precipitation and mechanochemical treatment, are tested in the present research work. The photodegradation of model wastewater pollutant Reactive Black 5 dye under UV light irradiation, using nanosized cobalt-ferrite type of materials, is investigated. The photocatalytic experiments established that the mechanochemically activated nano-dimensional cobalt-ferrite type of photocatalysts show higher photocatalytic activities than those of the co-precipitated ferrite type of samples. The degree of degradation of Reactive Black 5 dye varies within the range 61-99% for the studied nanostructured cobalt-ferrite type of photocatalysts.

Acknowledgements: The authors appreciate the financial support of the Bulgarian National Science Fund at the Ministry of Education, Youth and Science by Project ДИД 02/38/2009.

* E-mail: zzhel@ic.bas.bg

IMPACT OF CHEMICAL COMPOSITION ON PREPARATION OF NANODIMENSIONAL SPINEL FERRITES

K. Zaharieva*, Z. Cherkezova-Zheleva, B. Kunev, I. Mitov

Institute of Catalysis, BAS, Acad. G. Bonchev St., Block 11, 1113 Sofia, Bulgaria

The present research work deals the studies about changes in a chemical composition of nanosized zinc ferrite-type samples ($\text{Zn}_x\text{Fe}_{3-x}\text{O}_4$, $x=0.25, 0.5, 1$) obtained using different synthesis methods as co-precipitation [1] or co-precipitation and mechanochemical treatment. The mechanochemical activation of co-precipitated ferrite-type samples was performed at milling time – 30 min, 1 h for ZnFe_2O_4 and 2 h for $\text{Zn}_{0.5}\text{Fe}_{2.5}\text{O}_4$ and milling speed at 500 rpm. The different structures, phase and chemical compositions and magnetic behaviour of co-precipitated zinc ferrite-type materials [1] and mechanochemically activated samples were investigated by physicochemical techniques such as X-ray diffraction analysis and Moessbauer measurements at room and liquid nitrogen temperature. The mean crystallite size, lattice strain and unite cell parameter of spinel ferrite phase were also calculated. The relation between chemical composition and different synthesis methods was found.

[1] K. Zaharieva et al., Nanoscience and Nanotechnology (Eds. E. Balabanova, E. Mileva) 14 (2014) submitted.

* E-mail: zaharieva@ic.bas.bg

Keywords: mechanochemical treatment, zinc ferrite-type materials.

PREPARATION OF IMPROVED AND NANODIMENSIONAL CATALYTIC MATERIALS BY MECHANOCHEMICAL METHOD

Z. Cherkezova-Zheleva*

Institute of Catalysis, BAS, Acad. G. Bonchev St., Block 11, 1113 Sofia, Bulgaria

Mechanochemistry is a low-cost and reproducible way for preparation of new and nanomaterials with a desired properties with high yield and under simple and easy operating conditions. The method also enables work under environmentally friendly and essentially waste-free conditions. This makes mechanochemistry one of the most interesting techniques from an industrial point of view. Some of the main properties of mechanochemistry are very suitable for highly effective catalyst synthesis either as a step or as the main stage of preparation.

Number of examples of mechanochemical preparation of precursor or catalytic materials will be presented. Physicochemical and catalytic properties of these materials will be compared to samples obtained using different synthesis methods and shames including co-precipitation and thermal treatment. Phase composition, structure, dispersity and other important characteristics were investigated by powder X-ray diffraction, Moessbauer and infrared spectroscopy, thermal analysis, X-ray photoelectron measurements, electron microscopy, etc.

* E-mail: zzhel@ic.bas.bg

Keywords: mechanochemistry, synthesis, characterization, catalytic materials.

NEUTRON POWDER DIFFRACTION INVESTIGATION OF A HALF HOLE-DOPED BISMUTH-BASED MANGANITE

T. Malakova*, K. Krezhov

¹ Institute for Nuclear research and Nuclear Energy, Tzarigradsko chaussee 72, 1784 Sofia

The structural effects of partial replacement of diamagnetic Bi^{3+} for potential charge ordering and magnetic ordering phenomena in $\text{Bi}_{0.25}\text{Nd}_{0.25}\text{Sr}_{0.5}\text{MnO}_3$ have been studied and compared with previous evidence on $\text{Bi}_{0.25}\text{Nd}_{0.25}\text{Ca}_{0.5}\text{MnO}_3$ [1]. The analysis of the neutron and magnetization data suggests that in bismuth-based calcium perovskites the lone pair character of $6s^2$ Bi^{3+} orbitals is constrained rather than dominant.

[1] K.A. Krezhov, D. Kovacheva, E. Svab and F. Bourée. J. Phys: Condens. Matter, 17 (2005) S3139-S3147.

* E-mail: tanya_malakova@abv.bg

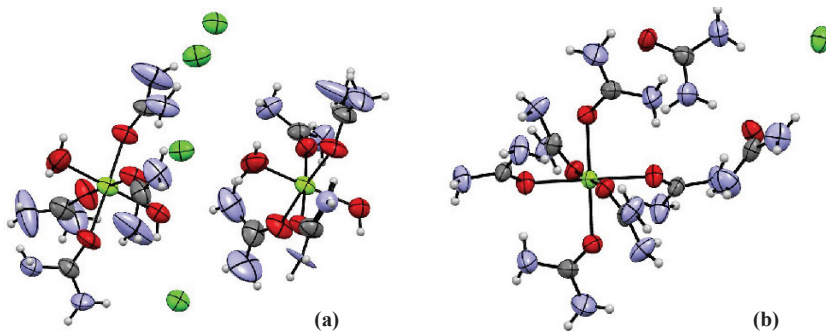
Keyword: perovskites, charge ordering.

SYNTHESIS AND CRYSTAL STRUCTURE OF MAGNESIUM CHLORIDE UREATES

K. Kossev, R. Nikolova, B. Shivachev

*Institute of Mineralogy and Crystallography "Acad. Iv. Kostov" Bulgarian Academy of Sciences,
Acad. G. Bonchev str., building 107, 1113 Sofia, Bulgaria*

The structural peculiarities of urea molecule such as planar geometry, good donor-acceptor properties, high dipole moment, presence of π -bond and ability to form hydrogen bonds, make urea a suitable co-crystallizing agent. Urea molecules replace completely or partially the crystallization water in the structure of the inorganic crystal hydrates and thus complexes of urea with various transition and non-transition metals have been studied. The present communication concerns the structural characterization of two new complexes of urea with magnesium chloride tetraurea dihydrate $[\text{Mg}(\text{OC}(\text{NH}_2)_2)_4((\text{H}_2\text{O})_2)]\text{Cl}_2$ (**1**) and hexakis(urea) magnesium chloride – urea. $[\text{Mg}(\text{OC}(\text{NH}_2)_2)_6]\text{Cl}_2$ (**2**). Crystals of the compounds (**1**) and (**2**) were obtained at room temperature by slow evaporation of an aqueous solution of magnesium chloride and urea in a molar ratio 1/4 and 1/10 respectively. In (**1**) Mg octahedral coordination is formed from four urea and two water molecules while in (**2**) Mg octahedral coordination involves six urea molecules Fig. 1.



* E-mail: k_kossev@yahoo.com

Keywords: Urea, Magnesium complex, single crystal.

AUTHOR INDEX

A

Abdallah, M. • 26
 Abrashev, M. • 112
 Achimovičová, M. • 64
 Adam, A. M. • 27
 Aleksandrova, V. • 73
 Aleksandrov, L. • 65, 87
 Aleksovska, S. • 36, 68
 Andreeva, L. • 82, 84
 Aneva, Z. • 32
 Angelova, A. • 27
 Angelova, R. • 109
 Angelova, S. M. • 83
 Angelov, B. • 27
 Angelov, V. • 28
 Angel, R. J. • 15
 Apostolova, M. D. • 41
 Apostolova, T. • 46
 Aripova, M. Kh. • 29, 30
 Aripov, J. • 30
 Aroyo, M. • 22
 Atanasova-Vladimirova, S. • 38
 Atanasov, L. • 80
 Avdeev, G. • 72, 112
 Averin, I. • 85
 Avramova, I. • 74, 75

B

Babakhanova, Z. A. • 30
 Bachvarova-Nedelcheva, A. • 48, 94
 Bakalska, R. • 98
 Baláž, M. • 63
 Baláž, P. • 63, 64
 Barbov, B. • 31
 Bineva, I. • 32
 Birol, T. • 24
 Bismayer, U. • 16
 Blagoev, B. • 93
 Blaskov, V. • 64, 74, 75
 Bocker, C. • 72, 112
 Bojinova, A. • 56, 57, 66, 85, 90
 Boshkov, N. • 109

C

Chakarova, S. • 32
 Cherkezova-Zheleva, Z. • 37, 89, 106, 115, 116, 117
 Chernev, G. • 97
 Colova, I. • 73

D

Dakova, I. • 33, 40
 Dakov, V. • 33
 Dal Santo, V. • 104
 Degen, Th. • 46
 Delcheva, Z. • 91

Dencheva, S. • 34
 Detcheva, A. • 110
 Dimitriev, Y. • 26, 48, 87
 Dimitrov, A. • 39
 Dimitrova, I. • 65
 Dimitrov, D. • 57, 66, 85, 90
 Dimitrov, M. • 35, 104
 Dimitrovska-Lazova, S. • 36
 Dimova, S. • 37
 Dimova, L. • 38, 44, 45, 108
 Divarova, V. • 39
 Djambazov, P. • 114
 Djambazov, S. • 97, 114
 Djerahov, L. • 40
 Dodoff, N. I. • 41
 Donkova, B. • 42
 Dortmann, Th. • 46
 Doukov, T. • 43
 Drechsler, M. • 27
 Dyulgerov, V. M. • 44, 45

E

El-Deeb, B. • 77
 Eliyas, A. • 64, 74, 75, 116

F

Faulques, E. • 55
 Ferdov, S. • 105
 Fernandes, M. H. V. • 73
 Filippov, S. K. • 27

G

Ganguli, A.K. • 115
 Ganguly, A. • 115
 Garbev, K. • 17, 18
 Gasharova, B. • 17, 18
 Gateshki, M. • 46
 Gavrilova, R. • 80
 Gechev, S. M. • 47
 Gegova, R. • 48
 Gencheva, G. • 32, 49, 51, 52, 76, 99, 103
 Genova, I. • 104
 Gentsheva, G. • 65
 Georgieva, R. • 110
 Georgieva, S. • 93
 Georgieva, Zh. • 49
 Goranova, D. • 50
 Gorolomova, P. • 32, 51, 103
 Gospodinov, M. • 111
 Griesmar, P. • 70
 Grudeva, V. • 109
 Gugov, I. • 72, 112

H

Harizanova, R. • 72, 112
 Harizanova, S. • 71
 Hassaan, A. • 113

Hatzidimitriou, A. • 19
 Hegetschweiler, K. • 52
 Henych, J. • 35
 Hristova-Vassileva, T. • 32

I

Ibrahim, Mohamed M. • 53
 Iordanova, R. • 48, 87, 94
 Ivanova, G. • 93
 Ivanova, N. • 94
 Ivanova, R. • 35
 Ivanova, Vi. • 54, 92
 Ivanova, Y. • 26, 110
 Ivanov, E. • 28
 Ivanov, V. G. • 55

J

Jegova, G. • 96
 Jossifov, C. • 37

K

Kadinov, G. • 63, 89
 Kalvachev, Yu. • 31, 100
 Kaneva, N. • 56, 57, 66, 85
 Karadjova, I. • 33, 40
 Karadjova, V. • 58
 Karakirova, Y. • 75
 Karamanov, A. • 59
 Karashanova, D. • 109
 Karatodorov, S. • 84
 Kasabova, N. • 74, 75
 Kirov, G. • 34
 Kocsis, B. • 22
 Koleva, K. • 60
 Kolev, H. • 115
 Kolevski, A. • 50
 Kolev, T. • 98
 Koseva, I. • 78, 108
 Kossev, K. • 44, 61, 118
 Kostova, B. • 63, 86, 95
 Kostova, I. • 79
 Kostova, N. G. • 64
 Kostov, R. I. • 62
 Kotsilkova, R. • 28
 Kouzmanova, Y. • 65
 Kovacheva, D. • 36, 65, 68, 93, 104, 108, 109
 Krasteva, L. • 66
 Krebs, B. • 32, 51
 Krezhov, K. • 117
 Kuneva, M. • 67
 Kunev, B. • 37, 116
 Kurakalva, R. M. • 40
 Kurteva, V. • 99
 Kurteva, V. B. • 83
 Kushev, D. N. • 41

L

Lalia-Kantouri, M. • 19, 41
 Lazarova, G. • 57
 Lazarova, Ts. • 68
 Lekova, V. • 39

Lesieur, S. • 27
 Levi, Z. • 32
 Lilova, V. • 69
 Lilov, E. • 27, 69

M

Malakova, T. • 117
 Manasieva, D. • 58
 Mangold, S. • 111
 Marinkova, D. • 70
 Marinova, V. • 111
 Markov, P. • 71, 78, 87
 Mathis, Y.-L. • 18
 Mazhdrakova, A. • 72
 Michel, M. • 70
 Mihailova, B. • 96, 111
 Mihailova, I. • 73
 Mihailov, V. • 84
 Mihaylov, L. • 78
 Mikli, V. • 82, 84, 93
 Milanova, M. • 106
 Milenova, K. • 74, 75, 116
 Miletic, V. • 41
 Mimouni, R. • 81
 Mirčeski, V. • 36
 Mirtcheva, G. • 76
 Mitov, I. • 37, 60, 89, 106, 116
 Mkrtchyan, R. V. • 29
 Mladenov, M. • 93, 109
 Momekov, G. • 32, 51, 52, 76
 Mondal, S. • 115
 Moss, D. • 18
 Mostafa, Nasser Y. • 77
 Mouhovski, J. T. • 47
 Mustafa, M. • 80, 81

N

Nam, T. O. • 29
 Naydenov, A. • 115
 Nesheva, D. • 32
 Nihtianova, D. • 71, 78, 87
 Nikiforov, N. • 69
 Nikolchina, I. A. • 83
 Nikolova, R. • 41, 44, 45, 61, 105, 118
 Nikolov, P. • 74, 75
 Nikolov, V. • 78, 108

P

Paneva, D. • 89
 Papazova, K. • 56, 57, 66, 85, 90
 Patronov, G. • 79
 Paulmann, C. • 111
 Pejova, B. • 32
 Pelovsky, Y. • 86
 Pentcheva, R. • 21
 Perez-Mato, J. M. • 22
 Petkova, P. • 80, 81
 Petkova, V. • 42, 63, 86, 95
 Petkov, P. • 27, 54
 Petkov, R. • 80
 Petrova, A. A. • 83

Petrova, N. • 61
 Petrova, R. • 49, 51, 76, 83, 99, 103
 Petrov, O. • 41, 107
 Petrov, S. • 38
 Petrov, V. • 82
 Petrunov, V. • 84
 Piroeva, I. • 38
 Polad, S. • 24
 Pronin, I. • 85

R

Racheva, P. • 39
 Radev, L. • 73
 Raicheff, R. • 93, 109
 Raichev, D. • 90
 Rakovsky, S. • 74, 75
 Rashkova, M. • 96
 Rashkov, R. • 50
 Rasio, N. • 104
 Raykova, R. • 70
 Ristic, M. S. • 19
 Rothe, J. • 23
 Rüssel, C. • 72, 112

S

Salvado, I. M. M. • 73
 Sbirkova, H. I. • 88
 Scotti, N. • 104
 Serafimova, E. • 95
 Serafimova, E. • 86
 Shalaby, A. • 87
 Shvachev, B. • 38, 44, 45, 49, 51, 61, 76, 83, 88, 99, 103, 105, 107, 118
 Shopska, M. • 63, 89, 115
 Simova, S. • 51, 99
 Sinigersky, V. • 37
 Siuleiman, S. • 90
 Sloan, J. • 55
 Smith, D. C. • 55
 Stambolova, I. • 64, 74, 75
 Stanchovska, S. • 71
 Staneva, A. • 87
 Stanimirova, Ts. • 91
 Stemmermann, P. • 17
 Štengl, V. • 35
 Štěpánek, P. • 27
 Stoeva, Z. • 79
 Stoilova, A. • 54, 92
 Stoilova, D. • 58
 Stojnova, K. • 39
 Stoyanova, A. • 94
 Stoyanova-Ivanova, A. • 82, 84, 93
 Stoyanova, R. • 71
 Stoyanov, L. • 109
 Stoyanov, V. • 95

T

Tasci, E. • 22
 Tasci, E. S. • 24

Terzieva, S. • 82, 84, 93
 Titorenkova, R. • 96
 Todorova, E. • 97
 Todorova, M. • 98
 Todorova, S. • 99, 115
 Todorova, T. • 100
 Tomov, I. • 101
 Tonchev, D. • 79
 Tonchev, S. • 67
 Tonchev, V. • 50, 102
 Tosheva, T. • 49, 103
 Trifonova, Y. • 54, 92
 Tsekova, D. • 103
 Tsoncheva, T. • 35, 60, 104
 Tsvetanova, L. • 105
 Tsvetkov, M. • 106
 Tumbalev, V. • 82, 84
 Tzvetanova, Y. • 107
 Tzvetkov, P. • 36, 78, 108

U

Ugrinov, A. • 49, 52

V

Valchev, V. • 100
 Varbanov, S. • 49, 103
 Vasileva, P. • 40
 Vasilev, P. • 80, 81
 Vassileva, P. • 110
 Vassilev, N. • 103
 Vassilev, N. G. • 41
 Vassilev, S. • 74, 75, 101
 Velcheva, V. • 52
 Veleva, S. • 109
 Velikova, N. • 26, 110
 Velinov, N. • 60, 64, 115
 Vitova, T. • 25, 111
 Vitov, O. H. • 47
 Vladislavova, L. • 112
 Vueva, Y. • 110

W

Wildner, M. • 58

Y

Yakushova, N. • 85
 Yaneva, S. • 113
 Yoleva, A. • 114
 Yordanova, A. • 78
 Yordanova, I. • 115
 Yotova, L. • 70, 113

Z

Zaharieva, K. • 37, 106, 116
 Zaleski, A. • 93
 Zarev, S. • 49
 Zhecheva, E. • 71
 Zhelyazkova, Y. • 103
 Zianna, A. • 19